Structure and macromolecular properties of *Weissella confusa* and *Leuconostoc citreum* dextrans with a potential application in sourdough

Ndegwa Henry Maina

ACADEMIC DISSERTATION

To be presented, with the permission of the Faculty of Agriculture and Forestry of the University of Helsinki, for public examination in lecture hall B2 (Raisio Oyj:n Tutkimussäätiön sali), Viikki, 1st June 2012, at 12 noon.

University of Helsinki
Department of Food and Environmental Sciences
Chemistry and Biochemistry Division
Helsinki 2012

Custos: Professor Vieno Piironen
Department of Food and Environmental Sciences
Food Chemistry Division
University of Helsinki, Finland

Supervisors: Docent Liisa Virkki
Department of Food and Environmental Sciences
Chemistry and Biochemistry Division
University of Helsinki, Finland

Professor Maija Tenkanen
Department of Food and Environmental Sciences
Chemistry and Biochemistry Division
University of Helsinki, Finland

Reviewers: Dr. Luc Saulnier
Biopolymers - Interactions and Assemblies unit
INRA, Nantes Research Centre, France

Professor Thomas Peters
Institute of Chemistry
Center for Structural and Cell Biology in Medicine (CSCM)
University of Lübeck, Germany

Opponent: Dr. Gregory L. Côté
Renewable Product Technology Research Unit
National Center for Agricultural Utilization Research
Agricultural Research Service
U.S. Department of Agriculture, USA

ISBN 978-952-10-7983-2 (paperback)
ISBN 978-952-10-7984-9 (PDF, http://ethesis.helsinki.fi)
ISSN 0355-1180

Unigrafia
Helsinki 2012

.....Man shall not live and be upheld and sustained by bread alone, but by every word that comes forth from the mouth of God. Matthew 4:4 Amplified Bible.

Ndegwa H. Maina 2012. Structure and macromolecular properties of *Weissella confusa* and *Leuconostoc citreum* dextrans with a potential application in sourdough (dissertation). EKT-Series 1553. University of Helsinki, Department of Food and Environmental Sciences. 93 + 57 pp.

Abstract

Over the past few years, interest in dextrans produced by lactic acid bacteria (LAB) has experienced a renaissance because of their prospective application as natural hydrocolloids in fermented products. Though the benefits of dextrans as hydrocolloids in sourdough bread have been the subject of several studies, only in a few of these studies have the structural features of the potential dextrans been elucidated. In this thesis the structure and macromolecular properties of *W. confusa* E392 and *L. citreum* E497 dextrans were studied to understand their functionality in sourdough. Since functionality also depends on concentration, an enzyme-assisted assay was developed to estimate the amount of dextrans produced in sourdough. The experimental part included several other dextrans for comparison and method development.

Structural analysis revealed that *W. confusa* E392 dextran contains few α-(1→3)-linked branches (3%), while *L. citreum* E497 dextran contains α-(1→2)- and α-(1→3)-linked branches (11% and 4%, respectively). Further details on the nature of these branches from the analysis of structural segments indicated that the α-(1→3)-linked branches in both dextrans are either a single unit or elongated by two or more α-(1→6)-linked glucosyl residues. Macromolecular characterization in aqueous solutions showed them to be high molar mass dextrans (10^7 g/mol). In dimethylsulfoxide (DMSO), however, the molar mass of the dextrans was lower (1.5 and 1.9 × 10^6 g/mol). The lower values in DMSO were considered to originate from individual dextran chains, while the values obtained in aqueous solutions were skewed by the presence of compact aggregates. The enzyme-assisted assay developed for dextran quantification was limited to dextrans with few branch linkages. *L. citreum* E497 dextran was therefore not quantifiable with this method. During 17-24 hours of fermentation, *W. confusa* E392 produced 1.1-1.6% dextran from an initial 10% sucrose. Preliminary studies indicate that the strain channeled the remaining glucose (the theoretical maximum glucose was 5%) to the production of oligosaccharides via dextransucrase acceptor reactions with maltose.

In conclusion, the study revealed that despite their simple monosaccharide composition, dextrans have a complex ramified structure even in the case of *W. confusa* E392 that only has a few branch linkages. Aqueous solutions of high molar mass dextrans contain compact aggregates, which, in addition to the ramified structure of dextrans, complicate their macromolecular characterization. Consequently, deducing the functional properties of dextrans in sourdough or any other food application is not straightforward. When comparing the functional properties of dextrans, the size (hydrodynamic properties and intrinsic viscosity), which reflects the shape and conformation of the dextrans, should be considered in addition to molar mass and structural features. Since food applications are aqueous systems, the functionality of dextrans may result from a contribution of both the properties of individual chains and compact aggregates.

Acknowledgements

This study was carried out at the University of Helsinki, Department of Food and Environmental Sciences, Chemistry and Biochemistry Division. The research was funded by the Finnish Funding Agency for Technology and Innovation, the Academy of Finland, the Glycoscience Graduate School, the Finnish Cultural Foundation and the Raisio Research Foundation; their financial support is greatly appreciated.

I express my sincere gratitude to God for every success, talent and ability He has given me, and for the strength and grace to complete this work. May You be glorified in everything I do. I am greatly indebted to my supervisors, Docent Liisa Virkki and Professor Maija Tenkanen. I thank Liisa for introducing me to NMR spectroscopy, excellent advice, support and encouragement throughout the study. It has been a privilege to work with you. I am deeply grateful to Maija especially for giving me a chance to work in her research group, for challenging me to go the extra mile and for being a mentor.

I am thankful to Professor Vieno Piironen for support during my doctoral studies, giving me good advice and for her comments on this dissertation. I greatly appreciate Professor Thomas Peters and Dr. Luc Saulnier for pre-examination of this dissertation. Thank you for critically evaluating this work and for the comments and suggestions you provided. I sincerely thank Professor Rosário Domingues and Associate Professor Dmitry Evtuguin for welcoming me to the University of Aveiro, Portugal. I am especially thankful to Professor Rosário Domingues for introducing me to the structural analysis of oligosaccharides by mass spectrometry.

I am grateful to my co-authors: Docent Hannu Maaheimo, Docent Päivi Tuomainen, Docent Jouni Jokela, Dr. Sami Heikkinen, Dr. Kati Katina, Dr. Riikka Juvonen, Dr. Leena Pitkänen, Dr. Liisa Johansson, Dr. Arja Laitila, Laura Flander, Henna Pynnönen and Minna Juvonen. Thank you for making your invaluable expertise available; you contributed to the success of this research. I am very thankful to my colleagues in the hemicellulose research group, with whom working on the many facets of carbohydrate research has been an immense pleasure. I specifically wish to thank Minna Malmberg and Laura Huikko for practical assistance with the laboratory work. I am grateful to all my colleagues in the D-building for creating a friendly work atmosphere. I thank Adelaide Lönnberg for language revision of this dissertation.

I express my heartfelt gratitude to my family, relatives and friends. I am indebted to my parents John Maina Gichinga and Mary Waithira Gichinga for their prayerful support and encouragement to pursue my doctoral studies. I thank my brother Wilson Gichinga and my sisters Jacqueline Njoki Maina and Peninah Muthoni Muiruri, for always believing in me and encouraging me. Finally I owe my dearest thanks to my precious wife Wambui Ndegwa and our three lovely princesses Waithira, Wanjiru and Wariri, to whom I dedicate this thesis. Life would be meaningless without you in my life. I am sincerely grateful for your love, enduring patience and for standing by me throughout this project.

Helsinki, May 2012

Ndegwa H. Maina

List of original publications

This thesis is based on the following publications:

I Maina NH, Tenkanen M, Maaheimo H, Juvonen R, Virkki L. 2008. NMR spectroscopic analysis of exopolysaccharides produced by *Leuconostoc citreum* and *Weissella confusa*. Carbohydr Res 343:1446-1455.

II Maina NH, Virkki L, Pynnönen H, Maaheimo H, Tenkanen M. 2011. Structural analysis of enzyme-resistant isomaltooligosaccharides reveals the elongation of α-(1→3)-linked branches in *Weissella confusa* dextran. Biomacromolecules 12:409–418.

III Maina. NH, Juvonen M, Jokela J, Virkki L, Domingues RM, Tenkanen M. 2011. Structural analysis of linear mixed-linkage glucooligosaccharides by tandem mass spectrometry. Submitted.

IV Maina NH, Pitkänen L, Heikkinen S, Tuomainen P, Virkki L, Tenkanen M. 2011. Macromolecular characterization of high-molar mass dextrans by size exclusion chromatography, asymmetric flow field flow fractionation and diffusion-ordered NMR spectroscopy. Submitted.

V Katina K, Maina NH, Juvonen R, Flander L, Johansson L, Virkki L, Tenkanen M, Laitila A. 2009. In situ production and analysis of *Weissella confusa* dextran in wheat sourdough. Food Microbiol 26:734-743.

The publications are reproduced with the kind permission of the copyright holders: Elsevier and the American Chemical Society. The publications are referred to in the text by their Roman numerals.

Contribution of the author to papers I to V:

I-III Ndegwa H. Maina planned the study together with the other authors. He performed all the experiments related to isolation and structural analysis of the dextrans. He had the main responsibility of interpreting the results and was the corresponding author of the papers.

IV Ndegwa H. Maina planned the study together with the other authors. He performed all the DOSY experiments. He had the main responsibility for the DOSY results and for writing the sections in the article related to this work.

V Ndegwa H. Maina planned the study together with the other authors. He performed all the experimental work to develop the enzyme-assisted assay for *in situ* analysis of dextrans and also evaluated the oligosaccharides produced during sourdough fermentation. He had the main responsibility for interpreting the results on dextran and oligosaccharide analysis and for writing the sections in the article related to this work.

Abbreviations

AsFlFFF	asymmetric flow field-flow fractionation
BIMO	branched isomaltooligosaccharides
c^*	critical overlap concentration
Da	Daltons
Dn/dc	refractive index increment
DMSO	dimethylsulfoxide
DOSY	diffusion-ordered spectroscopy
DQF-COSY	double-quantum filtered correlation spectroscopy
EPS	exopolysaccharides
ESI	electrospray ionization
FFF	field-flow fractionation
GC-MS	gas chromatography with a mass spectrometry detector
GOS	glucooligosaccharides
GPC	gel permeation chromatography
GRAS	generally recognized as safe
HePS	heteropolysaccharides
HILIC	hydrophilic interaction liquid chromatography
HMM	high molar mass
HMBC	heteronuclear multiple bond connectivity spectroscopy
H2BC	heteronuclear two-bond correlation spectroscopy
HoPS	homopolysaccharides
HPLC	high-perfomance liquid chromatography
HPSEC	high-perfomance size exclusion chromatography
HPAEC-PAD	high-perfomance anion exchange chromatography with pulse amperometric detection
HSQC	heteronuclear single-quantum coherence spectroscopy
IMO	isomaltooligosaccharides
[η]	intrinsic viscosity
LAB	lactic acid bacteria
LS	light scattering
LMM	low molar mass
NMR	nuclear magnetic resonance
MALDI	matrix-assisted laser desorption/ionization
M_w	weight average molecular weight
M_n	number average molecular weight
M_w/M_n	dispersity index
MRS-S	De Mann, Rogosa and Sharp agar containing 2% sucrose
MS	mass spectrometry
MS/MS	tandem mass spectrometry
MS^2	second MS/MS circle
MS^3	third MS/MS circle
m/z	mass to charge ratio
NOESY	nuclear overhauser effect spectroscopy
PFG	pulse field gradient
R_g	radius of gyration
R_h	hydrodynamic radius
RI	refractive index signal
ROESY	rotating frame nuclear overhauser effect spectroscopy
TOF	time of flight
TOCSY	total correlation spectroscopy

Contents

ABSTRACT 4
ACKNOWLEDGEMENTS 5
LIST OF ORIGINAL PUBLICATIONS 6
ABBREVIATIONS 7
CONTENTS 8
1 INTRODUCTION 10
2 REVIEW OF THE LITERATURE 12
2.1 Overview of exopolysaccharides from lactic acid bacteria 12
2.2 Dextrans 14
2.2.1 Structural properties 14
2.2.2 Biosynthesis 17
2.2.3 Dextran-hydrolyzing enzymes 19
2.3 Structural analysis of dextrans 20
2.3.1 Methylation analysis 21
2.3.2 NMR spectroscopy 23
2.3.3 Potential of mass spectrometry 25
2.4 Physicochemical properties of dextrans 27
2.4.1 Characterization of the macromolecular and rheological properties of dextrans 28
2.4.1 Diffusion-ordered NMR spectroscopy (DOSY) 30
2.5 Application of dextrans 33
2.6 Potential of dextrans in sourdough bread 33
3 AIM OF THE STUDY 37
4 MATERIALS AND METHODS 38
4.1 Microbial strains and isolation of dextrans 38
4.2 Monosaccharide composition analysis (I) 40
4.3 Enzyme-aided analysis of the dextrans (II and V) 40
4.3.1 Chromatographic profiling of the dextrans (II and V) 40
4.3.2 Preparation and isolation of enzyme-resistant oligosaccharides (II) 41
4.3.3 Development of an enzyme-aided assay for dextran quantification (V) 41
4.3.4 Preliminary studies on dextransucrase acceptor reaction products in sourdough 43
4.4 HPAEC-PAD analysis (II and V) 44
4.5 Methylation analysis (II) 45
4.6 Mass spectroscopy (II and III) 45
4.7 NMR spectroscopy (I, II and III) 46
4.8 Macromolecular characterization of *W. confusa* and *L. citreum* dextrans (IV) 47
4.8.1 HPSEC and AsFlFFF 47

4.8.2 DOSY 48
5 RESULTS 49
5.1 Isolation of the dextrans (I) 49
5.2 NMR spectroscopy analysis of the dextrans (I) 49
5.3 Enzyme-aided analysis of the isolated dextrans (II) 51
5.3.1 Action of the enzymes (II) 51
5.3.2 Chromatographic profiling of the native dextrans 52
5.4 Structural analysis of BIMO (II and III) 52
5.4.1 Isolation of the BIMO (II and III) 52
5.4.2 Methylation analysis of the BIMO from commercial dextran (II) 54
5.4.3 Structural analysis of BIMO (tetrasaccharides) by MS (III) 54
5.4.4 NMR spectroscopy analysis of the BIMO (II and III) 58
5.5 Macromolecular characterization of the dextrans 62
5.5.1 HPSEC and AsFlFFF 62
5.5.2 DOSY 64
5.6 *In situ* quantification of polymeric dextrans in dough 66
5.6.1 Dextrans in model dough 67
5.6.2 Dextran in sourdoughs 67
5.7 Dextransucrase acceptor reaction products in sourdough 68
6 DISCUSSION 69
6.1 Structural features of native dextrans 69
6.2 Enzymatic hydrolysis and chromatographic profiling of native dextrans 70
6.3 Fine structure of the dextrans by analysis of BIMO 71
6.3.1 Mass spectrometry analysis of fractionated BIMO 72
6.3.2 NMR spectroscopy analysis of fractionated BIMO 73
6.3.3 BIMO from *L. citreum* E497 dextran 74
6.4 Macromolecular properties of the native dextrans 75
6.4.1 HPSEC and AsFlFFF 75
6.4.2 DOSY 77
6.5 *In situ* analysis of dextrans produced during sourdough fermentation 78
7 CONCLUSION 81
REFERENCES 83
Original publications
About the author

1 Introduction

End product quality is an important consideration in food processing. Food quality, which can be defined as "fitness for consumption", encompasses several dimensions such as safety, nutrition, aesthetics, ethical factors and convenience (Claudio 2006). In most cases food quality maintenance or enhancement involves addition of food additives such as colorants, flavor enhancing agents and hydrocolloids. Unfortunately, such additives are subject to strict regulation and, additionally, current consumer trends are towards healthier and additive-free foods (Welman and Maddox 2003). Therefore, new technologies that produce healthier foods and utilize minimal or no additives are constantly being sought by the food industry. In the bread-making industry, solutions have been found by simply going back to traditional bread making, i.e. sourdough bread (Katina 2005).

Sourdough fermentation is an ancient process in which ground cereal grains are mixed with water and spontaneously fermented with lactic acid bacteria (LAB) and yeast that are naturally present in the flour or the environment (Hammes and Gänzle 1998; Kulp 2003). For optimal leavening, acidification and flavor production, traditional spontaneous sourdough fermentation was lengthy and the outcome varied depending on the raw material and general hygiene conditions. Thus, as Gelinas and Mckinnon (2000) maintain, once a sourdough with desirable characteristics was obtained, a portion was kept as a starter for subsequent sourdoughs. This technique was known as backslopping. The traditional sourdough fermentation processes dominated home-baked bread until the commercialization of bread making at the beginning of the 19th century (Wirtz 2003; Bobrow-Strain 2008).

The mechanization of bread-making processes for industrial production was, however, not compatible with the lengthy traditional sourdough fermentation processes (Decock and Cappelle 2005). Baker's yeast was therefore introduced for a predictable, reproducible and accelerated leavening process (Kulp 2003; Carnevali et al. 2007). Large-scale production also necessitated optimization of dough properties for mechanical handling and improvement of bread quality, such as a better shelf life. This led to the introduction of food additives, such as surfactants, hydrocolloids, antimicrobial agents and enzymes as baking aids, all of which are still commonly used today (Stampfli and Nersten 1995; Mondal and Datta 2008). Although these tools provided manufacturers with production efficiency, cost reduction and quality control, the aroma and flavor attributes of traditional artisan style home-baked bread were compromised (Katina 2005).

In order to utilize sourdough at an industrial level, research is needed to characterize the biochemical processes taking place during fermentation and to devise methods that can

optimize the beneficial factors. This is particularly important for ensuring consistency in day-to-day sourdough bread production. Currently, research is focusing on several aspects of sourdough, such as identification of the sourdough microflora, development of aroma and flavor components during the fermentation process, production and identification of antimicrobial components, and the impact of sourdough technology on the rheological properties and the shelf life of wheat bread (Katina 2005). Among these factors, those that enhance the rheological properties and retard the staling of bread are the focus of this thesis. These benefits have mainly been attributed to the production of exopolysaccharides (EPS) by certain LAB (Korakli et al. 2001; Katina et al. 2005; Tieking and Gänzle 2005). Tieking and Gänzle (2005) maintain that EPS have beneficial effects on the technological properties of dough and bread, including water binding capacity, dough rheology and machinability, dough stability during frozen storage, loaf volume and bread staling. Essentially, EPS act as hydrocolloids in bread and because they are produced *in-situ* during sourdough fermentation, they are not considered as additional food additives. Production of EPS *in-situ* is therefore a novel method for replacing hydrocolloid additives in food, which concurs with the current consumer trends (Katina 2005).

Currently, challenges in the utilization of EPS from LAB not only include the identification of potential strains and the enhancement of EPS production, but also the production of EPS with specific structures and sizes that impart the desired functional properties (De Vuyst and Degeest 1999; Welman and Maddox 2003). Such studies, including structural characterization of EPS, have focused extensively on LAB in dairy applications (Laws and Marshall 2001). On the contrary, though several studies have focused on determining the sourdough microflora (De Vuyst and Neysens 2005), only a few have carried out detailed structural analysis of the EPS produced. The structural details of EPS are necessary in order to understand their functionality in sourdough. In this thesis, dextrans produced by *Weissella confusa* E392 and *Leuconostoc citreum* E497 were studied to understand their functional properties in sourdough. The literature review provides an overview of EPS with an emphasis on dextrans, their structure, synthesis, physico-chemical properties and their utilization in sourdough. The experimental part summarizes the data presented in five publications (**I-V**) on the structural and macromolecular properties of the potential dextrans, *in-situ* quantification of dextrans produced during sourdough fermentation and the effect of the dextrans on the final bread.

2 Review of the literature

2.1 Overview of exopolysaccharides from lactic acid bacteria

The cell surface of LAB is composed of polysaccharides that can be components of the cell wall or may be external to the cell surface structure. The additional polysaccharides are generally referred to as EPS or capsular polysaccharides if they are strongly associated with the cell surface (Sutherland 1990; Ruas-Madiedo and De los Reyes-Gavilan 2005). Sutherland maintains that the microbial cell surfaces are not compromised without EPS and therefore they do not contribute to the integrity of the microbial cell structure (Sutherland 1990). It is also unlikely that the EPS are synthesized as storage polymers, since most EPS producing bacteria do not have the necessary enzymes for their degradation (Gänzle and Schwab 2009). Currently, the suggested biological role of EPS includes: protection of microbial cells against phages, protection against desiccation, stress tolerance (e.g. acid and oxidative stress), antibiotic resistance, adhesion, and biofilm formation (De Vuyst and Degeest 1999; Ruas-Madiedo and De los Reyes-Gavilan 2005; Gänzle and Schwab 2009).

The composition of microbial EPS is very diverse and may even include rare sugars such as L-fucose and L-rhamnose. Sutherland (1990) notes that a common distinction between EPS from eukaryotes and prokaryotes is the presence of pentoses, such as xylose and arabinose in eukaryotic EPS. Based on the mechanism of biosynthesis and the precursors required, EPS from LAB can be divided into two groups (Boels et al. 2001). The first includes EPS that are synthesized extracellularly by glycosyltransferases using a disaccharide as the substrate. EPS in this group are homopolysaccharides (HoPS) that include α-glucans (dextrans and reuterans) and β-fructans (levan and inulin), produced by glucosyltransferases (glucansucrases) and fructosyltransferases (fructansucrase), respectively, using sucrose as a glycosyl donor (Monsan et al. 2001). Raffinose can also be used as a substrate for β-fructans synthesis (Gänzle and Schwab 2009).

The second group includes HoPS and heteropolysaccharides (HePS) with irregular or regular repeating units that are synthesized from activated sugar nucleotide precursors. The HoPS in this group include β-glucan from *Lactobacillus* (Duenas-Chasco et al. 1998), *Streptococcus* and *Pediococcus* strains (Dueñas-Chasco et al. 1997; Ruas-Madiedo et al. 2002) and polygalactans from *Lactococcus lactis* strains (Gruter et al. 1992). HePS are structurally diverse and are composed of several monosaccharides such as D-glucose, D-rhamnose, D-galactose, D-fructose and N-acetyl amino sugars. HePS may also contain other organic and inorganic compounds (De Vuyst and Degeest 1999). The repeating units

in HePS that may include two to eight monosaccharides are usually synthesized in the cytoplasm by glycotransferases (Ruas-Madiedo et al. 2009) and polymerized extracellularly after translocation across the membrane as lipid-linked intermediates (De Vuyst and Degeest 1999).

The implication of the different biosynthetic pathways is reflected in the yield of the EPS produced. Generally, the yield of HePS from intracellular synthesis is low (50-600 mg/l) due to the competition between different metabolic pathways for the nucleotide precursors and because the synthesis is an energy-demanding process. The yield is further limited by the capacity of the lipid carrier, which is also involved in cell wall synthesis, and the efficiency of the extracellular polymerization process. In contrast, the yield of HoPS that are synthesized extracellularly is usually high (3-15 g/l), the activity of glycansucrases being the main limiting factor (De Vuyst and Degeest 1999; Gänzle and Schwab 2009). The energy required for this process derives from the cleavage of the glycosidic bond in sucrose (Monsan et al. 2001).

Interest in the study of EPS from LAB stems from their potential physiological and technological benefits. Physiologically, EPS from LAB are reported to elicit anti-tumor effects, immunostimulatory activity, cholesterol lowering ability and prebiotic properties. Nonetheless, more research, especially human intervention studies, is needed to provide more solid scientific evidence on these health-promoting effects (Ruas-Madiedo et al. 2009). Technologically, the physicochemical properties of EPS, such as viscosity, have motivated their utilization in food applications as, for example, biothickeners (De Vuyst and Degeest 1999, Patel et al. 2012). Since LAB have GRAS (Generally Recognized as Safe) status, they can be used for *in-situ* production of EPS during fermentation. This effectively provides a means to replace hydrocolloid additives in fermented products and, as Welman (2009) maintains, is the most practical and cost-effective way, and also suits the ~~–n~~atural product" image that consumers are currently demanding.

Therefore, by choosing the right strain and optimizing growth conditions, suitable starter cultures can be developed for acidification, flavor and aroma development and texture enhancement of fermented food products. This process has predominantly been explored in dairy applications, mainly with HePS-producing strains. Conversely, HoPS have mostly been exploited in sourdough applications (Waldherr and Vogel 2009). A likely reason for the prevalence of HoPS in sourdough is that HePS-producing strains are rarely isolated from fermented cereals, whereas HoPS producers are very common. The HoPS producers are also dominant in plant materials that contain sucrose (Gänzle and Schwab 2009). This study focuses on the HoPS produced in sourdough applications; thus further discussion will focus mainly on dextrans that are widely produced by sourdough-related microbes.

2.2 Dextrans

Dextran is a generic name for several α-glucans produced by LAB that belong to the *Leuconostoc*, *Lactobacillus, Streptococcus, Pediococcus* or *Weissella* genera (Smitinont et al. 1999, Naessens et al. 2005; Bounaix et al. 2009). According to Rehm (2010), dextrans were among the first microbial polysaccharides to be discovered. Studies on dextrans date back to the work of Louis Pasteur on viscosity development in wine in 1861. In 1874, Scheibler showed that viscosity in beet sugar juices was due to a carbohydrate that had a positive optical rotation and he thus called it ‗dextran' (Naessens et al. 2005).

2.2.1 Structural properties

According to Jeanes et al. (1954), the amount of α-(1→6) linkages in a specific dextran can vary from 50% to 97% of the total glycosidic linkages. Dextrans are currently divided into three classes according to their structural features (Figure 1). Class 1 dextrans have consecutive α-(1→6)-linked D-glucopyranosyl units and branch linkages via α-(1→2), α-(1→3) or α-(1→4). Class 2 dextrans (alternans) contain alternating α-(1→3) and α-(1→6) linkages with both α-(1→3) and α-(1→6) branch linkages (Côté 2002). Class 3 dextrans (mutans) have consecutive α-(1→3) linkages and α-(1→6) branch linkages (Robyt 1986). In agreement with previous deductions, alternans are not ‗true' dextrans (Seymour et al. 1979b; Côté 2002) and it may even be practical to abandon the classification and utilize the terms dextrans, alternans and mutans only. Henceforth in this thesis, the term dextran refers to Class 1 dextrans only.

Reutarans are related to dextrans in that they are also produced extracellularly from sucrose. According to the composite model of reuteran produced by *Lactobacillus reuteri* strain 35-5 (van Leeuwen et al. 2008b), reuterans are composed of α-(1→4)-linked glucosyl residues in the main chain with α-(1→6) branch linkages that are further elongated with α-(1→4)-linked glucosyl residues. The α-(1→4)-linked main chain is also irregularly interrupted by α-(1→6) linkages (6-*O*-monosubstituted glucosyl residues) (van Leeuwen et al. 2008b). Thus, unlike dextrans with α-(1→4) branch linkages, the α-(1→4) linkages in reuterans are more abundant than α-(1→6) linkages and are part of the main chain. An overview of the structural features of α-glucans from several strains is shown in Table 1. The structures of dextran from more strains can be obtained from Bounaix et al. (2009) and Slodki et al. (1986). As shown in Table 1, some dextrans can have two types of branches: α-(1→2)- and α-(1→3)- or α-(1→3)- and α-(1→4)-linked branches.

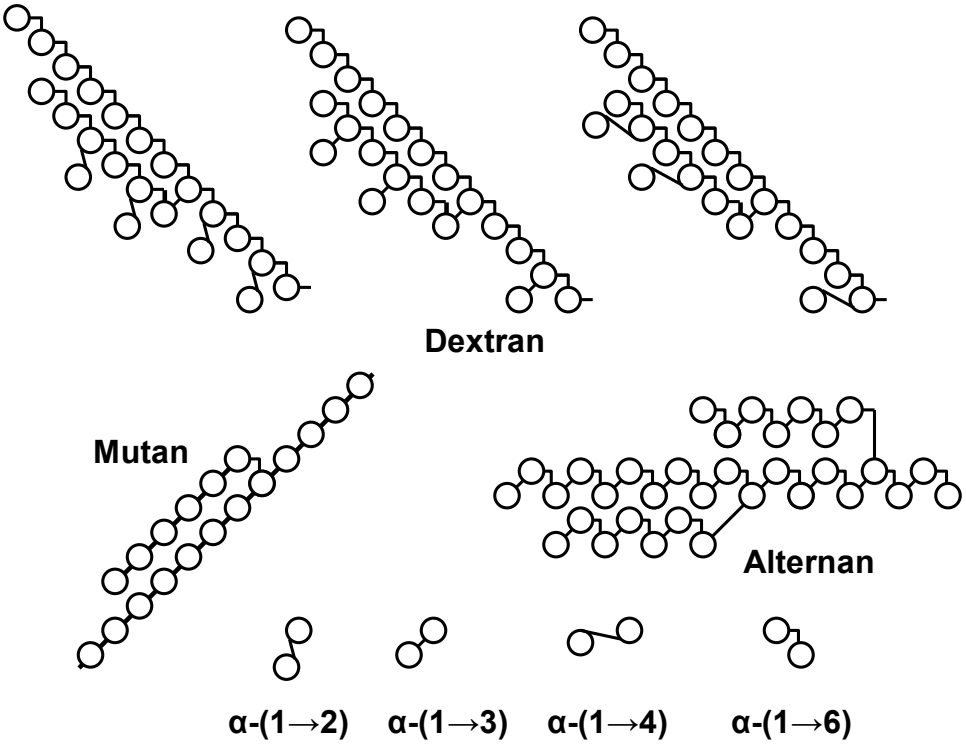

Figure 1. Schematic representation of dextrans, alternans and mutans (modified from Robyt 1986)

Although the structure of dextrans has been extensively studied, their fine structure, especially the length and spatial arrangement (topology) of the non-α-(1→6) linkages and extended branches, is still not fully understood (De Belder 1993). Generally, studies have shown that the α-(1→3)-linked branches in dextrans are single units or elongated by two or more α-(1→6)-linked glucosyl residues (Sidebotham 1974; Taylor et al. 1985) or in some cases elongated by α-(1→3)-linked glucosyl residues (Cheetham et al. 1990). Using sequential chemical removal of terminal D-glucosyl groups, Larm et al. (1971) concluded that 40% of the α-(1→3)-linked side chains in dextran produced by *Leuconostoc mesenteroides* NRRL B-512F contained one glucosyl residue, 45% were two glucosyl residues long, and the rest (15%) were longer. Based on physicochemical data, Ioan et al. (2001) concluded that the long branches in commercial *L. mesenteroides* B-512F dextran can have a molar mass of 29 000 g/mol (~179 glucosyl units).

Table 1. An overview of the glucosidic linkages (%) in α-glucans from several LAB strains. The values were obtained with methylation analysis except for *W. cibaria* and *W. confusa* dextrans which were obtained with NMR spectroscopy analysis.

Strains	**EPS**	**Glc*p*-(1→**	**α-(1→6)**	**α-(1→3,6)**	**α-(1→3)**	**α-(1→2,6)**	**α-(1→2)**	**Reference**
Lb. parabuchneri 33	Dextran	6	75	9	9			Kralj et al. 2004
Lb. sake Kg 15	Dextran	4	86	9	1			Kralj et al. 2004
Lb. reuteri. LB 180	Dextran	10	51	13	26			Kralj et al. 2004
Lb. reuteri ML1	Mutan-like	18	10	26	47			Kralj et al. 2004
L. citreum NRRL B-742[a]	Dextran (S)	38	25	28				Slodki et al. 1986
L. mesenteroides NRRL B-512F	Dextran	5.5	89	5.5				Larm et al. 1971
L. mesenteroides NRRL B-1355	Alternan	10	45	10	35			Slodki et al. 1986
L. mesenteroides NRRL B-523	Dextran	8	58	4	27		3	Slodki et al. 1986
L. mesenteroides NRRL B-1299	Dextran (S)	31	32	1	1	30	5	Slodki et al.1986
	Dextran (L)	20	53	5	5	16		Slodki et al. 1986
P. pentosaceus Ap-1	Dextran	8	85	7				Smitinont et al. 1999
P. pentosaceus Ap-3	Dextran	11	81	7				Smitinont et al. 1999
S. mutan GS-5	Dextran (S)		69		31			Kuramitsu and
	Insoluble glucan		48		52			Wondrack 1983
S. mutan 6715	Dextran (S)		64	36				Robyt 1986
	Mutan (I)		4	2	94			Robyt 1986
S. sobrinus MFe28[b]	Mutan	1	3		88			Russell et al. 1987
W. cibaria DSM 15878	Dextran		97		3			Bounaix et al. 2009
W. confusa DSM 20196	Dextran		97		3			Bounaix et al. 2009
		Glc*p*-(1→	**α-(1→6)**	**α-(1→4,6)**	**α-(1→4)**	**α-(1→3)**		
L. citreum NRRL B-742	Dextran (L)	14	73	12		1		Seymour et al. 1979a
Lb. reuteri LB 121	Reuteran	9	26	15	49			Kralj et al. 2004
Lb. reuteri ATCC 55730	Reuteran	9	11	13	69			Kralj et al. 2005

[a] 8% 4,6-*O*-disubstituted residue linkages [b]8% unknown linkages, *Lb.= Lactobacillus, L. =Leuconostoc, P. = Pediococcus, S. =Streptococcus W. =Weissella.* S = soluble, L = Less soluble, I = insoluble

Studies have also shown the elongation of α-(1→2)-linked branches in dextrans produced by *L. mesenteroides* NRRL B-1298 and NRRL B-1299 with α-(1→6)-linked glucosyl residues and branches elongated by non-α-(1→6)-linked glucosyl residues (Sidebotham 1974; Watanabe et al. 1980). As in reuterans, the occurrence of α-(1→2) or α-(1→3) linkages as interruptions of the α-(1→6) linkages in the main chain or in elongated branches in dextrans is also probable. For example, van Leeuwen et al. (2008a) reported the presence of 3-*O*-monosubstituted residues in the main chain and in the elongated branches of *Lb. reuteri* strain 180 dextran.

According to Sidebotham (1974), dextrans can have a comb-like, laminated or ramified structure as shown in Figure 2. The degree and type of branching (long or short) in a particular dextran is not only strain dependent but also seems to be affected by the temperature at which the dextran is produced. Sabatie et al. (1988) found that dextrans synthesized at 3, 10 and 20°C displayed an expanded conformation, while dextrans synthesized at 30°C were more compact and behaved like a globular protein due to increased ramification (Sabatié et al. 1988). Kim et al. (2003) showed that branching increased from 4.8% at 4°C to 14.7% at 45°C during cell-free synthesis of dextrans by a dextransucrase from *L. mesenteroides* B-512FMCM (Kim et al. 2003).

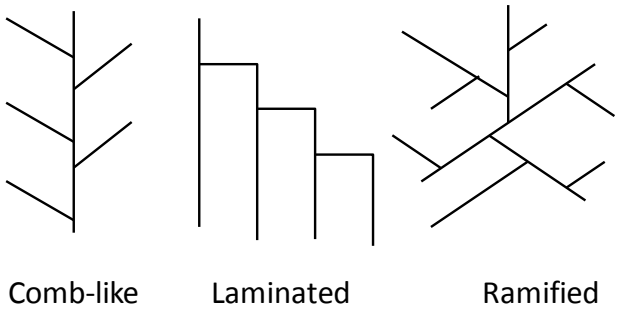

Figure 2. Schematic representation of the possible structures of dextrans (adapted from Sidebotham 1974).

2.2.2 Biosynthesis

Dextrans are synthesized extracellularly by dextransucrases (glucansucrases, EC 2.4.5.1) from sucrose. As reviewed by Leathers (2002), the optimal reaction conditions for dextransucrases are pH 5.0—6.5 and temperature ranging from 30—45°C. Although the catalytic mechanism of dextran synthesis has been the subject of several studies, the synthesis is still not fully understood. The proposed mechanisms have been reviewed by Monchois et al. (1999) and Monsan (2001). Currently there are two proposed mechanisms for dextran synthesis. Robyt et al. (1974) evidenced a highly processive mechanism that

involves two active sites. The synthesis occurs by addition of glucosyl residues to the reducing end of a dextranyl chain that is covalently linked to the dextransucrase (Robyt et al. 1974; Robyt et al. 2008). The synthesis occurs in a two-catalytic-site insertion mechanism that involves a set of three conserved amino acids (Asp551, Glu589 and Asp662) in a single active site. The mechanism suggests that the glucosyl units of sucrose and the growing dextranyl chains are covalently linked to Asp551 and Asp662. Glu589 donates a proton to the D-fructosyl group of sucrose and is in turn reprotonated by abstracting a proton from the C-6 hydroxyl group of the covalently linked D-glucosyl residue. The deprotonated glucosyl residue then launches a nucleophilic attack on the reducing end C-1 of the covalently linked dextranyl chains. The reaction continues until the dextranyl chain is transferred to water or an acceptor molecule, which terminates the polymerization process (Robyt et al. 2008).

In contrast, Moulis et al. (2006) concluded that the synthesis is a semi-processive mechanism, involves a single active site, and that the glucosyl residues are added to the non-reducing end of a growing dextranyl chain. The initial phase of the reaction involves formation of oligosaccharides using sucrose and glucose as acceptor molecules. The oligosaccharides formed, especially with glucose as an acceptor (isomaltooligosacharides, IMO), are then elongated to form high molar mass dextrans (HMM). Moulis et al. (2006) maintain that sucrose acceptor reaction products are minor, whereas fructose is used as an acceptor at later stages of the synthesis when its concentration has increased (Moulis et al. 2006). Recently, studies on a 117 kDa crystal structure of a glucansucrase fragment (GTF180-ΔN) from *Lb. reuteri* 180 have supported this non-reducing end growth mechanism (Vujicic-Zagar et al. 2010). The crystal structure confirmed that there was only one active site with no space for another covalently bound glucosyl residue or dextranyl chain (Vujicic-Zagar et al. 2010), which contradicts the mechanism proposed by Robyt et al. (2008). The native glucansucrase from this strain produces a dextran with 69% α-(1→6) and 31% α-(1→3) linkages (van Leeuwen et al. 2008a).

The above studies agree that, besides HMM dextran synthesis, the dextransucrases catalyze transfer of D-glucosyl residues from sucrose to the non-reducing end of mono- and oligosaccharide acceptors, such as glucose, fructose, maltose, isomaltose and sucrose, to form a series of oligosaccharide products. The disagreement, which still needs clarification, is whether the formation of HMM dextrans occurs by non-reducing or reducing end growth. Robyt et al. (1976) have further proposed that the acceptor reaction mechanism of the dextransucrase is also responsible for the formation of single unit branches in dextrans and the formation of elongated branches by transfer of dextranyl chains to acceptor dextran chains. Vujicic-Zagar et al. (2010) showed that maltose is held by GTF180-ΔN with its O6 pointing towards the catalytic site for the addition of α-

(1→6)-linked glucosyl residues. When isomaltotriose was the acceptor, it was held in a different mode, whereby its O3 hydroxyl group was oriented towards the active site. The latter binding mode was therefore proposed to be responsible for the formation of α-(1→3)-linked branches.

While the formation of α-(1→3) branch linkages in dextrans from *L. mesenteroides* NRRL B-512F (Table 1) are formed at the same active site as the chain-extending α-(1→6) linkages (Robyt and Taniguchi 1976), the formation of α-(1→2) branch linkages occurs at a different active site. Fabre et al. (2005) showed that the dextransucrase of *L. mesenteroides* NRRL B-1299 (Table 1) has two catalytic domains: CD1 and CD2. CD1 is primarily responsible for α-(1→6)-D-glucopyranosyl linkages whereas CD2 synthesizes α-(1→2) branch linkages (Fabre et al. 2005). Dextrans can also be produced from maltodextrins by some *Gluconobacter* strains, which usually leads to the formation of α-(1→4)-branched dextrans (Naessens et al. 2005).

2.2.3 Dextran-hydrolyzing enzymes

Several dextran-hydrolyzing enzymes with different specificities and modes of action are produced by bacteria, fungi and yeast. The enzymes have been utilized for various purposes such as enzyme-assisted structure elucidation and to partially hydrolyze dextrans for clinical purposes. The enzymes known to date are classified as endo-dextranases (EC 3.2.1.11), glucan-1,6-α-D-glucosidases (EC 3.2.1.70), glucan-1,6-α-isomaltosidases (EC 3.2.1.94), dextran-1,6-α-D-isomaltotriosidases (EC 3.2.1.95), and branched–dextran exo-1,2-α-glucosidase (EC 3.2.1.115) (Khalikova et al. 2005). As reviewed by Khalikova et al. (2005), extracellular endo-dextranases from fungi are common and usually show a higher enzyme activity when compared to dextranases from bacteria and yeast. The most commonly studied fungal endo-dextranases are from the *Penicillium* species (Khalikova et al. 2005). The fungal dextranases hydrolyze polymeric dextran to glucose, isomaltose, isomaltotriose and larger isomaltooligosaccharides, some of which may contain non-α-(1→6) linkages and are therefore resistant to further hydrolysis (Taylor et al. 1985). The endo-dextranases also hydrolyze isomaltooligosaccharides from the reducing end to release glucose. Hydrolysis of isomaltose is slow and may occur by initial condensation to isomaltotetraose then by hydrolysis to glucose and isomaltotriose (Khalikova et al. 2005).

Glucan-1,6-α-D-glucosidases are exodextranases that release the reducing end glucosyl unit in a stepwise fashion from polymeric dextran and isomaltooligosaccharides. Glucan-1,6-α-isomaltosidase (isomaltodextranase) and dextran 1,6-α-isomaltotriosidase (isomaltotriodextranase) are exodextranases that release isomaltose and isomaltotriose

from the non-reducing end of dextrans and isomaltooligosaccharides. *A. globiformis* T6 isomaltodextranase is unique since it is also capable of hydrolyzing α-(1→2, 3, and 4) linkages to release isomaltose. A debranching exodextranase (branched–dextran exo-1,2-α-glucosidase) that specifically releases α-(1→2)-linked glucosyl branches has been isolated from the *Flavobacterium* sp. strain M-73 (Khalikova et al. 2005).

2.3 Structural analysis of dextrans

A full description of the structural features of polysaccharides includes specification of the monosaccharide composition, anomeric configuration, ring conformation, sequence, linkages and molar mass (section 2.4). This usually requires an array of methods as shown in Figure 3.

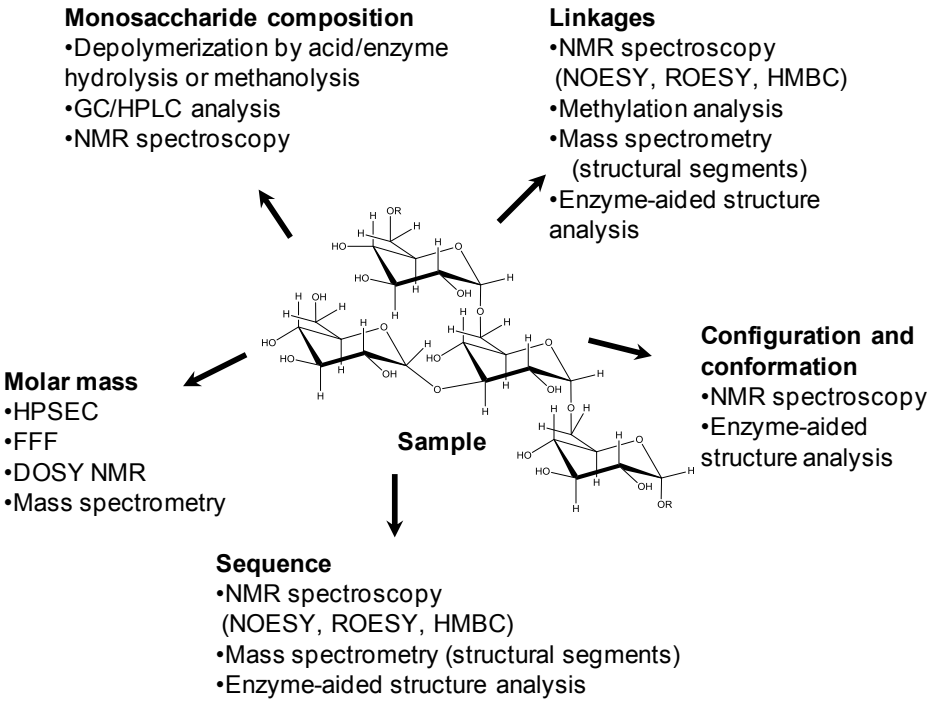

Figure 3. Methods used to determine the structural features of polysaccharides.

Structural analysis of dextrans has been performed with chemical methods such as peroxidate oxidation and methylation analysis (Jeanes et al. 1954; Slodki et al. 1986), enzyme-aided structural analysis (Mitsuishi et al. 1984), 1D ^{1}H and ^{13}C NMR spectroscopy (Seymour et al. 1976; Seymour et al. 1979b; Cheetham et al. 1990), and with two-dimensional (2D) NMR spectroscopy (Duenas-Chasco et al. 1998). In the following sub-sections the most commonly used methods, methylation analysis and NMR

spectroscopy, are reviewed. The potential of mass spectroscopy (MS) in studying the structures of dextrans is also discussed.

2.3.1 Methylation analysis

The principle of methylation analysis is first to label the free hydroxyl groups with an ether-linked methyl group. The permethylated sample is then hydrolyzed to free the hydroxyl groups involved in glycosidic linkages. The partially methylated monosaccharides are then derivatized into volatile molecules, in most cases by reduction and acetylation, for gas chromatography MS (GC-MS) analysis (Ciucanu and Kerek, 1984). The methylation analysis products are identified according to their retention time and MS fragmentation patterns, and their intensities are used to approximate the relative amount of different linkages, branch-point residues and terminal residues (Mulloy et al. 2008). However, quantification of methylation products should be handled with caution because incomplete permethylation of the sample under the reaction conditions used leads to erroneous results. Seymour et al. (1979a) showed that under-methylation selectively occurs at 3-hydroxyl groups in dextrans when using the Hakomori methylation procedure (Hakomori 1964), resulting in over-estimation of 3-*O*-monosubstituted glucosyl residues. Thus for dextrans, repeating the first permethylation procedure two or three times is recommended to ensure reliable results (Seymour et al. 1979a). Figure 4 shows a schematic structure containing the possible linkages in dextrans and Table 2 summarizes the methylation analysis products obtained from the residues. Although the linkages can be identified by methylation analysis, it does not provide information on the sequence of the linkages. For example, methylation analysis (Table 2) does not distinguish whether the 2, 3, or 4–*O*-monosubstituted residues are interruptions of the main chain (residue C, Figure 4) or branches extended via α-(1→2, 3, or 4)-linked glucosyl residues (residues E).

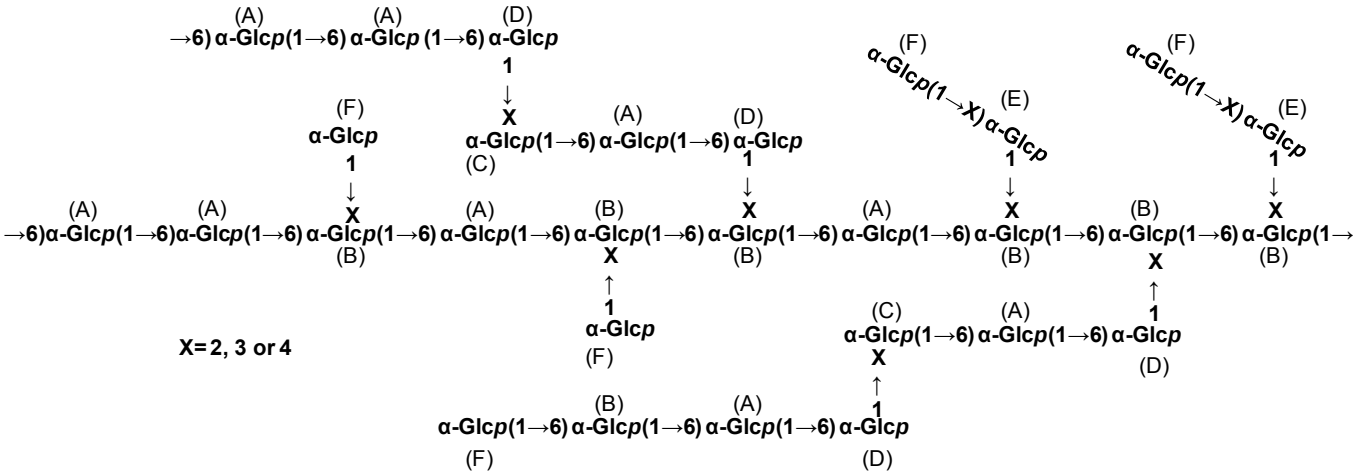

Figure 4. Schematic structure showing all glucopyranosyl residues in different chemical environments (A-F, Table 2). In addition to main chain α-(1→6)-linked residues, dextrans contain glucopyranosyl residues that are α-(1→x)-linked (where x=2, 3 or 4) occurring as internal monosubstituted residues or elongated branches (D and E) and as single unit terminal residues (F).

Table 2. Anomeric proton signals (ppm) and methylation analysis products of glucopyranosyl residues in different chemical environments, in the schematic dextran shown in Figure 4.

Residue	Description	Structure	Methylation products[a]	δ ^{1}H (ppm)[b]	Reference to NMR data
A	Main chain residues	→6)-α-D-Glc*p*-(1→6)-	2,3,4	4.96 - 4.99	Bounaix et al. 2009, van Leeuven et al. 2008a
B	Disubstituted residues	→2,6)-α-D-Glc*p*-(1→6)-	3,4	5.17 - 5.18	Duenas-Chasco et al. 1998
		→3,6)-α-D-Glc*p*-(1→6)-	2,4	4.97 - 4.98	van Leeuven et al. 2008d
		→4,6)-α-D-Glc*p*-(1→6)-	2,3		
C	Main chain interrupting residues with α-(1→2, 3 or 4) linkages	→2)-α-D-Glc*p*-(1→6)-	3,4,6		
		→3)-α-D-Glc*p*-(1→6)-	2,4,6	4.96 - 4.99	van Leeuven et al. 2008a
		→4)-α-D-Glc*p*-(1→6)-	2,3,6	4.96 - 4.97	van Leeuven et al. 2008b
D	α-(1→2, 3 or 4)-linked residues elongated with α-(1→6)-linked residues	→6)-α-D-Glc*p*-(1→2)-	2,3,4		
		→6)-α-D-Glc*p*-(1→3)-	2,3,4	5.32 - 5.35	van Leeuven et al. 2008a
		→6)-α-D-Glc*p*-(1→4)-	2,3,4	5.38 - 5.40	van Leeuven et al. 2008b
E	α- (1→2, 3 or 4) elongated branches	→2)-α-D-Glc*p*-(1→2)-	3,4,6		
		→3)-α-D-Glc*p*-(1→3)-	2,4,6	5.37 - 5.39	van Leeuven et al. 2008c
		→4)-α-D-Glc*p*-(1→4)-	2,3,6	5.39 - 5.40	van Leeuven et al. 2008c
F	Terminal residues	α-D-Glc*p*-(1→2)-	2,3,4,6	5.10 - 5.11	Duenas-Chasco et al. 1998
		α-D-Glc*p*-(1→3)-		5.35 - 5.36	van Leeuven et al. 2008c
		α-D-Glc*p*-(1→4)-		5.39 - 5.40	van Leeuven et al. 2008c
		α-D-Glc*p*-(1→6)-		4.96 - 4.97	van Leeuven et al. 2008c

[a] -*O*-methyl-glucosides, [b]Chemical shifts are average values from literature data.

2.3.2 NMR spectroscopy

NMR spectroscopy provides sufficient information to determine all the structural features of polysaccharides (Figure 3). The studies of Seymour et al. (1976-1980) can be credited for systematically laying the foundation for evaluating the NMR spectra of dextrans. Their general approach to dextran NMR spectra analysis can be summarized as follows:

1. The spectra of native dextrans are composite spectra of individual glucopyranosyl residues in different chemical environments (Figure 4). Note that each underivatized glucopyranosyl residue has seven proton signals (H-1—H-6a & 6b, Figure 5) and six carbon signals (C-1—C-6).
2. The anomeric region of native dextrans contains three types of resonance: the resonance of main chain residues and two minor resonances of equal intensity representing the branch point and the terminal residues.
3. The relative intensity of the anomeric resonances is proportional to the amount of that residue in the native polymer.
4. The more informative signals are from protons and carbons in the vicinity of the glycoside bond.
5. The total number of branch points equals the total number of terminal residues.
6. A neighboring group effect (e.g. for residues before and after a branch-point residue) may cause broadening or splitting of the affected residue.

The ^{1}H spectra of dextrans can be divided into two main regions: the anomeric region (4.4-5.5 ppm) and the bulk proton region (3-4.2 ppm) (Duus et al. 2000). The ^{13}C spectra have four regions: a) the anomeric region (97-103 ppm), b) the 70-75 ppm region associated with unbound C-2—C-5, c) the region between 60-70 ppm for bound and unbound C-6, and d) the 75-85 ppm region where bound C-2—C-5 are found (Seymour et al. 1976). Thus, comparing regions b and d, glycoside bond formation causes a downfield displacement of about 10 ppm for the carbon involved. The effect of glycoside bonds on ^{1}H chemical shifts of each proton in α-glucans (H-1—H-6a & 6b) has been demonstrated in a comprehensive study by van Leeuwen et al. (2008c).

The chemical shifts for individual glucopyranosyl residues can be assigned with 2D spectra that can include: double-quantum filtered correlation spectroscopy (DQF-COSY), total correlation spectroscopy (TOCSY), heteronuclear single-quantum correlation spectroscopy (HSQC), heteronuclear two-bond correlation spectroscopy (H2BC, Nyberg et al. 2005), and heteronuclear multibond connectivity (HMBC) spectra. 1D TOCSY or traces of each glucopyranosyl residue taken from 2D TOCSY spectra are particularly

useful for chemical shift assignment by evaluating the multiplicity of the signals from each residue. For glucopyranosyl residues, the anomeric protons appear as doublets (d) with a small coupling constant ($^3J_{H1,\ H2}$ ~3-4 Hz) for the α form (equatorial-axial configuration) and a large coupling constant (~7-8 Hz) for the β form (axial-axial configuration). H-2 in the α form appears as a typical doublet of doublets (dd) due to a small coupling to H-1 (axial-equatorial configuration) and a large coupling to H-3 (axial-axial configuration). In the β form, the H-2 appears as overlapping doublets (dd), due to the large coupling constants to both H-1 and H-3 (axial-axial configuration). H-3 and H-4 (both α and β forms) also appear as overlapping doublets (dd) due to large coupling constants (axial-axial configuration). H-5, H-6 a&b for both forms have a more complex pattern as they are coupled to more protons (Roslund et al. 2008). Figure 5 shows the multiplicity and assignment of the proton signals of the main chain α-(1→6)-linked glucopyranosyl residues in a typical dextran with a few α-(1→3) branches.

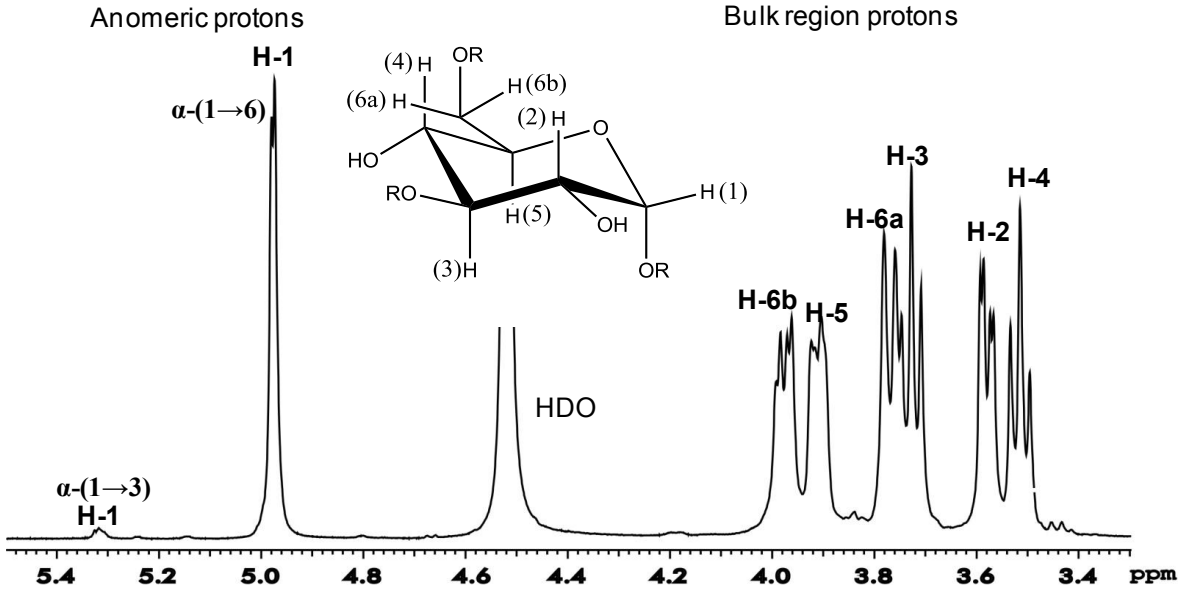

Figure 5. Typical spectra of a dextran with a few α-(1→3) branches. The protons from the main chain α-(1→6) residues are assigned. HDO=residual water (Maina unpublished results).

Determining the fine structural features from the NMR spectroscopy data of native dextrans is challenging because of the overlapping chemical shifts of glucopyranosyl residues in different environments (Table 2). For example, even though three anomeric resonances are expected in α-(1→3)-branched dextrans, the chemical shift of the 3,6-*O*-disubstituted branch point residue is not observed since it overlaps that of main chain α-(1→6)-linked residues. Furthermore, differentiating single unit and elongated α-(1→3) branches from the spectra of native dextrans is difficult as their anomeric signals cluster between 5.32 and 5.35 ppm (Table 2). Especially when the branch linkages are few, these

residues are best determined from the data of structural segments that can be produced by partial acid hydrolysis, Smith degradation or enzyme hydrolysis (Sidebotham 1974; Taylor et al. 1985; van Leeuwen et al. 2008a). An examination of 1D ^{1}H spectra of dextrans with only single unit branches and those containing α-(1→3) branches elongated with α-(1→3)- or α-(1→6)-linked glucopyranosyl residues can be found in the study by Cheetham et al. (1990). Table 2 summarizes the anomeric proton chemical shifts for some of the possible glucosyl residues in dextrans.

2.3.3 Potential of mass spectrometry

Mass spectrometry (MS) has become an important tool for determining the structures of carbohydrates, especially protein-linked glycans. Nonetheless, it is still underutilized in the structural analysis of dextrans. MS cannot be used to study the structure of intact high molar mass (HMM) dextrans, but can be highly resourceful in the study of structural segments (glucooligosaccharides, GOS) derived from partial hydrolysis of native dextrans or in evaluating acceptor reaction products of glucansucrases. MS has successfully been used to study gluco-disaccharides (Garozzo et al. 1990; Spengler et al. 1990; Hofmeister et al. 1991; Zhang et al. 2008) and GOS with one type of glycosidic linkage, α/β-(1→4) or α-(1→6), or both α-(1→4) and α-(1→6) linkages (Pasanen et al. 2007; Usui et al. 2009; Yamagaki and Sato 2009; Čmelík and Chmelík 2010).

Currently, the two main ionization techniques for MS analysis of carbohydrates are matrix-assisted laser desorption/ionization (MALDI) and electrospray ionization (ESI). The principles of these techniques and the application of MS in the structural analysis of oligosaccharides are reviewed by Zaia (2004). Combining liquid chromatography and MS detection with online electrospray ionization (ESI) or off-line matrix-assisted laser desorption/ionization (MALDI) is nowadays a routine procedure in analytical chemistry. In particular, developments in hydrophilic interaction liquid chromatography (HILIC) have significantly simplified online ESI-MS detection of oligosaccharides due to the utilization of MS-compatible eluents (Wuhrer et al. 2009). Thus, HILIC-ESI-MS is a powerful and prospective tool for LC-MS analysis of GOS mixtures.

Carbohydrates can be ionized in positive mode as proton adducts or as metal adducts (sodium or lithium adducts), and in negative mode as deprotonated ions or with an anion (e.g. a chloride ion) adduct. MS-based structural analysis of oligosaccharides relies on evaluation of structure diagnostic fragment ions in the tandem MS (MS/MS) spectra. The MS spectra of oligosaccharides contain two types of fragments: glycosidic cleavage and

cross-ring cleavage that are usually named according to the formal nomenclature (Figure 6) proposed by Domon and Costello (1988). The cross-ring cleavages (A-type fragment ions) of the reducing end residue are the most informative because they depend on the glycoside bond. The mechanisms for formation of these cross-ring cleavages have been demonstrated in various studies (Domon and Costello 1988; Spengler et al. 1990; Hofmeister et al. 1991).

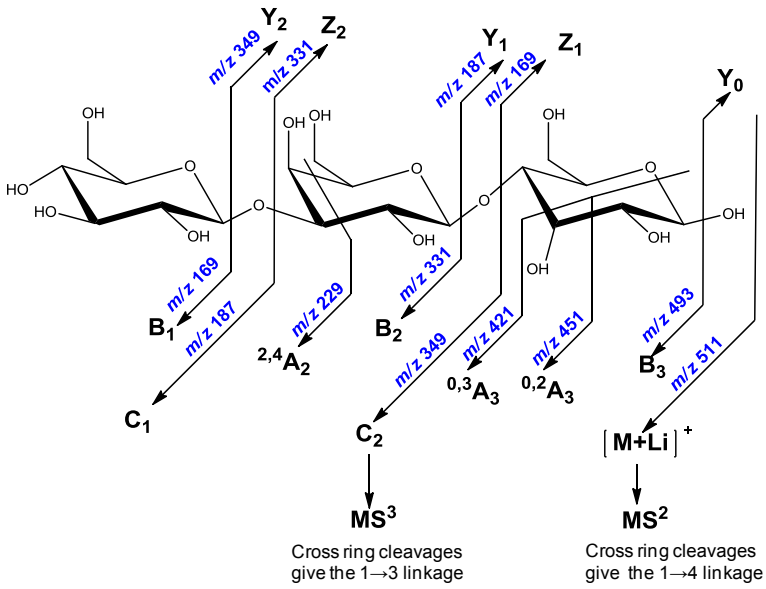

Figure 6. Schematic representation of a trisaccharide illustrating the nomenclature of fragment ions according to Domon and Costello (1988). The *m/z* values of lithium adduct ions and the ions isolated for MS^2 and MS^3 analysis to determine the (1→4) and (1→3) linkages, respectively, are shown.

In MS/MS analysis, sodium or lithium adduct ions in positive mode and negative mode ions yield the cross-ring cleavages required for structure analysis. Protonated ions fragment via glycoside bond cleavage only and therefore do not provide linkage information. The glycosidic cleavages, however, provide information concerning the sequence and size of the monosaccharide building blocks (Geyer and Geyer 2006). Therefore in each MS/MS cycle the diagnostic cross-ring cleavages, originating from the reducing end unit in the isolated product ion (Figure 6), are used to establish the glycosidic linkage (Garozzo et al. 1990; König and Leary 1998; Chai et al. 2001). Since MS does not distinguish isomeric monosaccharide building blocks, the presence of native substituents, such as N-acetyl, O-acetyl, methyl or carboxylic groups in oligosaccharides is usually advantageous in MS/MS. The additional mass of the substituents not only reveals the sequence of the monosaccharide units, but also assists in distinguishing fragment ions that would otherwise be isomeric. Thus, MS/MS analysis of GOS is not straightforward, especially for large and branched GOS that usually lack such groups.

2.4 Physicochemical properties of dextrans

The macromolecular properties of dextrans (weight average molecular weight (M_w), number average molecular weight (M_n), radius of gyration (R_g), hydrodynamic radius (R_h), intrinsic viscosity [η], and the second viral coefficient) have been studied by various groups (Senti et al. 1955; Nordmeier 1993; Wu, 1993; Ioan et al. 2000). The rheological properties have also been determined in several studies (Sabatié et al. 1988; Tirtaatmadja et al. 2001; Padmanabhan et al. 2003). Native dextrans have a broad molar mass distribution and have a typical M_w between 10^6—10^9 g/mol (Leathers 2002; Burchard 2005).

A general consensus among researchers is that the presence of long branches in dextran contributes significantly to their macromolecular and rheological properties, even if they are few (<5%) (Bovey, 1959; De Belder 1993; Ioan et al. 2000; Tirtaatmadja et al. 2001). In fact, Burchard (2005) notes that as molar mass increases, the hydrodynamic properties of dextrans approach that of compact hard spheres due to an increase in branching density. The molar mass dependence on R_g is shown in Equation [1]

$$R_g = KM_W^{\nu} \qquad [1]$$

where K is a constant and the exponent ν is 0.33 for a hard sphere, 0.5 for a random coil in a theta solvent, 0.588 for a random coil in a good solvent and 1 for a rigid rod (Burchard 1999). Typical ν values for dextran solution have been found to vary from 0.43-0.64 for HMM dextrans, indicating a random coil conformation. The lower ν values were for dextrans with more α-(1→3) branches that had a denser conformation (Irague et al. 2012).

Similarly, the non-linear Kuhn-Mark-Houwink relationship between [η] and M_w of dextrans arises from an increase in the size and density of branches at HMM (De Belder 1993; Tirtaatmadja et al. 2001). The molar mass dependence on [η] is shown in Equation [2]

$$[\eta] = KM_w^{\alpha} \qquad [2]$$

where K is a constant, and the exponent α, reported in the literature, is between 0.43 and 0.6 for dextrans with a M_w between 2000 and 10^5 g/mol and as low as 0.18 for highly branched dextrans (70 and 57% α-(1→6) linkages) (Tirtaatmadja et al. 2001).

Varying rheological properties have been reported for different dextran preparations. Tirtaatmadja et al. (2001) found that dextrans with M_w as high as 2.0×10^6 g/mol show

Newtonian viscosity behavior even at concentrations of 30% w/v and have a high critical overlap concentration (c^*) (Tirtaatmadja et al. 2001). The high c^* (concentration at which dextran solutions transition from dilute to semi-dilute) indicates a compact structure and low [η]. Xu et al. (2009), however, found non-Newtonian behavior of a 5.2×10^5 g/mol dextran at a concentration of 30% w/v. Recently, Irague et al. (2012) found that HMM dextran preparations that ranged from $0.76 \times 10^8 – 6.02 \times 10^8$ g/mol at 5% (w/v) displayed non-Newtonian shear thinning behavior. These conflicting results can be understood by considering the structural heterogeneity of dextran samples. At a specific concentration, while a dextran sample with long branches exhibits Newtonian viscosity behavior due to a compact structure, a dextran with the same molar mass but having single unit branches is less compact and thus shows non-Newtonian viscosity behavior at that concentration (Xu et al. 2009).

2.4.1 Characterization of the macromolecular and rheological properties of dextrans

The structure-function relationship of polysaccharides is deduced from understanding their structural, macromolecular and rheological properties (Figure 7). For dextrans, obtaining accurate data on these properties is not a straightforward task and can therefore lead to erroneous or inconsistent conclusions. Challenges in determining the structural properties of dextran have already been addressed.

When determining the macromolecular and rheological properties of dextrans, a key challenge is the solubility of native HMM dextrans and the presence of aggregates in the solutions analyzed. Both water-soluble and insoluble dextrans have been isolated from a single strain and it has been proposed that the flexible α-(1→6) linkages in dextrans cause high water solubility while an increase in α-(1→3) linkages results in lower solubility (Naessens et al. 2005; Watanabe et al. 1980). However, solubility may also be reduced by lyophilization of the isolated sample. Dextrans are also soluble in organic solvents, such as dimethyl-sulfoxide (DMSO), N,N-dimethylacetamide (DMA) and formamide (Heinze et al. 2006). Organic solvents, such as DMSO, are commonly used in the analysis of other α-glucans such as starch, due to their non-aggregative nature and better solubilization properties. DMSO solutions still require some salt (e.g. LiCl) to aid dissolution and to prevent aggregation due to hydrogen bonding (Schmitz et al. 2009).

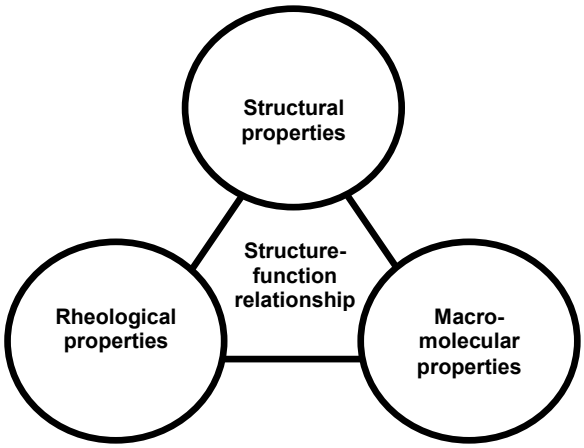

Figure 7. Properties required when determining the structure-function relationship of polysaccharides.

Another key challenge is the multi-dimensional distribution of native dextrans. Like other complex branched polysaccharides (polysaccharides with an irregular branching structure) such as amylopectin, dextrans not only have a molar mass distribution, but may also have a distribution in the density and length of branch chains (Figure 8) (Gidley et al. 2010; Vilaplana and Gilbert 2010). Thus, when dextrans are separated according to their hydrodynamic volume (V_h) (e.g. in high performance size exclusion chromatography, HPSEC), each V_h can represent a heterogeneous group of dextran molecules with different M_w that vary in length and branch density. This effect in HPSEC analysis has been referred to as ―imperfect resolution", ―structural polydispersity" or ―local polydispersity" (Vilaplana and Gilbert 2010).

The methods used to study the solution properties of dextrans include light scattering (LS) (Senti et al. 1955; Nordmeier 1993; Wu 1993), analytical ultracentrifugation (Setford 1999), HPSEC, and asymmetric flow field-flow fractionation (AsFlFFF) (Wittgren and Wahlund 1997; Ioan et al. 2000). After separation by e.g. HPSEC, the macromolecular properties of dextrans are usually determined with a combination of concentration-sensitive (differential refractometer) and molecular-weight-sensitive detectors (LS and/or viscometer detectors) (Mourey 2004). In HPSEC analysis of dextrans, Ioan et al. (2000) found that large molecules may drag through the column and co-elute with low molar mass (LMM) molecules. Since the large molecules dominate the LS signal, the accurate macromolecular parameters for the LMM fractions cannot be determined. Studies also show that HMM polysaccharides such as dextrans can degrade during HPSEC separation due to shearing (Cave et al. 2009; Striegel et al. 2009). Thus alternative methods, such as hydrodynamic chromatography and column-free field-flow fractionation, may be a better option (Gaborieau and Castignolles 2011).

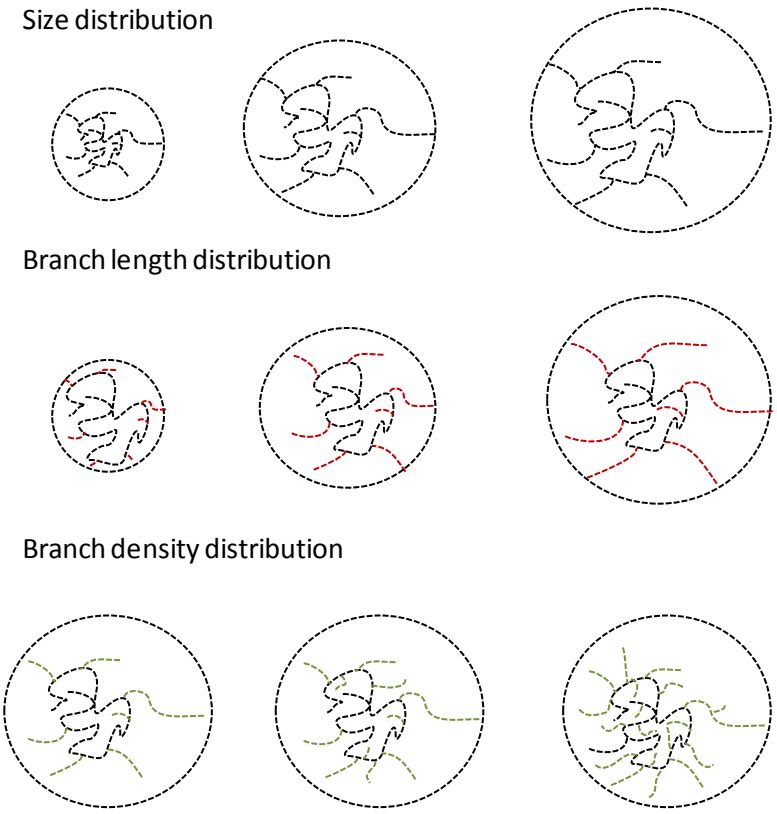

Figure 8. Schematic representation of the three distribution dimensions (size, branch length and branch density) of native dextrans

2.4.1 Diffusion-ordered NMR spectroscopy (DOSY)

NMR spectroscopy can also be used to determine the molar mass and R_h of dextrans by using the DOSY experiment. DOSY has been proposed as a versatile tool for estimating the molar mass and R_h of uncharged polysaccharides (Viel et al. 2003). As Nilsson (2009) points out, the term DOSY refers to a method for processing and displaying pulse field gradient (PFG) diffusion NMR data that results in a 2D plot with chemical shifts in one dimension and self-diffusion coefficients (D, m^2s^{-1}) in the other. The key features of a DOSY experiment shown in Figure 9 are briefly described here. A thorough evaluation of the DOSY experiment is provided in the review by Johnson (1999).

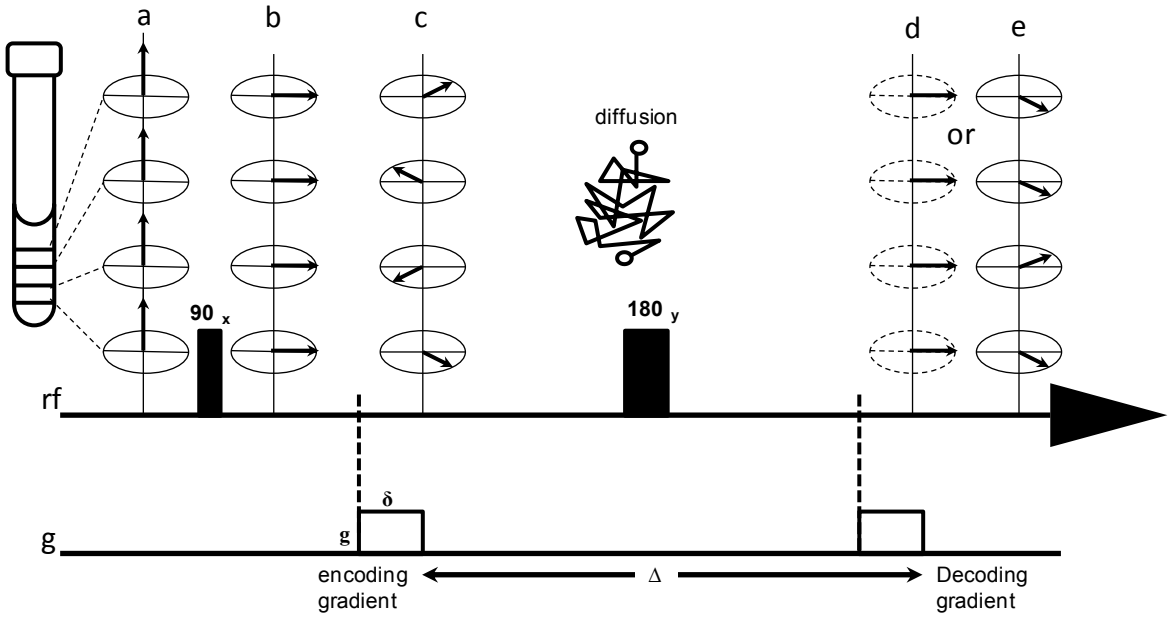

Figure 9. Schematic representation of the main components of a basic DOSY experiment. The NMR sample tube is divided into four slices and the effect of the pulse sequence on the spins at each stage of the experiment is shown in a,b,c and d/e. rf is the radio frequency pulse and *g* is the gradient pulse along the *z*-axis.

In a basic DOSY experiment (Figure 9), a 90° pulse is first applied to place the net magnetization in the *xy* plane and the phase of the spins is coherent (Figure 9b). A field gradient pulse is then applied along the *z*-axis. During this gradient pulse, a spatially varying magnetic field is created along the *z*-axis (in this example), which causes a variation of Larmor frequencies along this axis (Figure 9c). This is the encoding gradient as it labels the position of the spins (spins at a specific position along the *z*-axis will acquire a specific phase angle during the gradient pulse due to spatially different Larmor frequencies). The system is then allowed to evolve for a specific period Δ, during which a 180° pulse is specifically applied at Δ/2. During Δ, the diffusion will alter the spatial location of spins along the *z*-axis depending on their *D*. This period is therefore called the diffusion time. Diffusion along the *x*- and *y*-axes also occurs but can be ignored in this example, because the diffusion encoding and decoding gradients are applied along the *z*-axis. At the end of the period, a decoding gradient pulse is applied to refocus the spins. If diffusion does not occur during Δ, the spins are perfectly refocused and the maximum signal is obtained during acquisition (Figure 9d). However, if diffusion occurs during Δ, the refocusing is not perfect and the signal obtained during acquisition is diminished compared to the maximum signal (Figure 9e). Equation [3] defines the signal attenuation due to diffusion for this pulse sequence:

$$I=I_0\exp[-D\gamma^2g^2\delta^2(\Delta-\delta/3)-R] \quad [3]$$

where I is the intensity of the signal, I_0 is the equilibrium magnetization intensity, D is the self-diffusion coefficients (m^2s^{-1}), γ is the gyromagnetic ratio of the spins (rad $T^{-1}s^{-1}$), g is the gradient pulse (T m^{-1}) along a particular axis (z-axis in Figure 9), δ is the duration of the gradient pulse (s), Δ is the diffusion time, and R is a constant that takes nuclear relaxation into account (Antalek, 2002). Most DOSY experiments are carried out by varying the strength of the gradient pulse g in a number of steps to ensure that the sample signals decay by at least 95% of the maximum signal (Figure 10). δ or Δ can also be varied in DOSY experiments. Artifacts in DOSY spectra can arise from eddy currents, gradient field non-uniformity and convection currents. Several pulse sequence modifications and measurement setups to minimize their effects have been proposed as reviewed by Antalek (2002). The effects of gradient field non-uniformity and signal attenuation due to convection currents can also be reduced by restricting the sample volume to the section of the probe with the most uniform gradient field and efficient temperature control (Antalek 2002).

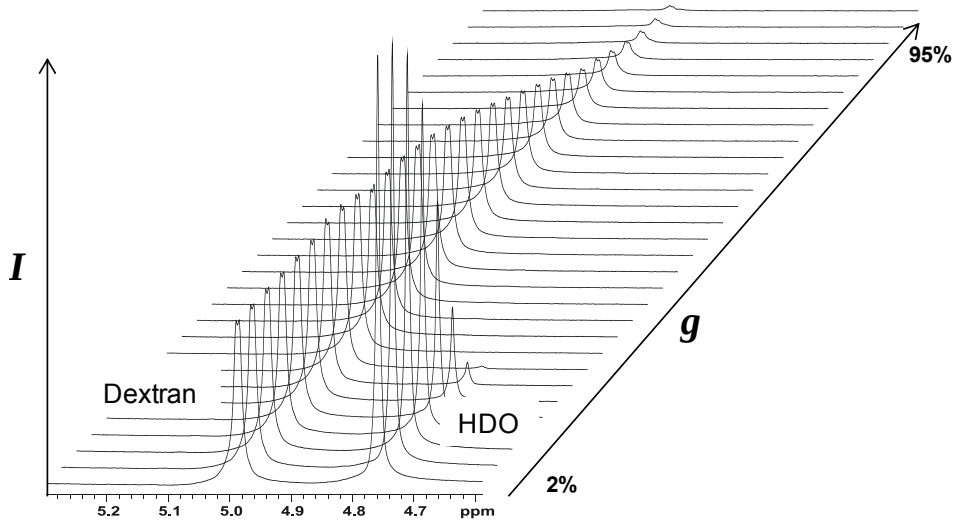

Figure 10. ^{1}H spectra of a dextran sample recorded with increasing gradient strengths. The anomeric signal of the main chain α-(1→6)-linked glucosyl residues in dextrans and residual water signal (HDO) are shown. The HDO signal decays faster than the signal from dextran because it diffuses faster, *i.e.* has a larger self-diffusion coefficient. The spectra were recorded at 600 MHz at 300K in D_2O. The strength of the gradient pulse (g) was varied from 2-95% of the maximum value in 30 steps. I is the intensity of the signals (Maina unpublished results).

By calibrating the diffusion dimension with structurally similar standards, DOSY can be used to determine the M_w of polymers (Chen et al. 1995; Politi et al. 2006; Barrère et al. 2009) according to equation [4]:

$$D=KM_W^{\alpha} \quad [4]$$

where K and α are scaling parameters that depend on the molecular architecture of the polymer, the viscosity of the solvent, and the temperature (Barrère et al. 2009). D is related to R_h by the Stokes-Einstein Equation [5]:

$$D=kT/6\pi\eta R_h \quad [5]$$

where k (J K^{-1}) is the Boltzmann constant, T is the temperature (K), and η (P) is the solvent viscosity. DOSY is advantageous since it is non-destructive and the same sample can be used for structural analysis. Furthermore, the experiment is carried out on a conventional NMR spectrometer and is therefore a suitable alternative where equipment such as HPSEC or AsFlFFF is not available.

2.5 Application of dextrans

Commercially produced dextran is used for various purposes in its native or chemically modified form. Native dextrans are used in clinical applications as blood-plasma substitutes. For this purpose, the optimum dextran should have low antigenicity, a molecular weight between 40 000 and 100 000 g/mol, and a high number of α-(1→6) linkages (Robyt 1986; Naessens et al. 2005). Dextran from *L. mesenteroides* B-512F has been widely used in this application since it is mainly composed of α-(1→6) linkages (95%). Native dextrans of different molecular weights serve as standards for size exclusion chromatography and as ingredients in cosmetics, bakery, and frozen dairy products (Heinze et al. 2006). The production of functional polymers by chemical modification of dextrans has been reviewed (Heinze et al. 2006). Dextran derivatives include cross-linked dextrans used in the production of Sephadex columns and bioactive dextran derivatives such as dextran sulfates and phosphates (Heinze et al. 2006). Currently, interest in dextran-producing strains and their respective dextransucrases for the production of prebiotic GOS is growing (Remaud-Simeon et al. 2000; Chung and Day 2002).

2.6 Potential of dextrans in sourdough bread

According to Waldherr and Vogel (2009), the functionality of dextrans and other hydrocolloids in dough and bread is related to two factors: the alteration of the dough‘s water-binding capacity and the interaction of hydrocolloids with dough components such

as gluten and starch. The increase in dough yield due to the water-binding capacity of HMM dextrans improves the freshness of the bread produced (Vandamme et al. 1997, Lacaze et al. 2007). By interacting with the dough gluten network, dextrans improve dough stability and gas retention. Dextrans also improve other dough parameters such as development time, consistency, strength and elasticity (Waldherr and Vogel 2009). Improvement of dough parameters is reflected in the final bread product as better bread volume, texture, mouth feel and crumb structure. By addition of 1-3% DW dextran in bread dough, Bohn (1961) reported 20% greater bread volume than in a control with no dextran. Lacaze et al. (2007) reported a 12% bread volume improvement in rye mixed bread containing dextran. Dextrans at a level of 5 g/kg have been shown to improve the viscoelastic properties of dough and the volume of the final breads more effectively than the same level of added fructans or reuterans (Tieking and Gänzle 2005). The effect of dextrans in sourdough bread seems to be affected by the molar mass and degree of branching of the dextrans utilized. Vandamme et al. (1997) and Lacaze et al. (2007) maintain that HMM linear dextrans are more efficient in improving bread volume than HMM highly branched dextrans.

Dextrans can be added to the bread recipe in two ways, *ex situ* as purified additives or by *in situ* production during sourdough fermentation. *In situ* production, which entails the addition of sucrose (commonly 10-15% DW) to the sourdough recipe, is more favorable since other metabolites produced during fermentation can improve the flavor, shelf life (antistaling and antimicrobial agents) and nutritional properties of the bread (Table 3) (Katina 2005). Although moderate acidification during fermentation has a positive effect on flavor, it has been shown that very intensive acidification can counterbalance the benefits of EPS produced *in situ* (Kaditzky et al. 2008). As reviewed by Arendt et al. (2007), acids increase the solubility of proteins and enhance the unfolding of gluten proteins, which subsequently leads to disentanglement and weakening of the gluten network.

Thus, successful utilization of sourdough entails optimization of both EPS production and other biochemical processes that take place during fermentation. Kaditzky and Vogel (2008) showed that more dextran was produced by *Lactobacillus reuteri* TMW 1.106 when the dough yield (DY) was high (DY 500 compared to DY 220), when the pH was regulated at the optimal pH for dextran synthesis, and when sucrose was replenished in a fed-batch fermentation. Dextran production was also fast and efficient when rye bran was added to the fermentation mixture (Kaditzky and Vogel 2008).

Table 3. Impact of the sourdough biochemical process on the final bread

Sourdough Biochemical process	**Final bread** (Improvements)
Acidification	Flavor, specific volume, texture
Production of volatile compounds	Flavor
Dietary fiber modification	Nutritional value
Proteolysis	Specific volume, flavor
EPS production (e.g. dextran)	Specific volume, texture, retardation of staling
Production of antimicrobial compounds	Shelf life

While the addition of dextran *ex situ* ensures consistency in the added amount for a positive impact on bread properties, an efficient method to ascertain the day-to-day reliability of *in situ* production is required. In most studies, dextrans in sourdough have been investigated by comparing the monosaccharide composition of water-extractable polysaccharides from sourdoughs with that of control samples that are, for example, fermented with strains that do not produce dextran (Korakli et al. 2001; Tieking et al. 2003; Di Cagno et al. 2006; Kaditzky and Vogel 2008). This method is unspecific and prone to error arising from the high glucose background from starch and maltooligosaccharides, as well as changes in the water-solubility of flour polysaccharides during sourdough fermentation. Furthermore, the water-solubility of dextrans varies depending on their structure, as discussed in section 2.4.1. Thus, a more efficient method is needed for evaluating the content of dextrans produced *in situ* during sourdough fermentation. An overview of the amount of HoPS produced by various strains during sourdough fermentation is provided in Table 4.

Table 4. Amount of HoPS produced *in situ* during sourdough fermentation

Strain	Sourdough	Sucrose g/kg DW	HOPS	HOPS g/kg DW	Yield %[e]	Reference
Lb. sanfranciscensis LTH2590	Wheat[a]	120	Fructan	2.0	3.3	Tieking et al. 2003
Lb. frumenti TMW 1.103	Wheat[b]	120	Fructan	0.3	0.5	
Lb. frumenti TMW 1.660	Wheat[b]	120	Fructan	1.0	1.7	
Lb. frumenti TMW 1.669	Wheat[b]	120	nd	0.7	1.2	
Lb. pontis TMW 1.675	Wheat[b]	120	nd	0.4	0.7	
Lb. reuteri TMW 1.106	Wheat[b]	120	nd	1.0	1.7	
W. *cibaria* WC4	Wheat[a]	160	Dextran	2.5	3.1	Di Cagno et al. 2006
Lb. sanfranciscensis LTH2590	Wheat[a]	100	Levan	5.2	10.4	Kaditzky et al. 2007
Lb. reuteri TMW 1.106	Wheat[b]	100	Glucan	6.2[d]	13.6	Kaditzky et al. 2008
W. *cibaria* 10M	Sorghum[c]	150	Dextran	0.6	0.8	Schwab et al. 2008
Lb. reuteri LTH5448	Sorghum[c]	150	Levan	1.6	2.1	
Lb. sanfranciscensis LTH2590	Wheat[a]	150	Levan	2.2	2.9	Galle et al. 2010
W. cibaria MG1	Sorghum[a]	150	Dextran	8.0	10.7	
	Wheat[a]	150		4.7	6.3	
W. kimchii F28	Sorghum[a]	150	Dextran	4.3	5.7	
	Wheat[a]	150		0.8	1.1	

Fermentation carried out at [a]30°C for 24h, [b]37°C for 24h, and [c]35°C for 24h, [d]calculated as anhydroglucose from the highest amount (~38 mmol glucose/kg flour) produced by the strain after 24h fermentation (dough yield 500) [e]Yield = the percentage of glucose or fructose in sucrose that is converted to HoPS. nd= not determined.

3 Aim of the study

This study is based on the hypothesis that LAB with GRAS approval can produce EPS *in situ* during sourdough fermentation, which have beneficial effects on dough rheology and on the properties of the final bread.

Based on this hypothesis, several questions can be asked:

A. What are the potential EPS producers for sourdough applications?
B. What are the structures of the EPS produced by the strains?
C. What are the physicochemical properties of the EPS?
D. How much EPS can a specific strain produce during the sourdough fermentation time?
E. What are the critical factors for efficient EPS production?
F. How are the structural and macromolecular properties of the EPS related to their functionality in sourdough applications?

This thesis mainly addresses questions B, C and D. The aim of the study was to determine the structural and macromolecular properties of dextrans produced by potential strains, and to develop a method for determining the amount of dextran produced *in situ* during sourdough fermentation. Initial experiments included five *Weissella* and four *L. citreum* strains, from which *W. confusa* E392 and *L. citreum* E497 were chosen for more elaborate studies.

The objectives of the study can be summarized as follows:

1. To determine the fine structure of the dextrans produced by *W. confusa* E392 and *L. citreum* E497, which have high potential for sourdough application (**I, II and III**).
2. To explore the prospects of MS in the analysis of structural segments produced from dextrans **(III**).
3. To develop a quick method for screening the structural features of dextrans produced by potential strains (**V**).
4. To determine the macromolecular properties of *W. confusa* E392 and *L. citreum* E497 dextrans (**IV**).
5. To develop a method for quantification of the amount of dextran produced *in situ* during sourdough fermentation (**V**).

4 Materials and Methods

This section gives a brief description of the materials and methods used to study the structure, macromolecular properties and *in situ* production of dextrans by strains with a potential application in sourdough. More details on the methods are presented in the original publications (**I-V**). A schematic summary of the methods used in relation to the objectives of this thesis (section 3) is shown in Figure 11. In the study, native dextrans were isolated for structure and macromolecular characterization. Dextran-hydrolysing enzymes were utilized to develop a method for profiling the structural variations in dextrans, to produce structural segments from the isolated dextrans and to estimate the amount of polymeric dextran and oligosaccharides produced during sourdough fermentation.

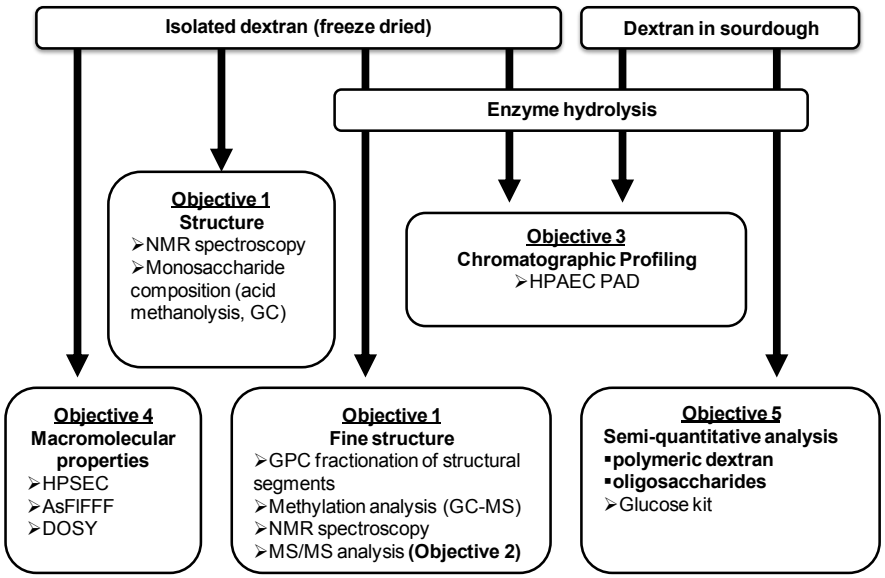

Figure 11. Schematic summary of the methods used in relation to the objectives of this study outlined in section 3.

4.1 Microbial strains and isolation of dextrans

Initial studies included several prospective LAB strains chosen on the basis of preliminary investigations at the Technical Research Center of Finland (VTT), where tens of strains originating from sourdoughs, cereals and vegetables were screened for dextran production efficiency. The screening was done by growing the strains on De Man, Rogosa and Sharpe agar (Oxoid, Bsingstoke, UK) supplemented with 2% (w/v) sucrose (MRS-S), and on culture media based on wheat flour with 2% sucrose (w/v) to mimic the sourdough environment. The strains were grown at 30°C for 2-7 days and the prospective LAB

selected based on their ability to form slimy cell cultures in both media. The selected strains for this study included five *Weissella* strains and four *L. citreum* strains (Table 5). Structurally different dextrans from *L. mesenteroides* NRRL B-512F (95% α-(1→6) and 5% α-(1→3) linkages, Larm et al. 1971) and *L. mesenteroides* NRRL B-1415 (86% α-(1→6) and 14% (α-(1→4) linkages, Abbott et al. 1966), and a reuteran from *Lb. reuteri* ATCC 55730 (81% α-(1→4) and 19% α-(1→6) linkages, Kralj et al. 2005), were included for method development and comparison.

Table 5. Microbial strains used in this study, their source and culture collection codes.

Strain[a]	Other culture collection codes	Source
Lb. reuteri ATCC 55730		
L. citreum VTT E-93504T	DSM 5577 ATCC 49730 NCDO 1837	Honey dew of rye ear
L. citreum VTT E-93497		Malting process
L. citreum VTT E-91082		Processed oat
L. citreum VTT E-90389		Split kernel of barley
L. mesenteroides NRRL B-512F	ATCC 10830A	Root beer
L. mesenteroides NRRL B-1415	VTT E-093126	
Weissella sp. VTT E-072748		Fermented bran
W. cibaria VTT E-072749		Fermented bran
Weissella sp. VTT E-072750		Fermented bran
Weissella sp. VTT E-083076		Fermented bran
W. confusa VTT E-90392	DSM20194 NCDO1975	Sour carrot mash

[a]In the text, strains from the VTT culture collections are abbreviated with the last three numbers and strains from the NRRL collection are abbreviated without NRRL, e.g. *W. confusa* VTT E-90392 = *W. confusa* E392 and *L. mesenteroides* NRRL B-512F = *L. mesenteroides* B-512F.

For structural analysis the native dextrans and reuteran were isolated after incubation of the strains for 5 days on MRS-S agar at 30°C in a carbon dioxide atmosphere. The cell mass was carefully harvested from the plates and suspended in 100-450 ml of sodium phosphate buffer saline. The suspensions were shaken for 10 min and allowed to stand for 30 min before centrifugation at 10 000 rpm for 40 min using a Sorvall RC-5C centrifuge (Du Pont Company, Delaware, USA) to separate the cells. Supernatants were collected and centrifuged again under the same conditions. Dextrans were recovered from the supernatant by precipitation with three volumes of ethanol. The precipitates were washed at least twice by redissolving and reprecipitation. The final precipitates were then redissolved in water and vacuum dried or lyophilized prior to further analysis. The native dextran isolated from *L. mesenteroides* B-512F was only sufficient for NMR spectroscopy

analysis. Other studies were therefore carried out with a commercially available dextran (GE Healthcare, Uppsala, Sweden) from this strain.

4.2 Monosaccharide composition analysis (I)

W. confusa E392 and *L. citreum* E497 dextrans were depolymerized by acid methanolysis (2 M HCl in methanol) and the monosaccharides trimethylsilylated according to the method of Sundberg et al. (1996). A five-point calibration curve was prepared using D-glucose that was also acid methanolized and derivatized as for the samples. The trimethylsilylated glucosides were analyzed by gas chromatography (GC). The monosaccharides were calculated as anhydro-glucose using a correction factor of 0.90.

4.3 Enzyme-aided analysis of the dextrans (II and V)

Commercially available dextran-hydrolyzing enzymes were employed in this investigation for a three-fold purpose: First, to develop a quick method for screening the structural features of dextrans by chromatographic profiling of enzyme-resistant oligosaccharides. Second, since the resistant oligosaccharides are structural segments of the native dextran, determination of their structures provided further details on the fine structure of the dextrans. Third, the enzymes were utilized to develop a quantitative assay to determine the amount of dextran produced in sourdough. Preliminary studies were also carried out to qualitatively and quantitatively determine the oligosaccharides produced by dextransucrase acceptor reactions with the maltose present in sourdough.

The enzymes used included *Chaetomium erraticum* dextranase from Sigma-Aldrich, (Germany) and *Aspergillus niger* α-glucosidase from Megazyme (Ireland). The enzymatic activity of the dextranase (195 808 nkat/ml) was determined using a similar method to the one used for β-glucanase activity (Zurbriggen et al. 1990). The activity of the α-glucosidase (16 670 nkat/ml) was provided by the manufacturer. An α-glucosidase from *Bacillus stearothermophilus* (Megazyme, Ireland), which only has activity towards α-(1→4) linkages, was also included in the study of dextransucrase acceptor products.

4.3.1 Chromatographic profiling of the dextrans (II and V)

Dextran solutions (3-5 mg/ml) in 0.05 mM sodium citrate buffer pH 5.5 were prepared and hydrolyzed with 10 000 nkat/g dextranase and 1 000 nkat/g *A. niger* α-glucosidase for

48 h at 30ºC. The reaction was terminated by placing the samples in a boiling water bath for 10 min, after which the profile of residual oligosaccharides in the hydrolysate was determined by high-performance anion exchange chromatography with pulse amperometric detection (HPAEC-PAD). To study the action of the enzymes, *W. confusa* E392 dextran was hydrolyzed with both enzymes and with dextranase only. During the hydrolysis, 1 ml samples were collected after 10 min, 0.5, 1, 2, 4, 6, 8, and 24 h, for HPAEC-PAD analysis.

4.3.2 Preparation and isolation of enzyme-resistant oligosaccharides (II)

The enzyme-resistant oligosaccharides from *W. confusa* E392, *L. citreum* E497 dextrans and commercial dextran from *L. mesenteroides* B-512F (referred to henceforth as commercial dextran) were isolated for structural analysis. For this purpose, 0.5 g of *W. confusa* E392 and *L. citreum* E497 dextrans, and 1 g commercial dextran were dissolved in 15 ml buffer and hydrolyzed with both enzymes for 48 h at 30ºC. Subsequently, the enzyme-resistant oligosaccharides in the hydrolysates were fractionated by gel permeation chromatography (GPC) with a Biogel P2 column (5 × 95 cm; Bio-Rad, Hercules, CA, USA). The hydrolysates were first filtered with 0.45 μm membrane filters (Acrodisc 13, Pall Corporation, Ann Arbor, Michigan, USA) and injected into the column. The flow rate was first kept at 0.5 ml/min overnight to elute the void volume (600 ml), then adjusted to 2 ml/min for collection of 5 ml fractions. The fractions were analyzed to access their composition by HPAEC-PAD. Similar fractions were pooled and freeze-dried for further analysis by MS and NMR spectroscopy.

4.3.3 Development of an enzyme-aided assay for dextran quantification (V)

In order to determine the amount of dextran produced during sourdough fermentation, an enzyme-aided assay was developed. The strategy was to specifically hydrolyze dextran and then quantify the released glucose.

Model dough

In the first step of the method development, pure dextran from *W. confusa* E392 was mixed with wheat flour and water to evaluate the recovery of dextran from a complex dough matrix. The model doughs were prepared by mixing flour, purified dextran (1.3-1.5% DW) and water. The doughs were then freeze-dried and homogenized. The procedure for hydrolysis (Figure 12) of the dextran was similar to the one used in the analysis of β-glucan (Megazyme, Ireland). In this procedure, the samples are first washed

with aqueous ethanol (50% v/v) to remove free sugars and maltooligosaccharides. A sample, hydrolyzed with α-glucosidase only, was nonetheless included for correction of background glucose. The glucose released from dextrans was quantified with a commercial glucose kit (K-GLUC, Megazyme, Ireland).

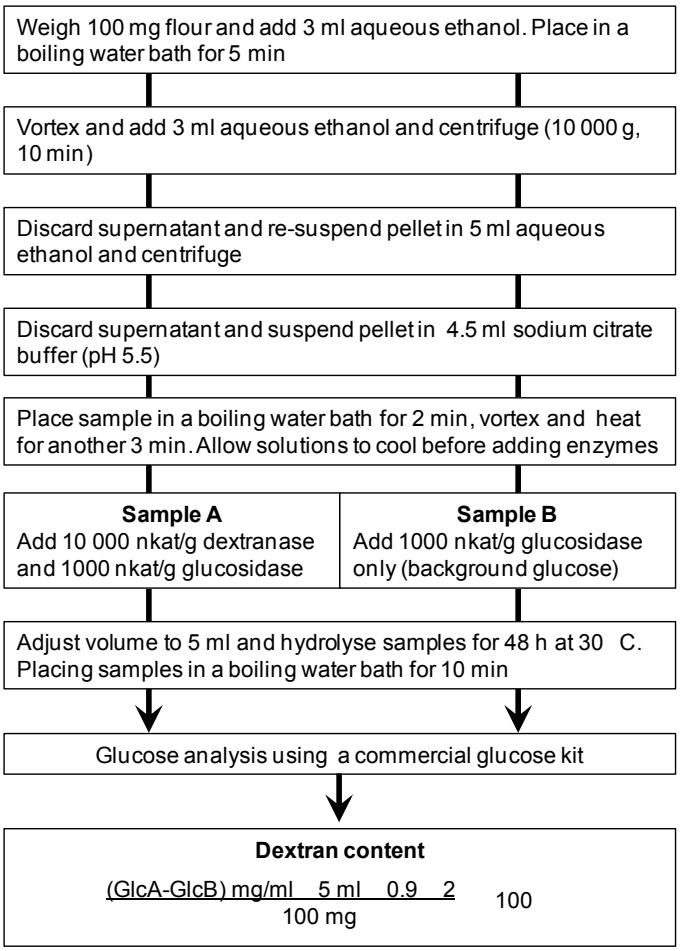

Figure 12. Schematic representation of the procedure used for quantification of dextrans in model dough and sourdoughs. In the calculation, 0.9 is a correction factor for anhydro-glucose and 2 is a correction factor determined from the recovery of dextran added to model doughs.

Sourdoughs

Eight different sourdough samples (Table 6) were prepared as described in paper **V**. The sourdoughs were divided into two series: one fermented for 24 h (24 h series) and the other fermented for 17 h (17 h series). In the 24 h series, sourdoughs fermented with *Lb. brevis* that does not produce dextran, and a sourdough fermented with *W. confusa* E392 without the addition of sucrose, were used as negative controls. In the 17 h series, the effect of static or dynamic (horizontal shaking) growth conditions on dextran production

was tested. In this series, *L. mesenteroides* B-512F sourdough was included for comparison and a *W. confusa* E392 sourdough that did not contain sucrose was used as a negative control. The sourdough samples were freeze-dried and homogenized, after which the content of dextran was determined in the same way as the freeze-dried model doughs described above (Figure 12). The enzyme dosages used for the sourdough samples were similar to those of the purified dextrans. Since the sourdoughs contained 10% (DW) sucrose, the theoretical maximum amount of dextran that could be produced during fermentation is 5% (50 g / kg flour). Thus the dosages of dextranase and α-glucosidase were 500 and 50 nkat/g of freeze-dried sourdough, respectively.

Table 6. Sourdough samples used for quantification of dextrans produced *in situ* during fermentation (paper **V**).

Sourdough	Strains	Incubation	Sucrose	Fermentation time (h)	EPS
1	*W. confusa* E392	Static	None	24	-
2	*W. confusa* E392	Static	10%	24	+
3	*Lb. brevis*	Static	None	24	-
4	*Lb. brevis*	Static	10%	24	+
5	*W. confusa* E392	Static	None	17	-
6	*W. confusa* E392	Static	10%	17	+
7	*W. confusa* E392	Shaking[a]	10%	17	+
8	*L. mesenteroides* B-512F	Static	10%	17	+

[a]Horizontal shaking at 150 rpm.

4.3.4 Preliminary studies on dextransucrase acceptor reaction products in sourdough

The formation of oligosaccharides due to the dextransucrase acceptor reaction with maltose in sourdough was evaluated by HPAEC-PAD analysis. For this preliminary study only sourdough 2 (Table 6) was used. The freeze-dried sourdough sample was treated as shown schematically in Figure 13. After suspending the samples in buffer, polymeric dextran was removed by filtration using Amicon Ultra-0.5 centrifugal filters (cut-off 100 000 g/mol, Millipore, USA) and the solutions analyzed by HPAEC-PAD. To identify the oligosaccharides that contained α-(1→6) linkages, a filtered solution was hydrolyzed with dextranase only and its HPAEC-PAD profile evaluated. These oligosaccharides were further quantified by analysis of glucose released after hydrolysis with both dextranase and *A. niger* α-glucosidase, using the glucose kit. Additionally, a sample was hydrolyzed with *B. stearothermophilus* α-glucosidase for correction of glucose originating from maltooligosaccharides.

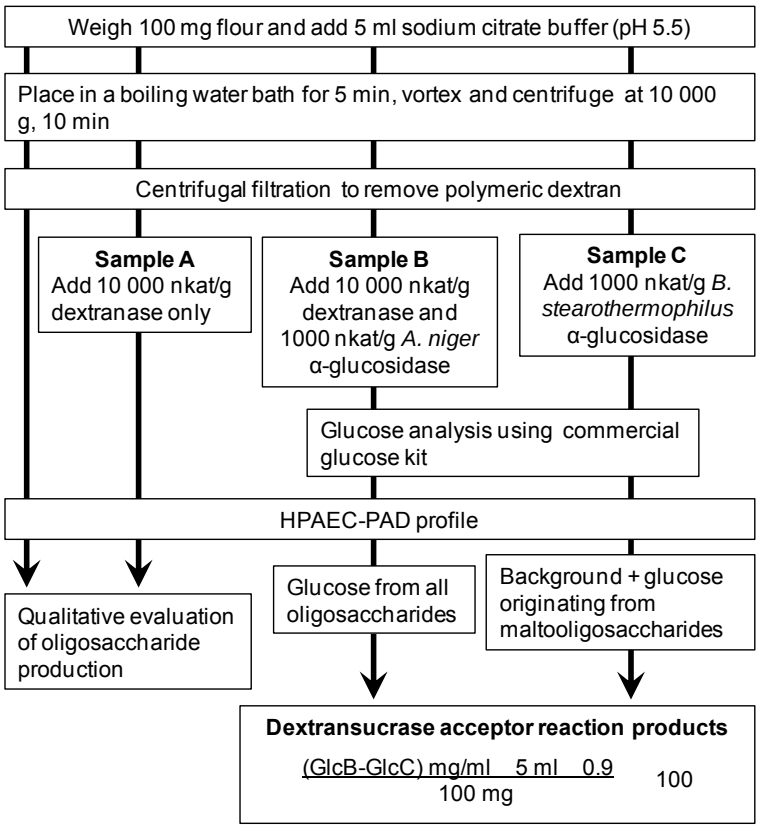

Figure 13. Scheme for qualitative and quantitative evaluation of oligosaccharides produced during sourdough fermentation. In the calculation, 0.9 is a correction factor for anhydro glucose.

4.4 HPAEC-PAD analysis (II and V)

The HPAEC-PAD equipment consisted of a Waters 717 autosampler, two Waters 515 HPLC pumps, an analytical CarboPac PA-100 column (250 x 4 mm, i.d, Dionex, Sunnyvale, CA, USA) and a Decade detector with a gold electrode (Antec Leyden, Zoeterwoude, The Netherlands). The analyses were carried out using the oligosaccharide method with a 100 mM NaOH to 1 M NaOAc gradient at a flow rate of 1 ml/min as described by Rantanen et al. (2007). Glucose (Merck, Darmstadt, Germany), isomaltose (IM2) and isomaltotriose (IM3, TCI Europe, Zwijndrecht, Belgium) were used as external qualitative standards. The samples were filtered through 0.45 μm membranes and the injection volume was 10μl.

4.5 Methylation analysis (II)

Methylation analysis was performed on enzyme-resistant oligosaccharides isolated after hydrolysis of commercial dextran according to the method of Ciucanu and Kerek (1984) with some modifications. Briefly, after permethylation, the samples were extracted with dichloromethane. The dichloromethane phase was evaporated and the samples dried under vacuum before hydrolysis with 2 M TFA for 2 h at 120ºC. The partially methylated glucosides were reduced and acetylated as described by Blakeney (1983). The methylation products were identified by GC-MS with a Hewlett-Packard 6890 instrument with an RTX column (60 m × 0.32 mm × 0.10 μm) (Agilent Technologies, Foster City, CA, USA). The analysis conditions were 170ºC (10 min) and a gradient from 4ºC/min to 200ºC (10 min).

4.6 Mass spectroscopy (II and III)

MS was carried out to determine the molar mass and structure of residual oligosaccharides isolated after enzymatic hydrolysis of *W. confusa* E392 and *L. citreum* E497 dextran. A comprehensive study was undertaken to first evaluate the possibilities of using MS to unequivocally determine the structures of GOS. The study therefore included several model GOS, mannobiose and two galactooligosaccharides as summarized in Table 7. Mass spectrometry was carried out with an Agilent 1100 Series LC/MSD Ion Trap XCT Plus with an electrospray ion source (Agilent Technology, Palo Alto, CA, USA). Prior to MS/MS analysis, 2-10 μl of each oligosaccharide (1-2 mg/ml) was mixed with 400 μl of MeOH:water:formic acid (50:49:1) solution (Reis et al. 2003). Additionally, 1-3 μl of 10 mg/ml lithium acetate (positive mode) or ammonium chloride (negative mode) was added to the samples. Samples were directly injected into the ESI unit at a flow rate of 10 μl/min. Before injection of each sample, the system was thoroughly cleaned by injecting an isopropanol:water (50:50) solution followed by methanol.

Table 7. Structure and origin of commercial model oligosaccharides used in the study.

	Oligosaccharide	Structure
	Disaccharides	
1	Mannobiose	α-D-Man*p*-(1→2)-D-Man[a]
2	Nigerose	α-D-Glc*p*-(1→3)-D-Glc[b]
3	Laminaribiose	β-D-Glc*p*-(1→3)-D-Glc[c]
4	Maltose	α-D-Glc*p*-(1→4)-D-Glc[d]
5	Cellobiose	β-D-Glc*p*-(1→4)-D-Glc[d]
6	Isomaltose	α-D-Glc*p*-(1→6)-D-Glc[e]
	Trisaccharides	
7	Maltotriose	α-D-Glc*p*-(1→4)-α-D-Glc*p*-(1→4)-D-Glc[b]
8	Isomaltotriose	α-D-Glc*p*-(1→6)-α-D-Glc*p*-(1→6)-D-Glc[e]
10	Panose	α-D-Glc*p*-(1→6)-α-D-Glc*p*-(1→4)-D-Glc[e]
11	Galactotriose	α-D-Gal*p*-(1→3)-β-D-Gal*p*-(1→4)-D-Gal[a]
12	β-Glucotriose	β-D-Glc*p*-(1→4)-β-D-Glc*p*-(1→3)-D-Glc[c]
	Tetrasaccharides	
13	Galactotetrose	α-D-Gal*p*-(1→3)-β-D-Gal*p*-(1→4)-α-D-Gal*p*-(1→3)-D-Gal[a]
14	β-Glucotetraose 1	β-D-Glc*p*-(1→4)-β-D-Glc*p*-(1→4)-β-D-Glc*p*-(1→3)-D-Glc[c]
15	β-Glucotetraose 2	β-D-Glc*p*-(1→4)-β-D-Glc*p*-(1→3)-β-D-Glc*p*-(1→4)-D-Glc[c]
16	Maltotetraose	α-D-Glc*p*-(1→4)-α-D-Glc*p*-(1→4)-α-D-Glc*p*-(1→4)-D-Glc[b]
17	Cellotetraose	β-D-Glc*p*-(1→4)-β-D-Glc*p*-(1→4)-β-D-Glc*p*-(1→4)-D-Glc[b]

Manufactured by [a]Dextra Laboratories, Reading, England, [b] Sigma-Aldrich Chemie, Steinheim, Germany, [c]Megazyme, Wicklow, Ireland, [d]Merck, Darmstadt, Germany, [e]TCI Europe, Zwijdrecht, Belgium.

4.7 NMR spectroscopy (I, II and III)

The structures of the polymeric dextrans and residual oligosaccharides were determined by NMR spectroscopy (**I-III**). The data were recorded on a Varian Unity 500/600 spectrometer (Varian NMR Systems, Palo Alto, CA, USA) using 5 mm triple-resonance pulsed-field gradient (PFG) probes. NMR samples were exchanged three times with D_2O, filtered and then placed in NMR tubes (Wilmad NMR tubes, 5 mm, ultra-imperial grade, Aldrich Chemical Company, Milwaukee, WI, USA). The measurements were performed at 23°C (oligosaccharides) and 50°C (native dextran) and the chemical shifts were referenced to acetone (δ_H = 2.225 ppm and δ_C = 31.55 ppm). 1D experiments and 2D DQF-COSY, TOCSY, HSQC, HMBC, H2BC, HSQC-TOCSY and nuclear overhauser enhancement spectroscopy (NOESY) experiments were used for chemical shift assignment and determination of glucoside bonds.

4.8 Macromolecular characterization of *W. confusa* and *L. citreum* dextrans (IV)

The macromolecular properties of *W. confusa* E392 and *L. citreum* E497 dextrans were analyzed by HPSEC, AsFlFFF and DOSY. Dextran standards with nominal M_w of 12 000 –270 000 and 670 000 g/mol (Dx 12-Dx 670) from Fluka (Buchs, Switzerland) and standards with nominal M_w of 490 000, 3 500 000 and 11 900 000 g/mol (Dx 490-Dx 11900) from Polymer Standards Service (Mainz, Germany) were used (**IV**).

4.8.1 HPSEC and AsFlFFF

The HPSEC and AsFlFFF equipment used in this study is described in detail in paper **IV**. The HPSEC analyses were performed in both aqueous (0.1 M $NaNO_3$) and DMSO-based (DMSO + 0.01 M LiBr) eluents, while AsFlFFF was carried out in aqueous solution (0.1 M $NaNO_3$) only. The flow rate in both HPSEC systems was 1 ml/min. The eluents were analyzed with a refractive index (RI) detector (VE 3580, Viscotek Corp., Houston, USA), and a combined light scattering (LS) and viscometric detector (270 Dual Detector, Viscotek Corp.). The HPSEC data (molar mass, [η], and R_η = viscometric radius) were processed with OmniSEC 4.5 software (Viscotek Corp.). A dn/dc value of 0.1435 ml/g for dextrans in aqueous solution (Vink and Dahlstrom 1967) and 0.072 ml/g (Basedow et al. 1978) for DMSO-based eluent were used. The concentration of the samples in aqueous solutions was 2 mg/ml and 3 mg/ml in DMSO.

In the AsFlFFF analysis, an exponentially decaying cross-flow (exponent 0.2) starting at 2 ml/min was used during separation while the detector flow was kept constant at 0.5 ml/min for dextran standards. Excess solvent from the upper part of the channel was pumped out at 0.5 ml/min before the detector outlet to intensify the detector signals. For the isolated dextran samples with HMM, a starting cross-flow of 1.5 ml/min and a faster decay (exponent 0.1) were used. The detector flow was 1 ml/min. The eluents were analyzed with an RI detector (PN 3150, Postnova Analytics, Landsberg/Lech, Germany) and a multi-angle light-scattering detector (MALS) (Brookhaven Instruments Corporation, Holtsville, NY, USA). The injection volume was 50 µl for standards and 20 µl for samples. The solution concentration for the dextran standards was 2 mg/ml and the concentration for *W. confusa* E392 and *L. citreum* E497 dextrans was 1 mg/ml.

4.8.2 DOSY

DOSY measurements were done to determine the self-diffusion coefficients D (m^2s^{-1}) of the dextran standards and samples, which were then related to M_w according to Equation [4]. The scaling parameters K and α were obtained by calibration with the dextran standards (nominal M_w ranging from 12 000 to 11 900 000 g/mol). D was also related to R_h by the Stokes-Einstein equation [5]. The experiments were performed in D_2O on a Varian Unity INOVA 600 spectrometer equipped with a 5 mm triple-resonance gradient probe head, incorporating three-axis gradient coils capable of delivering gradient amplitudes up to 64 G/cm on the z-axis. DOSY measurements were carried out at 300K using dilute solutions (< 1 mg/ml) of the dextran standards and samples. The standards and samples were exchanged twice with D_2O before analysis. Sample heights in the NMR tube were kept below 4 cm, and the experiments performed using the bipolar gradient pulse stimulated echo pulse sequences with convection compensation (BPPSTE-CC) (Jerschow and Müller 1997) to suppress the effects of eddy currents and especially the effect of convection currents. In all experiments, the gradient amplitude (g) was varied from 1% to 98% of the maximum in 30 steps with a total of 16 transients collected at each amplitude. The diffusion time (Δ) was kept constant (0.6 s), while the diffusion gradient pulse duration (δ) was optimized for each sample to ensure that, at the highest gradient, the signals decayed to at least 5% of the original intensity. Typical values for δ were between 1 and 6.5 ms. A 200 μs eddy current recovery delay was applied after each gradient. All experiments were done in triplicate. The NMR data was processed with the NPK algorithm (Delsuc and Malliavin 1998; Tramesel et al. 2007) incorporated in the NMRnotebook software (NMRtec, France) to obtain 2D DOSY spectra.

5 Results

5.1 Isolation of the dextrans (I)

Generally, the *Weissella* strains showed better growth and produced more dextran on MRS-S agar than the *Leuconostoc* strains. The cell mass from *L. mesenteroides* B-512F was more liquid, less viscous and easily dried on the media surface. Acid methanolysis (**I**) followed by GC analysis showed that the extracts from *W. confusa* E392 and *L. citreum* E497 contained 84.3 ± 4% and 83.6 ± 2% glucose, respectively. No other sugars were detected in the extracts.

5.2 NMR spectroscopy analysis of the dextrans (I)

All samples had a peak (E) for α-(1→6)-linked residues centered at δ_H 4.98 ppm (d, $J_{1,2}$ 3.2 Hz). Furthermore, the spectra of the dextrans had a broad peak B (an apparent triplet) for α-(1→3)-linked branches centered at δ_H 5.32 ppm. The *L. citreum* strains had additional peaks at δ_H 5.18 ppm (C) and 5.11 ppm (D) assigned to the α-(1→2) single unit terminal branches and the 2,6-*O*-disubstituted α-D-glucopyranosyl units, respectively. *Lb. reuteri* ATCC 55730 had a broad peak centered at δ_H 5.36 ppm (A), which is most likely from α-(1→4)-linked glucosyl residues. The peak at δ_H 4.52 ppm in the spectra is from HDO. The 1D ^{1}H spectra of dextrans from *L. mesenteroides* B-512F, *W. confusa* E392, *L. mesenteroides* B-1415, *L. citreum* E504, *L. citreum* E497 and *Lb. reuteri* ATCC 55730 are shown in Figure 14. The 1D ^{1}H spectra of dextrans from the other *Weissella* strains were similar to that of *W. confusa* E392, while those of *L. citreum* E389 and E1082 were similar to that of *L. citreum* E497.

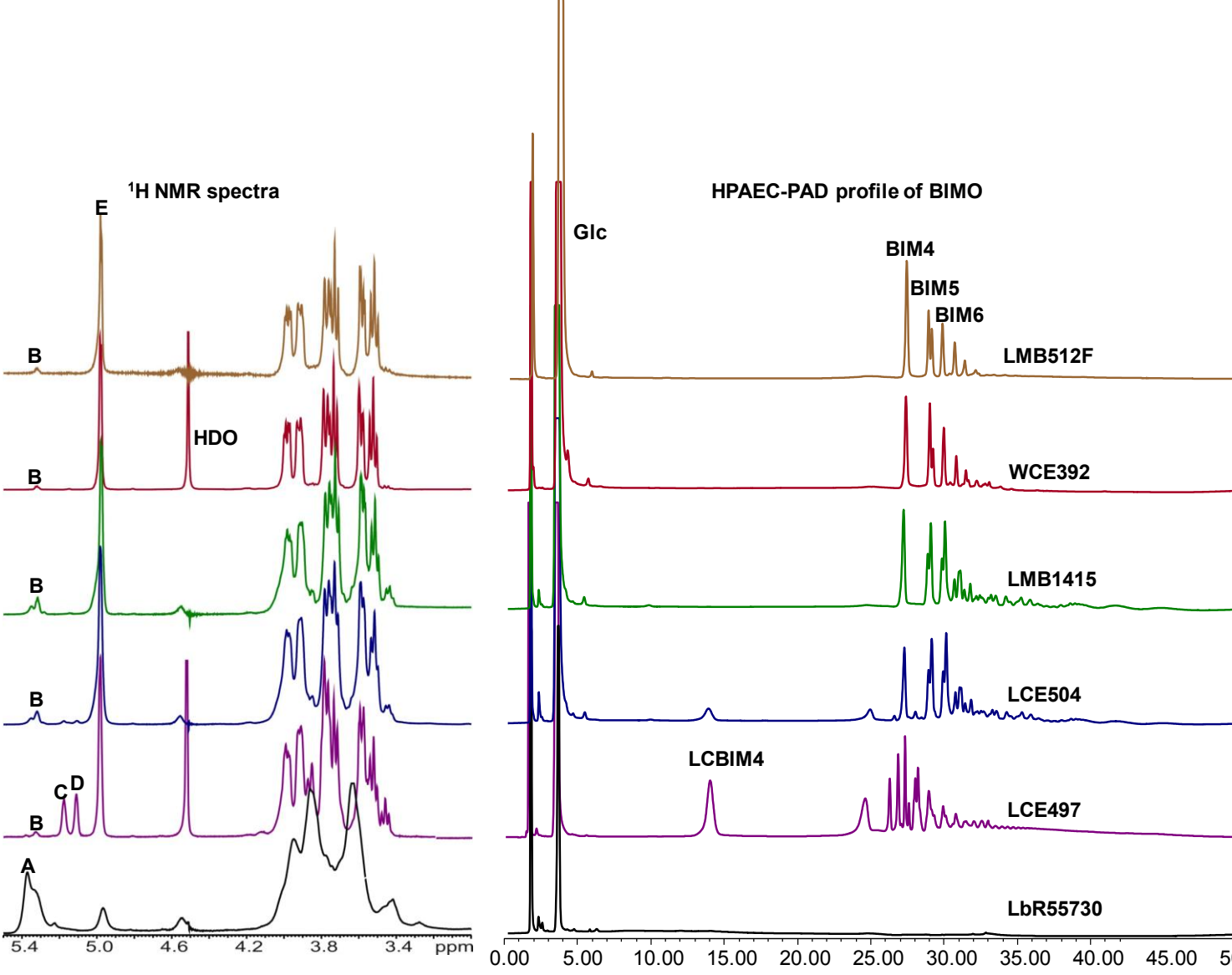

Figure 14. 1D ^{1}H spectra of dextrans (left) and the HPAEC-PAD profile (right) of resistant oligosaccharides (BIMO) remaining after enzymatic hydrolysis of dextrans from *L. mesenteroides* B-512F (LMB512F), *W. confusa* E392 (WCE392), *L. mesenteroides* B-1415 (LMB1415), *L. citreum* E504 (LCE504) and *L. citreum* E497 (LCE497). The 1D ^{1}H spectra of *Lb. reuteri* ATCC 55730 (LbR55730) reuteran and the HPAEC-PAD profile of its enzyme hydrolysate is also shown. The NMR spectra were recorded at 500 MHz in D_2O at 50°C and referenced to internal acetone (δ_H = 2.225 ppm and δ_C = 31.55 ppm). A = most likely α-(1→4)-linked glucosyl residues, B = α-(1→3)-linked branches, C = 2,6-*O*-disubstituted residues, D = α-(1→2)-linked branches and E = α-(1→6) linkages. The BIMO were obtained by hydrolysis of the dextrans and reuteran with *C. erracticum* (10 000 nkat/g) and *A. niger* α-glucosidase (1000 nkat/g) for 48 h at 30°C.

The relative amounts of linkages determined from the integral values of the anomeric protons in the dextrans are compared in Table 8. Dextrans from the *Weissella* strains and *L. mesenteroides* B-512F only had α-(1→3)-linked branches, 3% and 4%, respectively. *L. mesenteroides* B-1415 had 7% α-(1→3)-linked branches and 4% linkages (anomeric signal at δ_H 5.35 ppm) that were not determined. The *L. citreum* strains had both α-(1→2)- and α-(1→3)-linked branches in varying amounts. *L. citreum* E504 also contained 3% linkages (signal at δ_H 5.35 ppm) that were not determined. The *Lb. reuteri* ATCC 55730

reuteran contained 17% α-(1→6) linkages. The remaining 83% of the linkages were not rigorously determined but are most likely α-(1→4)-linked glucosyl residues in different chemical environments. Since the *Weissella* strains produced similar dextrans, only *W. confusa* E392 dextran was chosen for further study. Also, only *L. citreum* E497 dextran was studied further.

Table 8. Composition (%) of glycosidic linkages in the isolated dextrans and reuteran, determined from the integral values of the anomeric protons in their 1D ^{1}H NMR spectra (Figure 13). The NMR spectra were recorded at 500 MHz in D_2O at 50°C.

Strain	α-(1→6)	α-(1→3)	α-(1→2)	nd[b]
Weissella sp. E748	97	3		
Weissella sp. E749	97	3		
Weissella sp. E750	97	3		
W. cibaria E076	97	3		
W. confusa E392	97	3		
L. mesenteroides B-512F	96	4		
L. mesenteroides B-1415	89	7		4
L. citreum E504	89[a]	6	2	3
L. citreum E497	85[a]	4	11	
L. citreum E389	81[a]	2	17	
L. citreum E1082	77[a]	3	20	
Lb. reuteri ATCC 55730	17			83[c]

[a]Sum of 6-*O*-monosubstituted and 2,6-*O*-disubstituted glucosyl residues, [b]not determined, [c]most likely α-(1→4)-linked branches

5.3 Enzyme-aided analysis of the isolated dextrans (II)

5.3.1 Action of the enzymes (II)

W. confusa E392 dextran was first hydrolyzed with dextranase only, and samples were taken at various time points to evaluate the action of dextranase. The study showed that the main products of the endodextranase were glucose, IM2 and IM3 and enzyme-resistant oligosaccharides. However, with prolonged hydrolysis (48 h), IM3 was also hydrolyzed to IM2 and glucose. The presence of α-glucosidase resulted in hydrolysis of IM2 and IM3 to glucose and slightly changed the profile of the resistant oligosaccharides. Therefore, most of the residual oligosaccharides were already end products resulting from the prolonged action of dextranase, and represented the structurally complex, presumably branched

sections in the dextrans. The resistant oligosaccharides are therefore referred to as branched isomaltooligosaccharides (BIMO) in subsequent discussions.

5.3.2 Chromatographic profiling of the native dextrans

The isolated dextrans were hydrolyzed with a mixture of dextranase and α-glucosidase and the chromatographic profile of their BIMO compared. As shown in Figure 14, the profile of the BIMO varied with the structural complexity of the dextrans (Table 8). Dextran from *W. confusa* E392 and commercial dextran, both of which have a low degree of branching (<4%), had a very similar profile. The presence of 11% α-(1→2) linkages in *L. citreum* E497 dextran significantly changed the HPAEC-PAD profile of its BIMO. For *L. citreum* E504, the 2% α-(1→2) linkages did not significantly change its BIMO profile, when compared to that of *L. mesenteroides* B-1415, except for two peaks eluting between 13 and 25 min (Figure 14 LMB1415 and LCE504). Both dextrans contained a significant amount of α-(1→3) linkages (7% and 6%, respectively). Reuteran from *Lb. reuteri* ATCC 55730 only had a glucose peak and no BIMO in its profile.

5.4 Structural analysis of BIMO (II and III)

BIMO from *W. confusa* E392 and *L. citreum* E497 dextrans were isolated and their structures determined, in order to gain insight into the fine structure of these dextrans. For comparison, BIMO from commercial dextran were also isolated and analyzed.

5.4.1 Isolation of the BIMO (II and III)

BIMO from W. confusa E392 and commercial dextrans

BIMO remaining after hydrolysis of *W. confusa* E392 and commercial dextran were isolated by GPC using a Biogel P2 column. The isolated oligosaccharides from these dextrans were similar, with fractions occurring in three major BIMO pools (WCBIM4, WCBIM5 and WCBIM6, and LMBIM4, LMBIM5 and LMBIM6, respectively). Fractions that eluted prior to WCBIM6 and LMBIM6 were mixtures of various oligosaccharides (hexa-, hepta- and octasaccharides) and were therefore not analyzed further. ESI-MS (Table 9) confirmed that WCBIM4 and LMBIM4 were tetrasaccharides. WCBIM5 and LMBIM5 were composed of two isomeric pentasaccharides, while WCBIM6 and

LMBIM6 were hexasaccharides. WCBIM5 and LMBIM5 were analyzed as a mixture without further purification.

BIMO from L. citreum E497 dextran

GPC of BIMO from *L. citreum* E497 dextran resulted in only one sufficiently pure fraction for further analysis (LCBIM4, Figure 15). Fractions eluting prior to this fraction were mixtures of two or more oligosaccharides. Some of the pooled fractions are shown in Figure 15 (LCBIMO-A-D). ESI-MS analysis (not shown) indicated that fractions LCBIM4 and LCBIMO-D contained tetrasaccharides, while fraction LCBIMO-C was mainly composed of pentasaccharides. As shown in Figure 15, some of the BIMO fractions contained peaks that had a similar retention time to WCBIM4, WCBIM5-1&2 and WCBIM6.

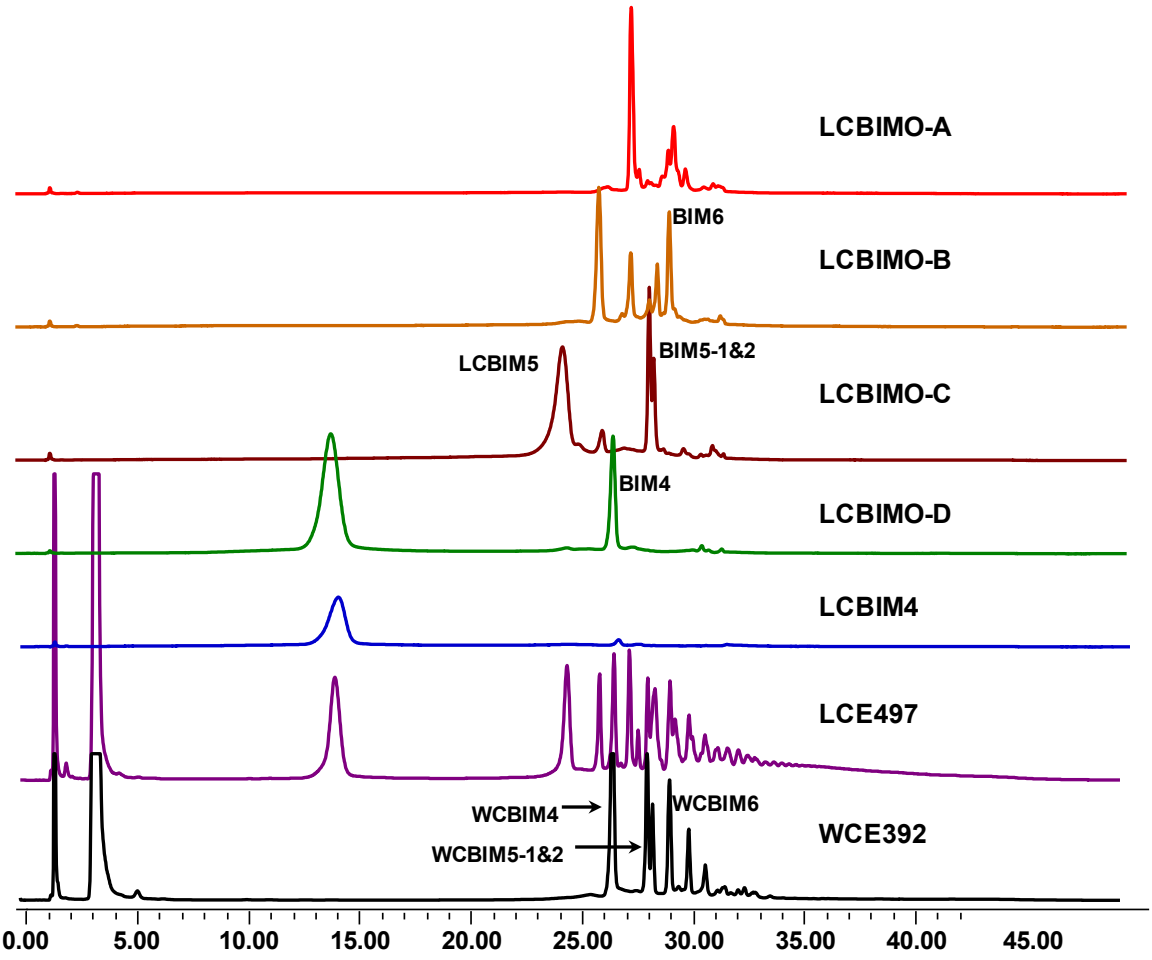

Figure 15. HPAEC-PAD chromatograms of some of the pooled fractions containing BIMO from *L. citreum* E497 dextran (LCBIMO-A-D and LCBIM4) isolated after 48 h hydrolysis with dextranase and α-glucosidase. The profile of the BIMO from the original *L. citreum* E497 dextran hydrolysate (LCE497) and that of *W. confusa* dextran (WCE392) are shown for comparison. BIM4, BIM5-1&2 and BIM6 are tentatively assigned based on retention time.

5.4.2 Methylation analysis of the BIMO from commercial dextran (II)

Methylation analysis was only performed on BIMO isolated from commercial dextran (LMBIM4-6), since all material obtained from *W. confusa* E392 dextran (WCBIM4-6) and *L. citreum* E497 dextran (LCBIM4) were kept for NMR spectroscopy analysis. The main glycosidic linkages in LMBIM4-6 are illustrated in Table 9. LMBIM4-6 contained 2,3,4,6-tetra-*O*-methyl- and 2,3,4-tri-*O*-methyl-glucosides originating from the non-reducing terminal residues, and 6-*O*-monosubstituted glucosyl residues, respectively. In addition, LMBIM4 and LMBIM5 contained 2,4,6-tri-*O*-methyl-glucoside, indicating the presence of 3-*O*-monosubstituted glucosyl residues. LMBIM5 and LMBIM6 also contained 2,4-di-*O*-methyl-glucosides, indicating the presence of 3,6-*O*-disubsituted glucosyl residues.

Table 9. Methylation analysis and MS data of the BIMO isolated after hydrolysis of commercial dextran with dextranase and α-glucosidase.

Oligosaccharide	Linkages obtained by methylation analysis				ESI-MS $[M+Na]^+$(*m/z*)
	Glc-(1→	→6)Glc-(1→	→3)Glc-(1→	→3,6)Glc-(1→	
LMBIM4	+	+	+	-	689
LMBIM5	+	+	+	+	851
LMBIM6	+	+	-	+	1013

5.4.3 Structural analysis of BIMO (tetrasaccharides) by MS (III)

To determine the structure of the isolated BIMO by MS, a comprehensive study (**III**) was undertaken that included various model linear GOS as shown in Table 7. Model disaccharides representing all the possible glycoside linkages were first analyzed in both positive and negative mode and their spectra used for comparison with the spectra of larger oligosaccharides. The fragment ions observed in the MS/MS spectrum were assigned according to the nomenclature of Domon and Costello (1988) (Figure 6). The ions in positive mode were analyzed as lithium or sodium adducts ($[M+Li]^+$), while ions in negative mode were analyzed as chloride adducts ($[M+Cl]^-$).

Model disaccharides

A summary of the structure diagnostic fragments in positive and negative mode for each glycoside linkage in the model disaccharides is shown in Table 10. A-type fragment ions (cross-ring cleavages, Figure 6) resulting from loss of 90 and 120 Da in positive mode, and loss of 78 and 120 Da in negative mode are diagnostic for α-(1→2) linkages. A loss of 90 Da A-type fragment ion in positive mode and lack of A-type fragments in negative

mode spectra indicates the presence of α-/β-(1→3) linkages. The α- and β-(1→4) linkages are identified by a loss of 60 Da A-type fragment ion and a minor loss of 120 Da A-type fragment ion in positive mode. In negative mode, A-type ions at *m/z* 281, 263 and 221 due to loss of 60, 78 and 120 Da are diagnostic for α-(1→4) linkages, while a fragment ion at *m/z* 263 (loss of 78 Da) and a minor loss of 60 Da is diagnostic for β-(1→4) linkages. The α-(1→6) linkages are identified by the presence of all A-type fragment ions in positive mode. In negative mode, α-(1→6) linkages are confirmed by the presence of A-type fragment ions arising from loss of 60, 90 and 120 Da. As shown in Table 10, only α-(1→2) and α-(1→6) linkages produce significant B_2 ion (loss of 18 Da), which can therefore be used in structure elucidation.

Table 10. Structure diagnostic fragment ions in positive and negative mode. Positive mode was carried out with lithium adducts and negative mode with chloride adducts.

		Positive mode			**Negative mode**				
	Linkage	**A-type fragments**			**B_2**	**A-type fragments**			
Ion *m/z*		289	259	229	323	281	263	251	221
Neutral loss		60	90	120	18[a]	60[a]	78[a]	90[a]	120[a]
Mannobiose	α-(1→2)		+	+++	++		+		+
Nigerose	α-(1→3)		+						
Laminaribiose	β-(1→3)		+						
Maltose	α-(1→4)	++				+	+		+
Cellobiose	β-(1→4)	++		+			+		
Isomaltose	α-(1→6)	+++	++	+	+	+		+	++

[a]Neutral losses expressed as loss from deprotonated molecular ions at *m/z* 341. **+++**=signal above 56% relative abundance, **++**=signal between 26 and 55% relative abundance and **+**=signals below 25% relative abundance.

Model tri- and tetrasaccharides

Using the principles determined with model disaccharides, the study showed that the positive mode and negative mode spectra were adequate to confirm the linkages in model tri- and tetrasaccharides that contained similar linkages (maltotriose, isomaltotriose, maltotetraose and cellotetraose). When the oligosaccharide contained different linkages, only the linkage at the reducing end could be unequivocally determined with the positive mode spectra. In contrast, the negative mode spectra enabled identification of all linkages in the oligosaccharides. Determination of the remaining linkages in positive mode was hindered by formation of isomeric fragments due to simultaneous loss of glucosyl residues from the reducing and the non-reducing end, which resulted in formation of isomeric C and Y ions (Figure 6) as illustrated with glucotriose in Figure 16.

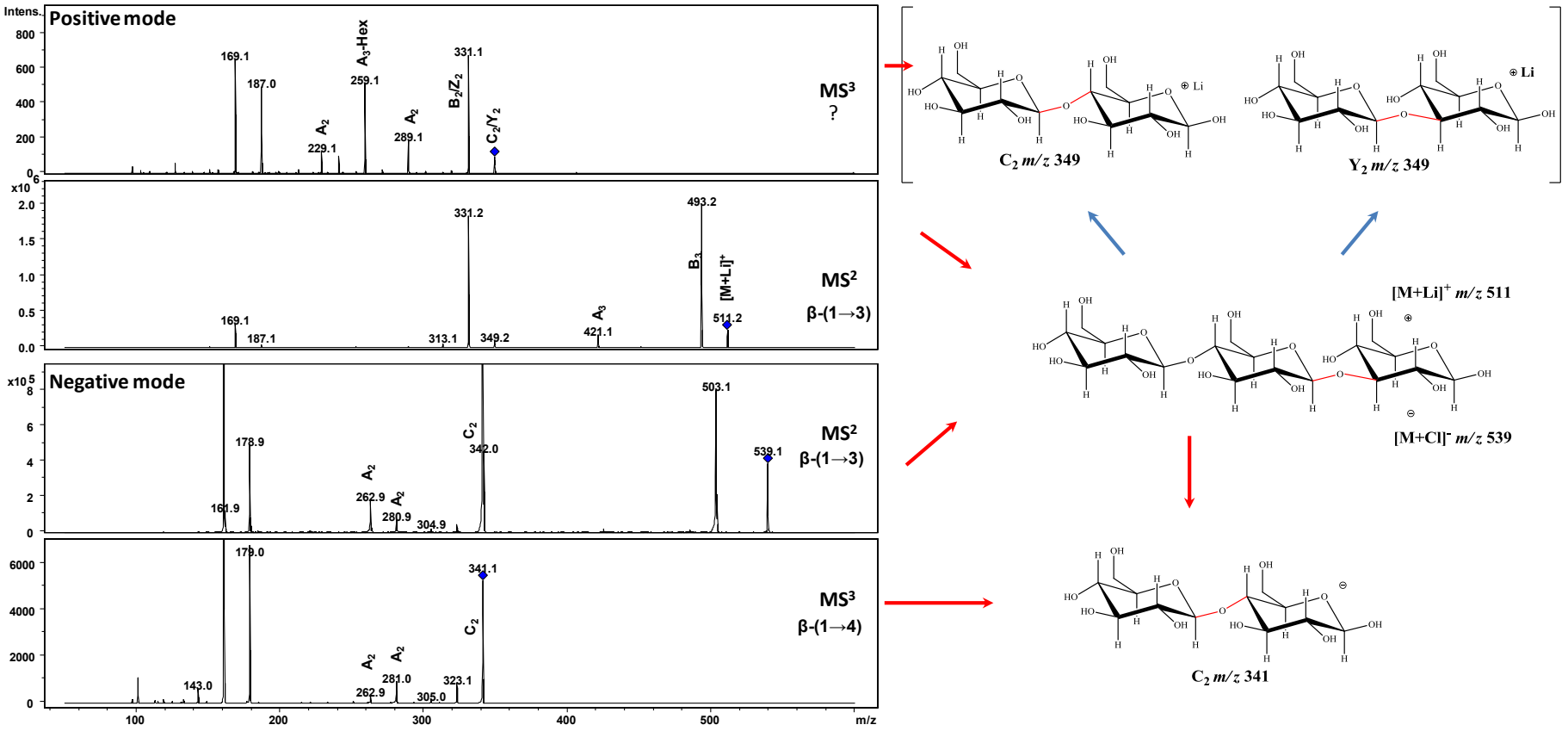

Figure 16. Positive and negative mode MS^2 and MS^3 spectra of glucotriose. A schematic representation of the C and Y ions isolated after MS^2 analysis is also shown. The positive mode MS was carried out with lithium adducts and the negative mode with chloride adducts.

Both the C and Y ions contributed the reducing-end cross-ring cleavage ions in the subsequent MS/MS cycle, making it difficult to determine the linkages. As seen in Figure 16, all A-type fragments arising from the C ion (1→3 linkage, loss of 90 Da) and from the Y ion (1→4 linkage, loss of 60 and 120 Da, Table 10) are observed in the positive mode MS^3 of glucotriose. Similar observations were made with the other model oligosaccharides. More details on these oligosaccharides are given in paper **III**.

Isolated WCBIM4 and LCBIM4

As with the model GOS, both positive mode and negative mode MS^2 analysis confirmed that the reducing end of WCBIM4 and LCBIM4 contain α-(1→6) linkages (Figure 17A and B). The presence of all A-type fragment ions (*m/z* 451, 421 and 391, and 289, 259 and 229) in the positive mode MS^2, MS^3 and MS^4 spectra suggested that the remaining two linkages were also α-(1→6) linkages. However, negative mode spectra showed that while the middle linkages in these oligosaccharides were α-(1→6) linkages (A-type fragment ions at 443,413 and 383), the linkages at the non-reducing end were not α-(1→6) linkages.

In the negative mode MS/MS spectra of WCBIM4 (Figure 17C), there are no ions below m/z 341 while in LCBIM4 (Figure 17D) the main A-type fragment ion arises from loss of 78 Da and the minor ion from loss of 120 Da. Thus, contrary to the results from the positive mode spectra, the negative mode spectra indicate that the non-reducing end of WCBIM4 contains an α-(1→3) linkage while LCBIM4 contains an α-(1→2) linkage. The significant B_2 ion at m/z 323, also observed in mannobiose (Table 10), further confirms the (1→2) linkage at the non-reducing end of LCBIM4. Thus the structure of WCBIM4 is (α-D-Glc*p*-(1→3)-α-D-Glc*p*-(1→6)-α-D-Glc*p*-(1→6)-D-Glc) and that of LCBIM4 is α-D-Glc*p*-(1→2)-α-D-Glc*p*-(1→6)-α-D-Glc*p*-(1→6)-D-Glc. Both were confirmed by NMR spectroscopy.

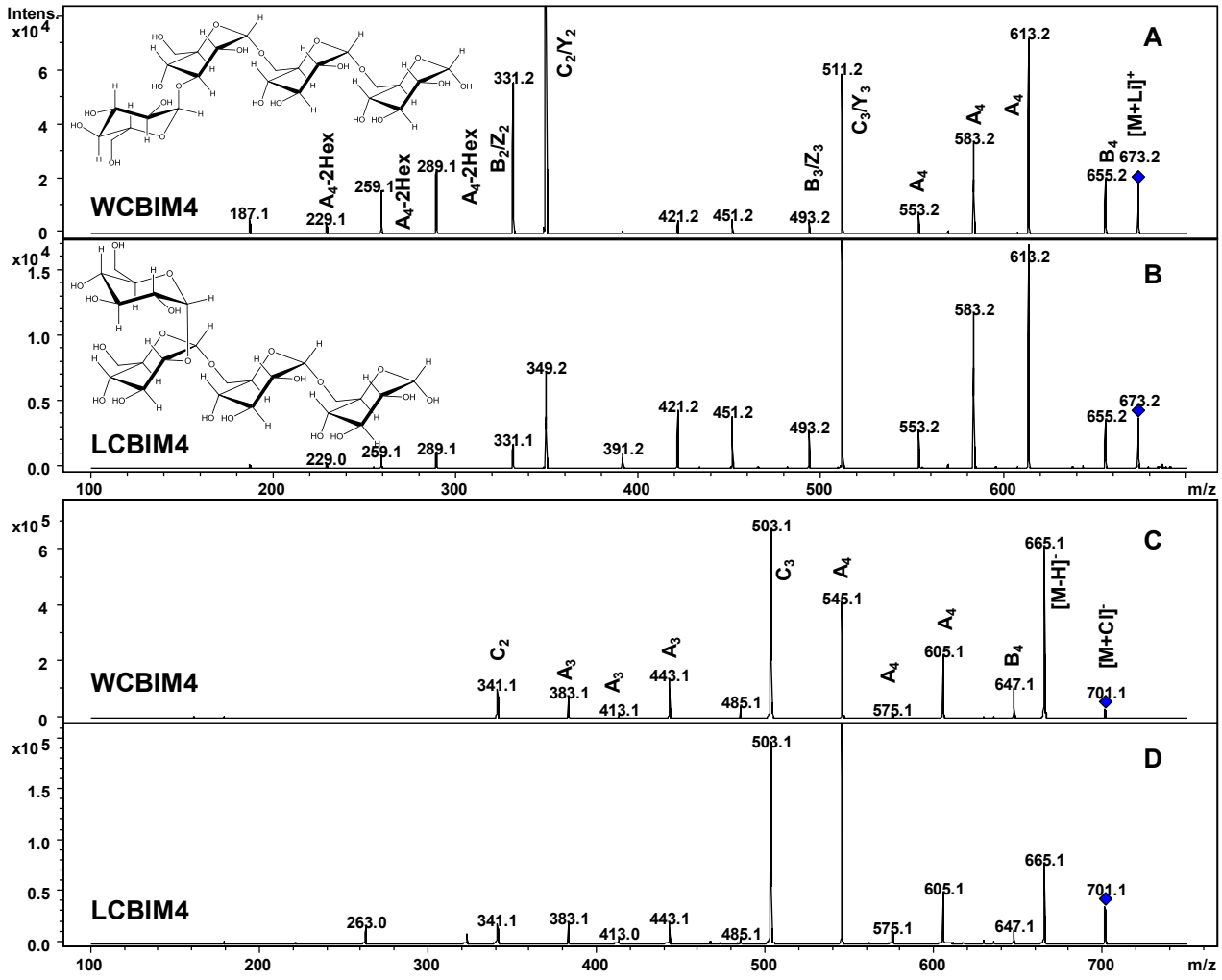

Figure 17. Positive (A and B) and negative mode (C and D) MS^2 spectra of WCBIM4 and LCBIM4.

5.4.4 NMR spectroscopy analysis of the BIMO (II and III)

This section summarizes the structures identified from NMR spectroscopy data. A detailed evaluation of the spectra and assignment of the chemical shift for each residue is given in **II** and **III**. The 1D ^{1}H NMR spectra of the BIMO (WCBIM4-6 and LCBIM4) are shown in Figure 18. Glucosyl residues in the BIMO are numbered A, B, and C (main chain) and A_1 and B_1 (residues in the branches) from the non-reducing end, with the reducing end residue referred to as Rα/Rβ (Figure 19).

Tetrasaccharides (WCBIM4 and LCBIM4)

The 1D ^{1}H NMR spectra of WCBIM4 contained anomeric signals at δ_H 5.35, 5.24, 4.97 and 4.68 ppm, with an integral ratio of 1: 0.4: 2: 0.6, respectively (Figure 18). Two of the anomeric signals were assigned to the α (δ_H 5.24 ppm) and β (δ_H 4.68 ppm,) anomers of the reducing end (Rα and Rβ, respectively). Thus, the integral ratio further verified that WCBIM4 was a tetrasaccharide. The anomeric proton at δ_H 5.35 ppm was assigned to a terminal non-reducing end α-(1→3)-linked glucosyl residue (residue A), while the two protons at δ_H 4.97 ppm were assigned to two internal (-α-D-Glc*p*-(1→6)-α-D-Glc*p*-(1→6)-) residues (B and C, respectively). Thus the structure of WCBIM4 was α-D-Glc*p*-(1→3)-α-D-Glc*p*-(1→6)-α-D-Glc*p*-(1→6)-D-Glc (3^3-α-D-glucosylisomaltotriose, Figure 19), which concurs with the negative mode MS data.

LCBIM4 had six anomeric signals at δ_H 5.35, 5.24, 5.17, 5.11, 4.96, and 4.68 ppm with an integral ratio of 0.1: 0.3: 1.1: 1.1: 1.2: 0.6, respectively. Based on the integral values, the anomeric signal at δ_H 5.35 ppm was considered to be an impurity, arising from a tetrasaccharide containing a terminal α-(1→3) linkage at the non-reducing end, as in WCBIM4. The HMBC spectrum of this sample (**III**) confirmed that the signal at δ_H 5.11 ppm was for an α-(1→2)-linked terminal glucose residue at the non-reducing end (A). The signal at δ_H 5.17 ppm was for an α-(1→6)-linked glucose residue next to the non-reducing end (B), while the signal at δ_H 4.96 ppm was for the internal glucose residue (C) that is α-(1→6)-linked to the reducing end residue. Accordingly, the structure of LCBIM4 was α-D-Glc*p*-(1→2)-α-D-Glc*p*-(1→6)-α-D-Glc*p*-(1→6)-D-Glc (2^3-α-D-glucosylisomaltotriose, Figure 19), which also concurs with the negative mode MS data.

Hexasaccharide (WCBIM6)

The 1D ^{1}H NMR spectrum of WCBIM6 (Figure 18) had six anomeric signals at δ_H 5.34 (d, $J_{1,2}$ 3.7 Hz), 5.32 (d, $J_{1,2}$ 3.7 Hz), 5.24 (d, $J_{1,2}$ 3.6 Hz), 4.99, 4.96 and 4.68 (d, $J_{1,2}$ 8.1 Hz) ppm, with an integral ratio of 0.2: 0.8: 0.4: 2.0: 1.8: 0.7, respectively. From the integral ratios, and considering that WCBIM6 is a hexasaccharide, the signal at 5.34 was considered to be an impurity. Similar to WCBIM4, the signals at δ_H 5.24 and 4.68 ppm were the α and β anomers of the (1→6)-linked reducing end glucosyl residue (Rα and Rβ). The signal at δ_H 5.32 ppm was for an elongated α-(1→3) branch point (residue B_1). This was substantiated by a correlation peak from the anomeric signal at δ_H 5.32 ppm to a bound C-3 (δ_C 82.3 ppm) on the HMBC spectrum (not shown) and the fact that it had a bound C-6 at δ_C 66.5 ppm. Furthermore, the H-5 chemical shift for this residue at δ_H 4.20 ppm was also unique, and has been established to be a structural reporter for a -α-(1→6)-α-D-Glc*p*-(1→3) unit (van Leeuwen et al. 2008a). The signal at δ_H 4.96 ppm was assigned

to two terminal non-reducing end α-(1→6)-linked glucosyl residues (A and A_1), while the signal at δ_H 4.99 ppm was for two unequivalent anomeric residues (3,6-*O*-disubstituted and 6-*O*-monosubstituted glucosyl residues B and C, respectively). The data therefore indicate that the structure of WCBIM6 was α-D-Glc*p*-(1→6)[α-D-Glc*p*-(1→6)-α-D-Glc*p*-(1→3)]-α-D-Glc*p*-(1→6)-α-D-Glc*p*-(1→6)-α-D-Glc (3^3-isomaltosylisomaltotetraose, Figure 19).

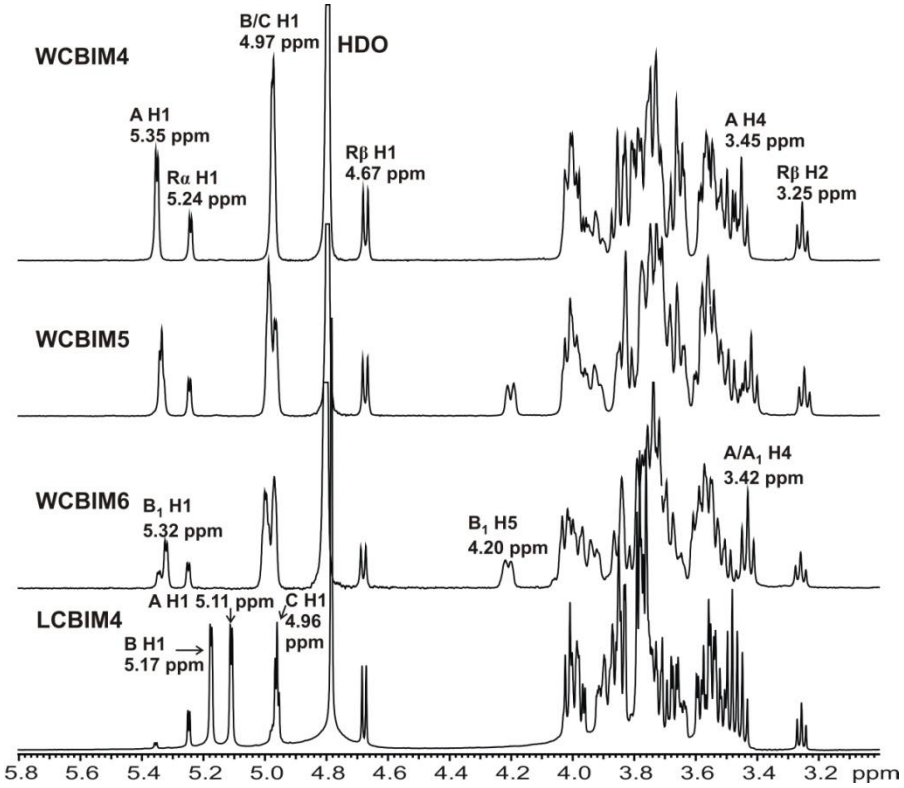

Figure 18. 1D ^{1}H spectra of WCBIM4-6 and LCBIM4 purified from the enzyme hydrolysate of *W. confusa* E392 and *L. citreum* E497 dextrans, respectively. The spectra were recorded at 500 MHz (WCBIM4-6) and 600 MHz (LCBIM4) in D_2O at 23°C. The peaks are referenced to internal acetone (δ_H = 2.225 ppm and δ_C = 31.55 ppm). Glucosyl residues are numbered A, B and C (main chain) and A_1 and B_1 (residues in the branches) from the non-reducing end, with the reducing end residue referred to as Rα/Rβ (see Figure 19).

Pentasaccharides (WCBIM5-1&2)

Conclusions could be drawn from the WCBIM4 and WCBIM6 assignments regarding the structure of the isomeric mixture in the pentasaccharide pool. The ^{1}H NMR spectrum of the mixture (Figure 18) showed six anomeric signals at δ_H 5.33 (d, $J_{1,2}$ 3.7 Hz), 5.32 (d, $J_{1,2}$ 3.7 Hz), 5.24 (d, $J_{1,2}$ 3.8 Hz), 4.98, 4.96 (d, $J_{1,2}$ 3.1 Hz) and 4.68 (d, $J_{1,2}$ 8.1 Hz) ppm. The signals at δ_H 5.24 and 4.68 ppm were assigned to the reducing end residues Rα and Rβ, respectively, and the signal at δ_H 4.96 ppm was assigned to the non-reducing end α-

(1→6)-α-D-Glc*p* terminal residue (A). The H-5 of the residue with an anomeric signal at δ_H 5.33 ppm occurred at 4.20 ppm, indicating that it is a -α-(1→6)-α-D-Glc*p*-(1→3)- unit. Unlike in WCBIM6, the anomeric proton at δ_H 5.32 ppm was for an α-(1→3)-linked terminal branch residue (A_1). This residue had an unbound C-6 at δ_C 61.6 ppm and it had an H-4 triplet signal at δ_H 3.45 ppm, which has been shown to be a structural reporter for terminal residues (van Leeuwen et al. 2008c). The single at δ_H 4.98 ppm was for two unequivalent residues, one with a bound C-6 and the other with an unbound C-6 (δ_c 66.6 and 61.6 ppm, respectively).

The data therefore showed that the isomeric pentasaccharides differed in the position of their α-(1→3)-linked glucosyl residue, one being a terminal branch unit and the other an internal residue. Based on NMR spectroscopy and methylation analysis data (data from LMBIM4-6 analogous to WCBIM4-6, Table 9), the structures of the pentasaccharides are most likely α-D-Glc*p*-(1→6)[α-D-Glc*p*-(1→3)]-α-D-Glc*p*-(1→6)-α-D-Glc*p*-(1→6)-α-D-Glc (3^3-α-D-glucosylisomaltotetraose) and α-D-Glc*p*-(1→6)-α-D-Glc*p*-(1→3)-α-D-Glc*p*-(1→6)-α-D-Glc*p*-(1→6)-α-D-Glc (3^3-isomaltosylisomaltotriose), henceforth referred to as WCBIM5-1 and WCBIM5-2, respectively. A schematic representation of the structures of WCBIM4-6 and LCBIM4 is shown in Figure 19.

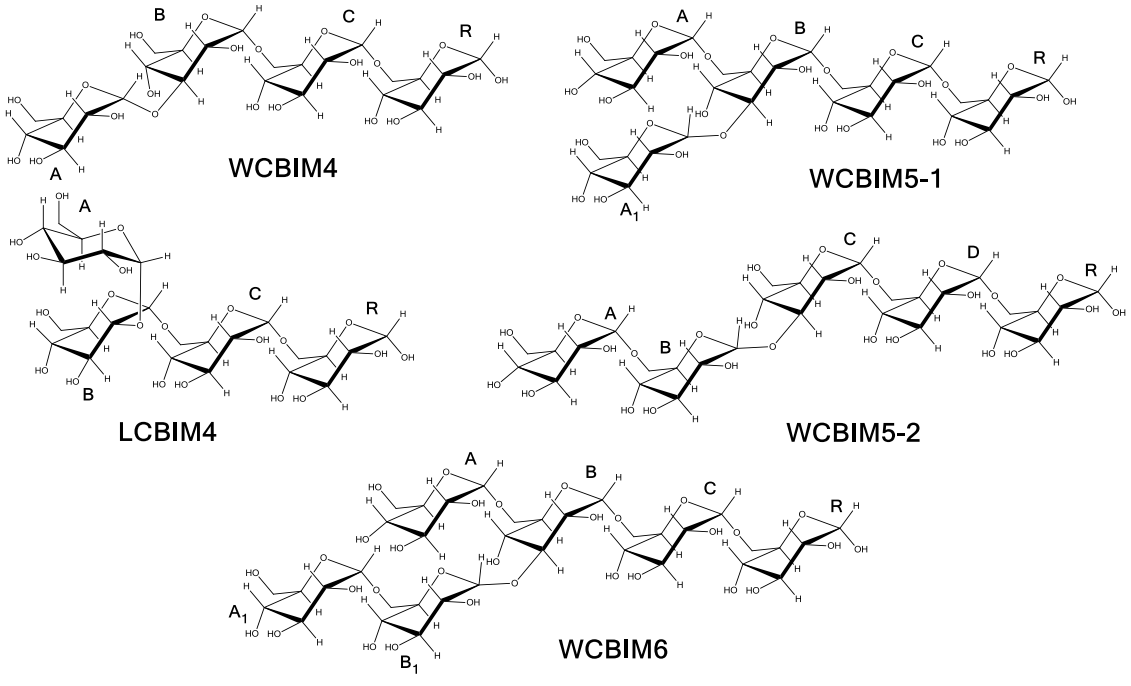

Figure 19. Structures of WCBIM4, WCBIM5-1, WCBIM5-2, and WCBIM6 obtained after enzymatic hydrolysis of *W. confusa* E392 dextran and LCBIM4 from enzymatic hydrolysis of *L. citreum* E497 dextran. The glucosyl residues are labeled A, B, C, D (main chain) and A_1, B_1, (residues in the branches) from the non-reducing end with the reducing end residue referred to as residue R in all cases.

5.5 Macromolecular characterization of the dextrans

The macromolecular properties of the isolated dextrans were determined in a comparative study involving HPSEC, AsFlFFF and DOSY. HPSEC was carried out in DMSO and aqueous solution to evaluate the effect of solvent on the macromolecular properties of the dextrans. DOSY was used for the first time to study HMM dextrans.

5.5.1 HPSEC and AsFlFFF

The HPSEC chromatograms (aqueous solution) and AsFlFFF fractograms of *W. confusa* E392 and *L. citreum* E497 dextrans are shown in Figure 20. The HPSEC chromatogram of *W. confusa* E392 dextran shows only one major peak for both RI and LS signals. The peak eluting between 17 and 19 minutes is for low molar mass materials in accordance with HPSEC elution theory. In the AsFlFFF fractogram of this sample, although only one major RI peak is observed, the LS peak is bimodal. The strong LS signal at higher retention times most likely originates from the large aggregates, which although present in low quantities scatter more light and therefore dominate the LS signal. It should be noted that in AsFlFFF the elution is in the order of increasing molar mass. Both the HPSEC chromatogram and the AsFlFFF fractogram of *L. citreum* E497 had only one major peak.

The macromolecular parameters of the samples based on these analyses are shown in Table 11. The values obtained with HPSEC in DMSO are also shown. HPSEC and AsFlFFF in aqueous solution gave similar M_w values for *W. confusa* E392 dextran (6.2 and 6.4 × 10^6 g/mol, respectively), while for *L. citreum* E497 dextran the results were significantly different (11.3 and 62.8 × 10^6 g/mol, respectively). HPSEC in DMSO gave lower M_w values than the values obtained with aqueous solution, 1.5 × 10^6 g/mol for *W. confusa* E392 dextran and 1.9 × 10^6 g/mol for *L. citreum* E497. The Mark-Houwink plot for dextran standards and samples (Figure 21) in both DMSO and aqueous solutions showed a curvature at HMM, indicating loss of self-similarity, most likely due to an increase in the length of branch linkages in the HMM dextrans.

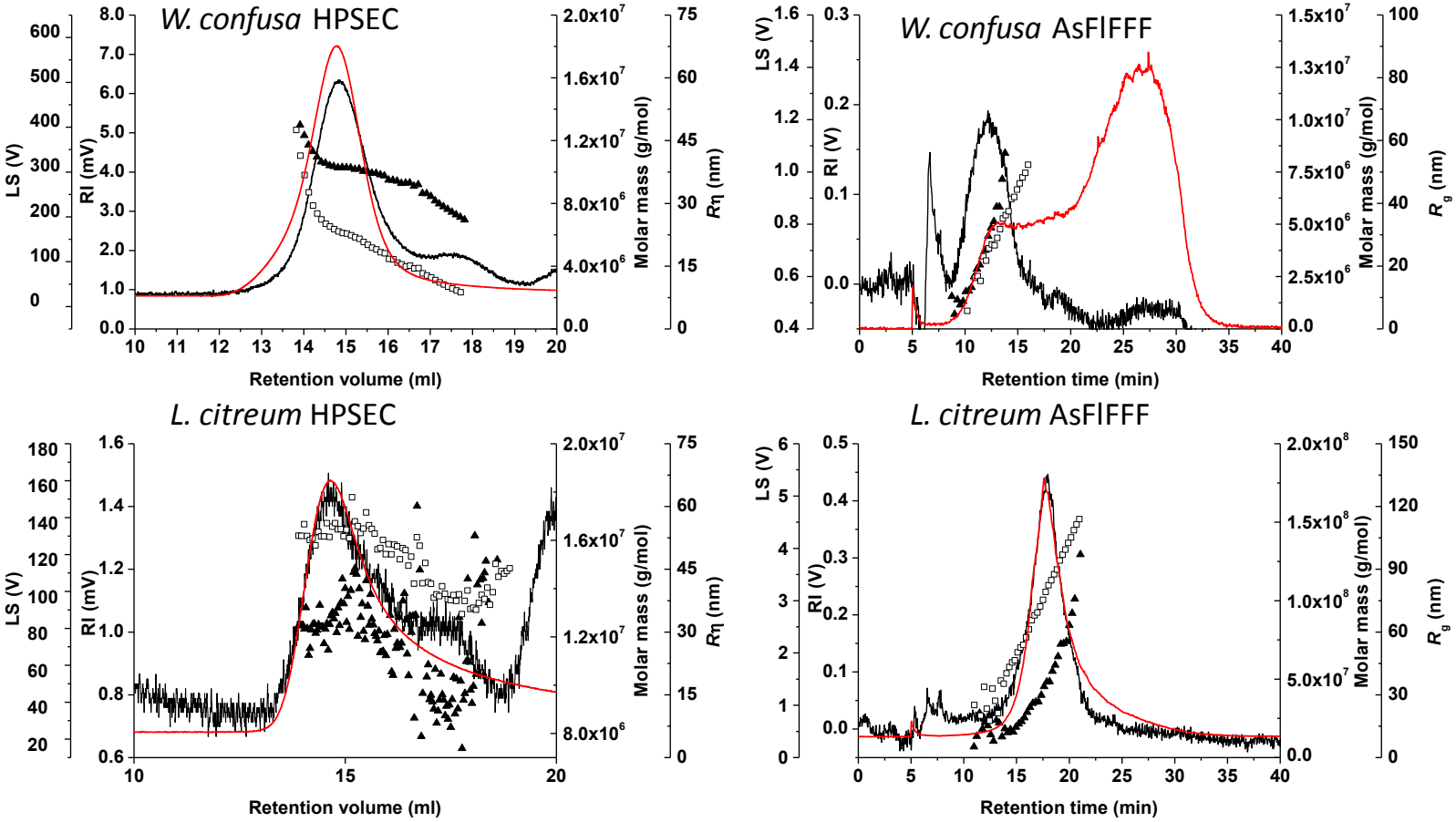

Figure 20. Refractive index (RI, black line) and light scattering at 90° (LS 90°, red line) profiles, from HPSEC and AsFlFFF analysis (aqueous solutions) of *W. confusa* E392 and *L. citreum* E497 dextrans. The molar mass distribution (triangles), viscometric radius (R_η) (HPSEC, squares) and radius of gyration (R_g) (AsFlFFF, squares) are also shown.

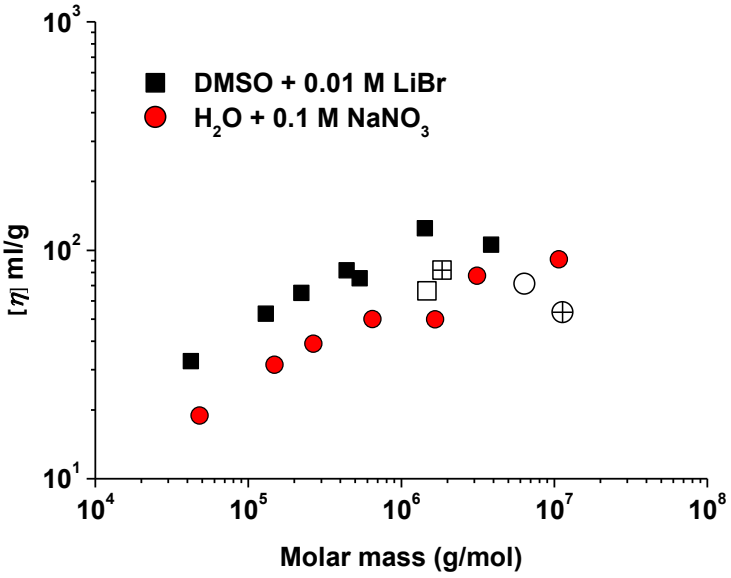

Figure 21. Mark-Houwink plot showing the relationship between the average molar mass (M_w) and average intrinsic viscosity ([η]) of the dextran standards and samples. The dextran from *W. confusa* E392 is marked with an open square (DMSO) and open circle (aqueous solution), and the dextran from *L. citreum* E497 with similar symbols containing a cross.

Table 11. Macromolecular properties of *W. confusa* E392 and *L. citreum* E497 dextrans determined with HPSEC, AsFlFFF and DOSY.

Sample	Method	$M_w \times 10^{-3}$ (g/mol)	M_w/M_n	[η] (ml/g)	R_h (nm)	R_g (nm)
W. confusa E392	HPSEC (DMSO)	1 473	1.08	66	24	51
	HPSEC (aq)	6 373	1.04	71	38	59
	AsFlFFF	6 168	1.84			30
	DOSY	23 860			55	
L. citreum E497	HPSEC (DMSO)	1 849	1.05	82	29	78
	HPSEC (aq)	11 330	1.05	65	45	54
	AsFlFFF	62 800	1.63			79
	DOSY	26 920			58	

5.5.2 DOSY

DOSY experiments were carried out at 300K using dilute solutions of the dextran standards and samples. To eliminate signal attenuation by convection and artifacts from gradient non-linearity, sample heights were kept below 4 cm and the BPPSTE pulse sequence that includes convection compensation (BPPSTE-CC) utilized. Overlaid DOSY

spectra from the dextran standards with nominal M_w of 150 000 g/mol (Dx 150), 670 000 g/mol (Dx 670) and *W. confusa* E392 dextran obtained with NMRnotebook are shown in Figure 22. The dextran standards had narrower peaks in the diffusion dimension than dextran isolated from *W. confusa* E392, probably due to the molecular dispersity of the isolated dextran sample. The *D* values for the dextran standards and samples obtained from the DOSY spectra ranged from 3.8—105 $\times 10^{-12}$ m^2s^{-1} and the calculated R_h values from 2.1—58 nm (Table 12). The *D* value for residual water (HDO) was the same for all the samples (~ 2.2 $\times 10^{-9}$ m^2s^{-1}).

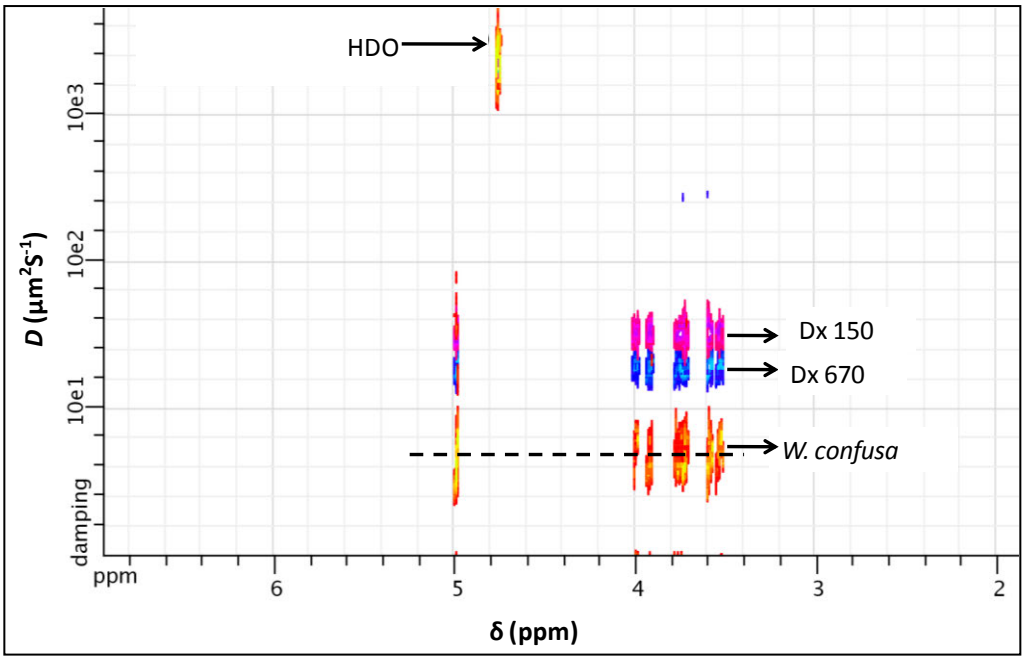

Figure 22. Overlaid DOSY spectra of the dextran standards with nominal molar mass of 150 000 g/mol (Dx 150), 668 000 g/mol (Dx 670) and the dextran produced by *W. confusa* E392. The DOSY data were measured at 300K in D_2O using the BPPSTE pulse sequence with convection compensation.

Figure 23 compares the calibration curve utilized in this study with that of Viel et al. (2003). The M_w of the dextran standards measured with light scattering, as specified by the manufacturer, gave the best calibration curve (Figure 23). For example, the M_w of Dx 490 (490 000 g/mol based on universal calibration with pullulan standards) distorted the calibration curve, whereas the value obtained with light scattering (1 520 000 g/mol) gave a better fit. The scaling parameters K and α (equation 2) obtained from the calibration curve were 5.47 × 10^{-9} and -0.425, respectively. The M_w values calculated from the DOSY data for *W. confusa* E392 and *L. citreum* E497 dextrans were 23.8 × 10^6 and 26.9 × 10^6 g/mol, respectively (Table 11).

Table 12. Diffusion coefficients (D) and hydrodynamic radii (R_h) of the dextran standards and samples determined with DOSY in D_2O at 300K.

Dextran[a]	Self-diffusion coefficient $D \times 10^{-12}$ (m^2s^{-1})[b]	Hydrodynamic radius R_h (nm)
Dx 12	104.7 ± 0.5	2.1
Dx 50	53.7 ± 0.2	4.1
Dx 150	32.6 ± 0.3	6.7
Dx 270	26.9 ± 1.1	8.2
Dx 490	13.9 ± 0.1	11.0
Dx 670	19.2 ± 0.1	15.8
Dx 3 500	9.6 ± 0.4	22.9
Dx 11 900	4.3 ± 0.1	51.1
W. confusa E392	4.0 ± 0.1	55.0
L. citreum E497	3.8 ± 0.1	57.9

[a]Dx 12 = Dextran 12 000 g/mol, [b] n = 3.

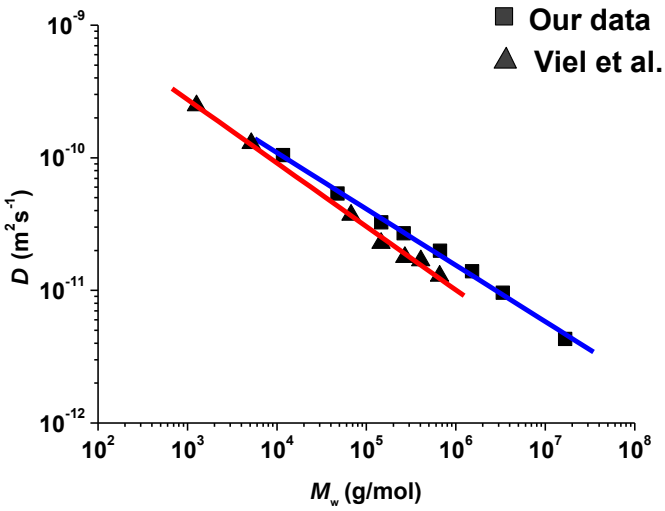

Figure 23. Double logarithmic plot of D values from the DOSY spectra against M_w of the dextran standards. Squares represent data obtained in this study, with the BPPSTE pulse sequence with convection compensation at 300K in D_2O. The M_w values measured with light scattering, according to the manufacturer's product sheets, were used in the calibration curve. The data of Viel et al. (2003) (triangles) obtained with the BPPSTE pulse sequence with a longitudinal eddy current delay at 300K are also shown.

5.6 *In situ* quantification of polymeric dextrans in dough

An enzyme-assisted assay to quantify dextran in sourdough was developed in this study. Preliminary tests showed that that *C. erraticum* dextranase did not have activity towards barley β-glucan or starch and was therefore specific to dextran hydrolysis. The yield of

glucose after hydrolysis of pure dextran with both dextranase and *A. niger* α-glucosidase was 68-70% for *W. confusa* E392 and commercial dextrans and only 29% for *L. citreum* E497 dextran. Thus further method development focused on *W. confusa* E392 dextran.

5.6.1 Dextrans in model dough

The average recovery of dextran from freeze-dried model doughs containing polymeric *W. confusa* E392 dextran was 51 ± 2%. Thus, an additional yield loss of about 20% occurred when dextran was present in a complex dough matrix. Therefore, the amount of dextran in freeze-dried sourdoughs was estimated using a correction factor of 2 (Figure12).

5.6.2 Dextran in sourdoughs

The amount of dextran in the sourdough samples is shown in Table 13. Since *Lb. brevis* does not synthesize dextran, the values obtained for its sourdoughs (0.15-0.18%) were considered as the assay background. This amount was also similar to that obtained when the sourdoughs fermented with *W. confusa* E392 did not contain sucrose (negative controls). Thus, taking into account this assay background (~0.2%), the amount of polymeric dextran produced by *W. confusa* E392 in the sourdoughs containing sucrose was between 1.1 and 1.6% (11-16 g/kg DW). As presented in Table 13, *L. mesenteroides* B-512F did not produce dextran since the level of dextran in its sourdough was similar to that of the assay background.

Table 13. Amount (% DW) of dextran produced *in situ* during sourdough fermentation.

Sourdough	Strains	Sucrose	Dextran[a,b] (% DW)
1	*W. confusa* E392	None	0.28 ± 0.07
2	*W. confusa* E392	10%	1.8 ± 0.1
3	*Lb. brevis*	None	0.18 ± 0.04[c]
4	*Lb. brevis*	10%	0.15 ± 0.01[c]
5	*W. confusa* E392	None	0.23 ± 0.06
6	*W. confusa* E392	10%	1.3 ± 0.1
7	*W. confusa* E392	10%	1.7 ± 0.1
8	*L. mesenteroides* B-512F	10%	0.19 ± 0.06

[a]The amount of monosaccharides was calculated as anhydro-glucose using a correction factor of 0.90. [b]The amount of dextran in the freeze-dried sourdoughs was calculated as shown in Figure 12. [c]Since *Lb. brevis* does not synthesize dextran, these values were considered to be the assay background. n = 3

5.7 Dextransucrase acceptor reaction products in sourdough

The presence of maltose in sourdough caused the formation of a series of oligosaccharides via the acceptor reaction mechanism of dextransucrases (Figure 24A). To estimate the content of these oligosaccharides, the free glucose background and glucose originating from maltooligosaccharides was determined in a sample that was only hydrolyzed with *B. stearothermophilus* α-glucosidase, which has specificity for α-(1→4) linkages (Figure 24B). As described in Figure 13, this value was subtracted from the amount of glucose obtained after hydrolysis of all GOS present, with dextranase and *A. niger* α-glucosidase (Figure 24C). Accordingly, the estimated amount of oligosaccharides formed by dextransucrase in sourdough 2 (Table 6) was 4.0% (40 g/kg DW).

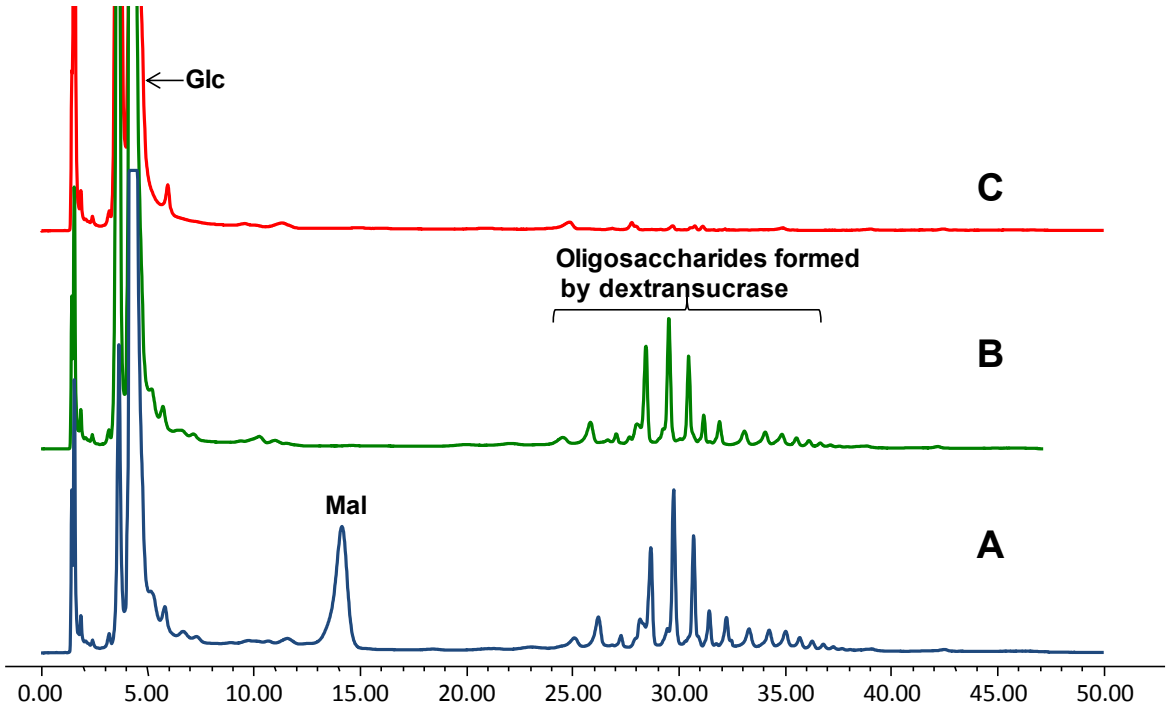

Figure 24. HPAEC-PAD chromatograms showing the profile of oligosaccharides in sourdough 2 (see Table 6): A) before enzyme hydrolysis, B) after hydrolysis with *B. stearothermophilus* α-glucosidase that has specificity for α-(1→4) linkages and C) after hydrolysis with dextranase and *A. niger* α-glucosidase.

6 Discussion

6.1 Structural features of native dextrans

The structural features of native dextrans were mainly determined from NMR spectroscopy data. Initial studies involved several *Weissella* and *Leuconostoc* strains with potential sourdough application. Subsequent studies, however, focused on *W. confusa* E392 and *L. citreum* E497 dextrans only, which were the most efficient dextran producers compared to the other *Weissella* and *L. citreum* strains. Two *L. mesenteroides* strains (B-512F and B-1415) that produce dextrans, and reuteran-producing *Lb. reuteri* ATCC 55730, were also included for comparison. As presented in Table 8, except for *Lb. reuteri* ATCC 55730 which produces reuteran, all the strains produced dextrans. The ratio of linkages in *Lb. reuteri* ATCC 55730 (83% α-(1→4) and 17% α-(1→6), Table 8) corresponded well with the values reported previously of 81% and 19%, α-(1→4) and α-(1→6) linkages, respectively (Kralj et al. 2005). The structural features of *Weissella* dextrans were distinctive in that they all contained a low degree of branching (< 3% α-(1→3)-linked branches). Bounaix et al. (2009) also found that *Weissella* strains isolated from sourdough produced dextrans with few branch linkages. This could possibly be a general feature of dextrans from *Weissella* species, and may also reflect a conservation of their glucansucrase gene family compared to *Leuconostoc* species. *Leuconostoc* species are known to produce a more diverse variety of dextrans with varying amounts and type of branch linkages, and even different structures such as alternans (Côté and Robyt 1982; Slodki et al. 1986)

The *L. mesenteroides* B-512F dextran contained 4% α-(1→3)-linked branches, which concurs with literature values (5% α-(1→3) linkages) (Larm et al. 1971; Cheetham et al. 1990). *L. mesenteroides* B-1415 dextran contained 7% α-(1→3)-linked branches and another 4% that were not determined. Contrary to this, previous studies show that dextran from this strain contains 14% α-(1→4)- and a negligible amount of α-(1→3)-linked branches (Abbott et al. 1966). As discussed later in section 6.3.2, the HPAEC-PAD retention times of the main BIMO from this strain resembled those of *W. confusa* E392, indicating a significant presence of α-(1→3)-linked branches in this dextran. The *L. citreum* strains produced dextrans with both α-(1→2)- and α-(1→3)-linked branches, although some of the linkages in *L. citreum* E504 were not identified (Table 8). Similar dextrans have also been reported for various *L. mesenteroides* strains such as NRRL B-1298, NRRL B-1299, NRRL B-1396, and NRRL B-1399 (Slodki et al. 1986).

A general observation on the dextran structures reported here and in the literature is that α-(1→3)-linked branches are almost always present, occurring as the only branches or in addition to α-(1→2)- or α-(1→4)-linked branches. Slodki et al. (1986) and Duenas-Chasco et al. (1998) have reported dextrans from *L. mesenteroides* NRRL B-1254 and *Lactobacillus* spp. G-77, respectively, that only contain α-(1→2)-linked branches. Dextrans with all types of branch linkages (α-(1→2)-, α-(1→3)- and α-(1→4)-linked branches) have also been reported previously (Slodki et al. 1986), although erroneous conclusions due to analytical artifacts, especially in early studies that only utilized chemical derivatization methods, cannot be ruled out. Furthermore, since more than one dextran can be produced by a single strain, it would be important to determine whether these branches occur within a single population of dextran molecules or whether they are part of different populations. As discussed in the case of *L. mesenteroides* NRRL B-742 dextrans, the proportion of different dextrans from a single strain may fluctuate depending on the fermentation conditions (Côté and Ahlgren 2000).

Previous studies that have reported more than one dextran from a single strain have utilized differential alcohol fractionation to separate the different fractions. According to Robyt (1986), in most cases, the less soluble fraction (L) precipitates at 36-37% alcohol, while the more soluble fraction (S) precipitates at 40-44% alcohol. For instance, *L. mesenteroides* NRRL B-1355 produces both alternan (S fraction) and dextran (L fraction) (Côté and Robyt 1982). In this case, structural analysis performed without fractionation would probably indicate a highly α-(1→3)-branched dextran due to the high content of α-(1→3) linkages in alternans.

The occurrence of α-(1→3)-linked branches in most dextrans may be ascribed to the fact that dextransucrases form these branch points at the same active site used for elongation of α-(1→6)-linkages in the dextrans (Robyt and Taniguchi 1976; Vujičić-Žagar et al. 2010). On the contrary, the α-(1→2)-linked branches require an additional catalytic site (Fabre et al. 2005) and are therefore only produced by specific dextransucrases. To the knowledge of this author, no dextrans with both α-(1→2)- and α-(1→4)-linked branches and no α-(1→3)-linked branches have been reported.

6.2 Enzymatic hydrolysis and chromatographic profiling of native dextrans

Dextran hydrolyzing enzymes were used to develop a quick method for profiling structural variation in dextrans, to obtain structural segments (BIMO) from *W. confusa* E392 and *L. citreum* E497 dextrans, and to develop an enzyme-assisted assay for dextran analysis (see

section 6.5). The action of the *C. erracticum* endodextranase used in this study was comparable to that of endodextranases reported previously (Khalikova et al. 2005). Glucose, IM2, IM3 and BIMO were the main reaction products of this endodextranase. However, IM3 was hydrolyzed to glucose and IM2 with prolonged hydrolysis (**II**).

The chromatographic profiles (HPAEC-PAD) of the BIMO were unique to the structural features of the hydrolyzed dextran (Figure 14). Therefore, enzyme-aided chromatographic profiling can be a very useful tool for screening the structural variation of dextrans produced by various strains or in different fermentation conditions. The procedure is straightforward and does not require excessive purification of the dextrans from other polysaccharides and macromolecules. As shown in paper **V,** Figure 1B, the profile of BIMO after *in situ* enzymatic hydrolysis of polymeric dextran was sufficient to indicate minimal structural changes in *W. confusa* E392 dextran produced in the complex sourdough environment. Enzyme-aided chromatographic profiling is also advantageous because the hydrolysis is reproducible. The versatility of this method can be improved if the structures of the BIMO are known and quantitative evaluation correlated to the type and degree of branching in a particular dextran. For example, LC analysis with HILIC coupled to online MS (with ESI) and evaporative light scattering detection would be the most ideal set-up for this purpose, to derive both structural and quantitative information in a single run. Efforts towards such a strategy are already in progress and the structures of some BIMO (section 6.3) are reported here. Additionally, a comprehensive study to evaluate the potential of MS in the structural analysis of the neutral underivatized BIMO is also included in this thesis.

6.3 Fine structure of the dextrans by analysis of BIMO

The fine structure of dextrans is not fully understood. Especially in NMR spectroscopy data of native HMM dextrans, signals from glucosyl residues in various chemical environments (Figure 4) may overlap (Table 2), leading to simplified conclusions on the structure of the dextran. In paper **I**, the signal at δ_H 5.32 ppm in the 1D ^{1}H spectra of *W. confusa* E392 and *L. citreum* E497 dextrans was not fully assigned due to its low abundance. However, there was enough evidence in the literature (Cheetham et al. 1990), to suggest that the dextrans contained both single unit and elongated α-(1→3)-linked branches. On the contrary, although previous studies have reported the elongation of α-(1→2)-linked glucosyl branches with α-(1→6)-linked glucosyl residues and also non-α-(1→6)-linked glucosyl residues in dextrans produced by *L. mesenteroides* NRRL B-1298 and B-1299 (Sidebotham 1974; Watanabe et al. 1980), the α-(1→2)-linked branches in *L. citreum* E497 dextran were single unit branches.

To further evaluate the nature of branch linkages in *W. confusa* E392 and *L. citreum* E497 dextrans, structural segments (BIMO) produced enzymatically were studied. BIMO from commercial dextran were also studied for comparison. Three major BIMO pools were obtained from *W. confusa* E392 and commercial dextrans (WCBIM4, WCBIM5 and WCBIM6, and LMBIM4, LMBIM5 and LMBIM6, respectively, paper **II**, Figure 2,) while fractionation of *L. citreum* E497 BIMO resulted in several impure fractions, except for LCBIM4 (Figure 15). WCBIM5 and LMBIM5 were composed of isomeric pentasaccharides (WCBIM5-1/LMBIM5-1 and WCBIM5-2/LMBIM5-2) and were analyzed without further purification.

6.3.1 Mass spectrometry analysis of fractionated BIMO

MS analysis of the BIMO was carried out as part of a comprehensive study to evaluate the possibility of unequivocally determining the glycosidic linkages in underivatized BIMO. Thus, several GOS, mannobiose and two galactooligosaccharides representing different glycoside linkage combinations were included in the study. Mannobiose and galacto-oligosaccharides were used, since the fragmentation patterns of hexoses are relatively similar.

The strategy for structural analysis of oligosaccharides by MS/MS involves sequential isolation and fragmentation of C-type fragment ions (Figure 6) that have one sugar unit less than the precursor molecular ion. Preferably, fragmentation should proceed in a stepwise manner with loss of glycosyl residues from the reducing end to the non-reducing end. The glycoside linkages are assigned by cross-ring cleavage of the reducing end residue. As shown in Table 10, the cross-ring cleavages depend on the glycoside linkage and are observed as a loss of 60, 90 or 120 Da in positive mode and as a loss of 60, 78, 90 or 120 Da in negative mode MS spectra. Thus, at each MS/MS stage the cross-ring cleavages of the ~~"n~~ew" reducing end residue in the isolated ion assigns the consecutive glycosidic linkages (Garozzo et al. 1990; Asam and Glish 1997).

Since the relative abundance of the fragment ions depends on the instrumentation, fragmentation method and adduct used, this study began by evaluating the typical cross-ring cleavages of reducing-end glycosyl residues using model disaccharides. The fragmentation behavior of the disaccharides observed here (Table 10) were in accordance with the results obtained in previous studies in both positive mode (Spengler et al. 1990; Hofmeister et al. 1991; Asam and Glish, 1997; Simoes et al. 2007; Zhang et al. 2008) and negative mode (Garozzo et al. 1990; Mulroney et al. 1995; Jiang and Cole 2005; Čmelík and Chmelík 2010).

The results from model oligosaccharides (trisaccharides and tetrasaccharides) showed that the reducing-end linkage of underivatized GOS can be deduced unambiguously from both positive and negative mode spectra. The remaining linkages, however, were only deducible from negative MS/MS spectra. The main drawback in positive mode was loss of glycosyl residues from the non-reducing end, leading to the formation of Y-type ions that were isomeric to the required C-type ions as illustrated in Figure 16. A disadvantage in negative mode was that the intensities of the fragment ions significantly reduced in MS/MS analysis, which limited the number of MS/MS cycles attainable (**III**).

In this MS/MS study, only BIMO containing one non-reducing end (WCBIM4 and LCBIM4) were included. More studies with model compounds are needed to determine the fragmentation behavior of trifunctional branch points (disubstituted residues) in GOS. The structure of WCBIM4 deduced from negative mode MS spectra was 3^3-α-D-glucosylisomaltotriose, while LCBIM4 was 2^3-α-D-glucosylisomaltotriose. These structures were also confirmed by NMR spectroscopy.

6.3.2 NMR spectroscopy analysis of fractionated BIMO

NMR spectroscopy analysis confirmed that BIMO from *W. confusa* E392 dextran (WCBIM4-6) and commercial dextran (LMBIM4-6) were similar. WCBIM4 contained an α-(1→3)-linked glucosyl unit at the non-reducing end (3^3-α-D-glucosylisomaltotriose). The isomeric pentasaccharides included one with a terminal α-(1→3)-linked branch unit (3^3-α-D-glucosylisomaltotetraose, WCBIM5-1) and another with an internal α-(1→3)-linked glucosyl residue (3^3-isomaltosylisomaltotriose, WCBIM5-2). The hexasaccharide (WCBIM6) had an α-(1→3)-linked isomaltosyl branch unit (3^3-isomaltosylisomaltotetraose). These findings were in agreement with the studies by Taylor et al. (1985), as discussed in paper **II**. The terminal α-(1→3)-linked glucosyl units in WCBIM4 and WCBIM5-1 originated from the single unit branch points, while the α-(1→3)-linked isomaltosyl units in the WCBIM5-2 and WCBIM6 originated from α-(1→3)-linked side chains elongated by two or more α-(1→6)-linked glucosyl residues in the native *W. confusa* E392 dextran. Although WCBIM6 clearly originates from elongated branches, WCBIM5-2 could also originate from internal α-(1→3)-linked residues (3-O-monosubstituted glucosyl units, residues D, Figure 4).

The BIMO fractions from *W. confusa* E392 dextran and commercial dextran represented α-(1→3)-linked glucosyl residues in four chemical environments (Figure 19): 1) an α-(1→3) linkage at the non-reducing end with a characteristic anomeric signal at δ_H 5.35 ppm (WCBIM4), 2) an α-(1→3) linkage in a single unit branch point (WCBIM5-1, anomeric signal at δ_H 5.32 ppm), 3) an α-(1→3)-linked internal glucosyl residue (between

α-(1→6)-linked glucosyl residues, WCBIM5-2, anomeric signal at δ_H 5.33 ppm), and 4) an α-(1→3) linkage at a branch point that is further elongated by α-(1→6)-linked glucosyl residues (WCBIM6, anomeric signal at δ_H 5.32 ppm). This clearly shows that based on anomeric signals, distinction of α-(1→3)-linked glucosyl residues in different chemical environments is challenging. However, the H-5 signal of α-(1→3)-linked internal residues and α-(1→6)-elongated branches occurs at δ_H 4.20 ppm and can therefore be used to substantiate their existence. This unique H-5 at δ_H 4.20 ppm has been previously established as a structure reporter for α-(1→6)-α-D-Glc*p*-(1→3)-structural units (van Leeuwen et al. 2008a). As shown in paper **II** (Figure 3), a similar signal (occurring at δ_H 4.19 ppm) is present in the ^{1}H 1D spectrum of the native *W. confusa* E392 dextran.

When considering the HPAEC-PAD profile of BIMO shown in Figure 14, except for *L. citreum* E497 and *Lb. reuteri* ATCC 55730, the retention times of BIMO from the dextrans of the other strains are relatively similar, differing mainly in the ratio of some of the peaks. In paper **II,** it was suggested that the first peak eluting between 26 and 29 min is WCBIM5-2 and the second is WCBIM5-1. Since WCBIM5-1 originates from single unit branches and WCBIM5-2 is from elongated branch points or α-(1→3)-linked internal residues, the ratio of these peaks in *L. mesenteroides* B-1415 and *L. citreum* E504 BIMO suggests that the native dextrans of these strains contain more single unit branches than the latter type of α-(1→3)-linked residues. In contrast, *W. confusa* E392 dextrans and commercial dextran contain more elongated branch points or α-(1→3)-linked internal residues. Larm et al. (1971) found that *L. mesenteroides* B-512F dextran contains at least 40% single unit α-(1→3)-linked branches and a total of 60% α-(1→3)-linked branches elongated by two or more α-(1→6)-linked glucosyl residues. These figures correspond well with the higher content of LMBIM5-2 than LMBIM5-1 observed here (Figure 14). Thus, since enzyme hydrolysis is reproducible, it is possible to correlate quantitative analysis of BIMO produced enzymatically with the structure of the dextran.

6.3.3 BIMO from *L. citreum* E497 dextran

Fractionation of BIMO in the Biogel P2 column occurs in accordance with their polymerization degree (DP). BIMO from *L. citreum* E497 dextran occurred in several fractions containing more than one oligosaccharide except for LCBIM4 (Figure 15). Both MS/MS analysis and NMR spectroscopy data confirmed that LCBIM4 was a tetrasaccharide with an α-(1→2)-linked glucosyl residue at the non-reducing end (Figure 19, 2^3-α-D-glucosylisomaltotriose). Fraction LCBIMO-D was composed of two tetrasaccharides. Based on their HPAEC-PAD retention times (Figure 15), the first one is analogous LCBIM4 and the second one is similar to WCBIM4 (3^3-α-D-glucosylisomaltotriose).

Fraction LCBIMO-C was composed mainly of pentasaccharides according to ESI-MS analysis (not shown). Purification of this fraction by anion exchange (not shown) has been successful, and structural analysis of the first peak eluting between 23 and 25 min (HPAEC-PAD) indicates that it contains a single unit α-(1→2)-linked branch point. The remaining two peaks are still under investigation, although their retention time suggests that they are similar to WCBIM5-1 and WCBIM5-2. A peak eluting at the same time as WCBIM6 can also be seen in LCBIMO-B (Figure 15). These findings concur with the presence of both α-(1→2) and α-(1→3) linkages in the native *L. citreum* E497 dextran and therefore fractionation of the BIMO based on DP enabled visualization of BIMO from each type of branch point. Analysis of the remaining fractions will confirm whether any of the α-(1→2) linkages are elongated.

6.4 Macromolecular properties of the native dextrans

The macromolecular features of the dextrans were determined in both aqueous and DMSO solutions to determine the possible effects of the solvent on their solution properties. In addition, the macromolecular properties were determined with different methods, two involving fractionation of the sample (HPSEC and AsFlFFF) and one without fractionation (DOSY).

6.4.1 HPSEC and AsFlFFF

In general, the HMM dextran solutions (both aqueous and DMSO) were cloudy, indicating the presence of undissolved material. The low solubility of the HMM samples was also reflected in the low sample recovery (< 50%) in both solvents; consequently, the solutions were not representative of the whole sample. Irague et al. (2012) recently reported better recoveries (> 71%) for HMM dextrans (up to 10^8 g/mol) produced by cell-free enzymatic synthesis with mutant dextransucrases. Notably, the high recoveries may have been obtained by Irague et al. (2012) because the solutions were analyzed directly from the reaction media without precipitation or freeze-drying.

As shown in Table 11, the obtained molar mass values differed depending on the solvent or method used. In DMSO, the molar mass of *W. confusa* E392 and *L. citreum* E497 dextrans were lower and not significantly different (1.5×10^6 and 1.9×10^6 g/mol, respectively) from the values obtained with aqueous solution in HPSEC (6.4×10^6 and 11.3×10^6 g/mol, respectively) and especially in AsFlFFF (6.2×10^6 and 62.8×10^6 g/mol,

respectively). These discrepancies in molar mass result from a contribution of several factors, of which aggregation plays a major role.

As reviewed in section 2.4.1, poor solubility, local polydispersity, and the presence of aggregates in dextran solutions complicate evaluation of their macromolecular properties. Although DMSO is considered a better solvent for dissolution of α-glucans, the results obtained in this study indicated a tendency of the HMM dextran to aggregate even in DMSO (paper **IV**, Figure 5). Despite this time-dependent aggregation, the lower molar mass values of these dextrans in DMSO were considered to reflect the molar mass of individual dextran chains, while values obtained in aqueous solution were mainly from aggregates. In both solvents, R_g, R_h were higher for *L. citreum* E497 dextran than for *W. confusa* E392 dextran, which coincides with the higher M_w value of *L. citreum* E497 dextran. The [η] for the dextran samples were higher in DMSO than in water (Table 11), indicating a more extended solution conformation of the dextrans in DMSO.

In his conclusion on light scattering of polysaccharides, Burchard (2005) noted that aggregates in polysaccharide solutions are metastable and do not dissociate even at the lowest concentrations. He additionally concluded that whether the aggregates dissociate in HPSEC due to high shear or they are simply filtered away is still uncertain (Burchard 2005). Recent findings have also demonstrated the degradation of HMM polysaccharides such as alternan due to the high shear in HPSEC (Cave et al. 2009; Striegel et al. 2009). Thus shear dissociation and/or shear degradation of the aggregates may explain the lower molar mass values obtained in HPSEC compared to AsFlFFF where samples are separated in an open column with minimal shear. In the case of *W. confusa* E392, however, both HPSEC and AsFlFFF gave similar molar mass values (6.4×10^6 and 6.3×10^6 g/mol, respectively). This may arise because some of the aggregates in this sample were separated in AsFlFFF analysis (Figure 20). It should be noted that even at low concentrations, the aggregates dominate the LS signal (Figure 20) and therefore the molar mass value calculated when aggregates are not resolved in HPSEC or AsFlFFF analysis is predominantly that of the aggregates.

As a consequence, the presence of aggregates in dextran solutions results in over-estimation of their molar mass values, which can lead to incorrect conclusions on the functionality of dextrans. As an example, Tirtaatmadja et al. (2001) indicated that a 2.0×10^6 g/mol commercial *L. mesenteroides* B512F dextran showed Newtonian behavior at a concentration of 30% w/v, which they therefore related to the presence of elongated branches (ramification). Nonetheless, it is likely that the molar mass of this sample is skewed by the presence of aggregates. AsFlFFF analysis of a similar commercial dextran preparation (paper **IV,** Figure 2), which is also reported to have an M_w of 2.0×10^6 g/mol

by the manufacturer, resolved the aggregates and individual chains in the sample. The individual chains had a higher concentration according to the RI signal and, therefore, the effective M_w of the sample when aggregates were not considered was ~500 000 g/mol. In another example, although the non-linear Kuhn and Mark-Houwink plot (Figure 21) is mainly attributed to an increase in branch linkages with increasing molar mass (i.e., the molecules are no longer self-similar), the presence of compact aggregates in the solutions analyzed may also contribute to the non-linearity.

6.4.2 DOSY

Compared to HPSEC and AsFlFFF, DOSY gave relatively similar molar mass values for *W. confusa* E392 and *L. citreum* E497 (23.9×10^6 and 26.9×10^6 g/mol, respectively, Table 11). The D_2O solutions used in this analysis most likely contained aggregates and, therefore, true *D* values for single chains were not determined. As the samples were polydisperse, the *D* values and corresponding molar mass values obtained in DOSY are a statistical average of their distribution (Callaghan and Pinder 1983). Overall, the magnitude of these values (10^7) was in satisfactory agreement with molar mass values obtained with aqueous HPSEC and AsFlFFF, indicating that DOSY can be used to estimate the molar mass of HMM dextrans. This result compliments the findings of Viel et al. (2003) on the versatility of DOSY to assess the molar mass of neutral uncharged polysaccharides. In the study of Viel et al. (2003), dextran and pullulan standards with a lower mass range (1270-853 000 g/mol) were used.

A comparison of the calibration curves determined here and by Viel et al. (2003) shows that they are parallel (Figure 23) to each other and therefore gave different scaling parameters (K and α, Equation [4]). This may have resulted from systematic errors in either of the studies, possibly because of differences in the pulse sequences utilized and other instrumental factors. In this study, keeping the sample height below 4 cm did not eliminate signal attenuation by convection and, therefore, a pulse sequence that included a convection compensation element was utilized. Thus, even though several studies (Suárez et al. 2006; Säwén et al. 2010) have relied on the scaling parameters obtained by Viel et al. (2003) using pullulan standards ($K = 8.2 \times 10^{-9}$ m^2s^{-1} and $\alpha = -0.49$), the results obtained here suggest that it may be necessary to determine these parameters for each experimental set-up. The scaling parameters obtained here were 5.47×10^{-9} and -0.425, respectively, and are comparable to the results of Politi et al. (2006) ($K = 4.24 \times 10^{-9}$ m^2s^{-1} and $\alpha = -0.417$) obtained with dextran standards ranging from 10 000 to 500 000 g/mol.

6.5 *In situ* analysis of dextrans produced during sourdough fermentation

In situ production of dextran in sourdough can easily be affected by factors such as contamination of the sourdough with microbes that compete for the added sucrose. Thus a simple method to evaluate the amount of dextran produced in sourdough would be highly beneficial for quality control. In this study, an enzyme-assisted assay to specifically quantify dextran in sourdough was developed. The enzymes included *C. erracticum* endodextranase and *A. niger* α-glucosidase, which hydrolyzed dextran to glucose and BIMO. As indicated in the results, with these enzymes it was only feasible to develop the assay for *W. confusa* E392 dextran, since the recovery of glucose from *L. citreum* E497 dextran was only 29%. Utilization of another commercially available *Penicilium* sp. endodextranase (not shown) did not further improve the yield from either of the dextrans. The assay developed is only semi-quantitative, since the recovery of *W. confusa* E392 dextran in freeze-dried model doughs was only 51%. The lower recovery may be attributed to formation of complexes between dextrans and dough components such as proteins and starch that hinder the accessibility of the enzymes to the dextran chains. Preliminary tests carried out with model doughs without freeze-drying (not shown) gave better recoveries, although the standard deviations are higher. In future studies, debranching enzymes or *A. globiformis* T6 isomaltodextranase, for example, may be added to the enzyme cocktail for more efficient hydrolysis of dextrans — even those containing a high degree of branching.

Using the developed assay, the level of dextran produced by *W. confusa* E392 in 17 and 24 h sourdough fermentation was between 1.1 and 1.6% DW (11-16 g/kg), which was 3.4-3.9% less than the theoretical maximum (5%) synthesizable from 10% sucrose. This amount of dextran produced *in situ* by *W. confusa* E392 and the corresponding yield (% of glucose in sucrose converted to dextran, 22-32%) were significantly higher than reported previously (Table 4). The highest amount of dextran (1.6%) was obtained with 24 h fermentation (sourdough 2, Table 13). However, a comparable amount (1.5%) was obtained with horizontal shaking during 17 h of fermentation (sourdough 7, Table 13).

As discussed in paper **V,** *W. confusa* E392 concomitantly produced oligosaccharides and dextrans in sourdough (paper **V,** Figure 3). Similar oligosaccharides have also been described previously (Kaditzy and Vogel 2008; Schwab et al. 2008). The oligosaccharides contained maltose (paper **V**, Figure 3), most likely at the reducing end as demonstrated by Dols et al. (1997). Preliminary studies on these dextransucrase acceptor reaction products indicated that sourdough 2 (Table 6) contained 4.0% DW (40 g/kg) oligosaccharides (Figure 24). This amount clearly accounts for the glucose that is not converted to

polymeric dextran during sourdough fermentation, although a procedure to correct for maltose in these oligosaccharides would be required for a more accurate result.

The technological benefits of the sourdoughs containing *W. confusa* E392 dextran in wheat bread baking are described in detail in paper **V**. The breads had an improved specific volume, softness and shelf life compared to control breads without sourdough and bread containing sourdoughs with no dextran. Dextran-containing *W. confusa* E392 sourdough was not very acidic, which therefore did not override the positive technological and sensory properties of the final bread (**V**). The impact of the significant amount of oligosaccharides from sucrose is still not known. As reported for maltooligosaccharides, these acceptor reaction oligosaccharides may play a role in improving the shelf life of the breads as anti-staling agents (Leon et al. 2002). Sourdoughs containing *L. citreum* E497 dextran have also been tested. Despite the technological benefits, the breads had inadequate texture and flavor properties due to high acidification by this strain (unpublished results). Thus *W. confusa* E392 has a higher potential in wheat sourdough applications than *L. citreum* E497.

As indicated in the literature review, relating the structural features of dextrans to their functionality in sourdough or any other application entails accurate determination of the structural, macromolecular and rheological properties of the dextrans. From a structural perspective, the studies here show that a few branches do not necessarily equate to a very linear dextran. The α-(1→3) linkages in both *W. confusa* E392 and *L. citreum* E497 dextrans are elongated, though the actual length of these branches, which plays a crucial role in the functionality of dextrans (Tirtaatmadja et al. 2001), is still unknown. In the future, an α-(1→3) debranching enzyme that should act on polymeric dextran and have no activity towards α-(1→6) linkages could be employed for this purpose. The debranched dextrans can then be analyzed by HPSEC or AsFlFFF to determine the molar mass of the obtained fragments. Such a debranching enzyme, however, has not been reported to the knowledge of this author.

From a macromolecular perspective, the results obtained here with dextrans produced in simple MRS-S media may not fully reflect the properties of dextrans obtained *in situ* during sourdough fermentation. Although the profile of BIMO obtained after hydrolysis of *W. confusa* E392 dextran in sourdough indicated minimal structural changes (paper **V**), the dextransucrase acceptor reactions with maltose may compromise the molar mass of dextrans produced *in situ*. The results here show that the aqueous dextran solutions used in macromolecular characterization contained aggregates. Even at low concentrations, the aggregates dominated the LS signal and therefore cause over-estimation of the molar mass values obtained, which further complicates deduction of the functionality of the dextrans.

Thus, relating the structural and macromolecular properties of *W. confusa* E392 and *L. citreum* E497 dextrans to their functionality in sourdoughs requires further research. Nonetheless, the studies here provide foundational information on the dextrans produced by the strains and also provide insight into the challenges involved in determining the structural and macromolecular properties of HMM dextrans.

7 Conclusion

In this study, dextrans from strains with a potential use in sourdough were investigated. The research focused on the structural and macromolecular properties of dextrans produced by *W. confusa* E392 and *L. citreum* E497 to understand their functionality in sourdough. Enzymatic hydrolysis was used to develop a method for screening the structural variations in dextrans, to obtain BIMO used in evaluating the fine structure of the dextrans, and finally to aid quantification of dextrans in sourdough. Enzyme hydrolysis was preferred in this study because it is repeatable and thus quantitative analysis of the BIMO can be correlated to the structure of the dextran and can also be used for assessing structural changes in dextran produced in complex media.

Structural elucidation of dextrans by NMR spectroscopy, which has been used in several studies previously, is revisited in this thesis. The results clearly showed, in agreement with past research, that the structure of dextran is complex, tending towards a ramified structure even when there are few branch linkages. Analysis of BIMO evidenced the presence of elongated α-(1→3)-linked branches in *W. confusa* E392 and *L. citreum* E497 dextrans. In the spectra of native dextrans, the H-5 signal at 4.20 ppm can be used to substantiate the presence of elongated branches and/or α-(1→3)-linked internal glucosyl residue. Nevertheless, it is still not possible to establish whether the branches are elongated by two or more residues using this signal.

In the thesis, the possibility of using MS in the study of structural segments was explored. MS-based analysis would be a highly effective method, especially when coupled with liquid chromatography separation, to establish both the profile and structure of oligosaccharides in, for example, the enzyme hydrolysate used in this study. In a comprehensive study, this thesis demonstrates that despite the high MS/MS efficiency in positive mode, loss of non-reducing end residues via glycoside bond is a major drawback to structure elucidation. On the other hand, though negative mode provided solid data to unequivocally determine the structures of the oligosaccharides included in the study, its MS/MS efficiency was low. In the present study, the focus was mainly on branched oligosaccharides with a linear arrangement (i.e. they only had one non-reducing end). We can, however, anticipate that, for oligosaccharides with more than one non-reducing end, loss of branch point residues via glycoside bond cleavage will occur and strategies to overcome this hurdle are needed.

Macromolecular characterization of the dextrans produced by the strains was carried out in a comparative study that involved different solvents and methods. The challenge in this

study was the poor solubility of freeze-dried dextrans and the presence of aggregates in the samples analyzed. DMSO disrupted the aggregates and is therefore considered the solvent of choice when the molar mass of individual chains is required. However, as demonstrated with *W. confusa* E392 dextran, the DMSO solutions were metastable and seemed to aggregate with time. In this study, DOSY was used for the first time to determine the molar mass of HMM dextrans. The method gave promising results and can therefore be used as an alternative when HPSEC or AsFlFFF equipment is not available. With this method, the same sample can be used for structural, hydrodynamic radius and molar mass analysis.

At present, there is no commercially available specific enzyme assay for dextran quantification. Such a kit would be useful in quality control when dextran is produced *in situ* during sourdough or any other food fermentation process. However, several enzymes are required to completely convert dextran to quantifiable glucose. In this thesis, the enzyme-aided assay developed is semi-quantitative due to the low recovery of dextran from freeze-dried sourdough and is limited to dextrans with less than 5% α-(1→3) branching. In the future more enzymes may be included in the cocktail for more efficient hydrolysis of highly branched dextrans.

As shown here, few branches in dextrans does not automatically equate to a very linear dextran, which, as proposed in the literature, is a desirable feature for more effective functionality in sourdough applications. Possibly the size (R_g and R_h) or [η], which reflect the shape and conformation of the dextrans, are more appropriate parameters to consider when comparing the structure-function relationship of different dextrans in sourdough applications. Determination of these parameters is, however, a challenge, as the solutions of HMM dextrans can contain both individual dextran chains and compact aggregates. Nonetheless, since sourdough is an aqueous system, the functionality of dextran may result from a contribution of both the individual chains and aggregates. The preliminary study on oligosaccharides, produced concomitantly with dextrans in sourdough, showed that a significant amount of the glucose from sucrose is used in the acceptor reactions. Thus, the role of these oligosaccharides in improving the technological properties of sourdough bread should also be considered.

REFERENCES

Abbott D, Bourne EJ, Weigel H. 1966. Studies on dextrans and dextranases. 8. Size and distribution of branches in some dextrans. J Chem Soc C 9:827-831.

Antalek B. 2002. Using pulsed gradient spin echo NMR for chemical mixture analysis: How to obtain optimum results. Concepts Magn Reson 14:225-258.

Arendt EK, Ryan LAM, Dal Bello F. 2007. Impact of sourdough on the texture of bread. Food Microbiol 24:165-174.

Asam MR, Glish GL. 1997. Tandem mass spectrometry of alkali cationized polysaccharides in a quadrupole ion trap. J Am Soc Mass Spectrom 8:987-995.

Barrère C, Mazarin M, Giordanengo R, Phan TNT, Thvand A, Viel S, Charles L. 2009. Molecular weight determination of block copolymers by pulsed gradient spin echo NMR. Anal Chem 81:8054.

Basedow AM, Ebert KH, Ruland U. 1978. Specific refractive index increments of dextran fractions of different molecular weights. Makromol Chem 179:1351-1353.

Blakeney AB, Harris PJ, Henry RJ, Stone BA. 1983. A simple and rapid preparation of alditol acetates for monosaccharide analysis. Carbohydr Res 113:291-299.

Bobrow-Strain A. 2008. White bread bio-politics: purity, health, and the triumph of industrial baking. Cultural Geographies 15:19-40.

Boels IC, Kranenburg Rv, Hugenholtz J, Kleerebezem M, de Vos WM. 2001. Sugar catabolism and its impact on the biosynthesis and engineering of exopolysaccharide production in lactic acid bacteria. Int Dairy J 11:723-732.

Bohn RT, 1961. Addition of dextran to bread doughs, US Patent 2983613.

Bounaix M, Gabriel V, Morel S, Robert H, Rabier P, Remaud-Simeon M, Gabriel B, Fontagne-Faucher C. 2009. Biodiversity of exopolysaccharides produced from sucrose by sourdough lactic acid bacteria. J Agric Food Chem 57:10889-10897.

Bovey FA. 1959. Enzymatic polymerization. I. Molecular weight and branching during the formation of dextran. J Polym Sci A Polym Chem 35:167-182.

Burchard W. 1999. Solution properties of branched macromolecules. Adv Polym Sci 143:113-194.

Burchard W. 2005. Light scattering from polysaccharides. In: Dumitriu S, Eds. Polysaccharides -Structural diversity and functional versatility. Second Edition. Marcel Dekker, NY, USA. pp. 189-252.

Callaghan PT, Pinder DN. 1983. A pulsed field gradient NMR study of self-diffusion in a polydisperse polymer system: Dextran in water. Macromolecules 16:968-973.

Carnevali P, Ciati R, Leporati A, Paese M. 2007. Liquid sourdough fermentation: Industrial application perspectives. Food Microbiol 24:150-154.

Cave RA, Seabrook SA, Gidley MJ, Gilbert RG. 2009. Characterization of starch by size-exclusion chromatography: The limitations imposed by shear scission. Biomacromolecules 10:2245-2253.

Chai W, Piskarev V, Lawson AM. 2001. Negative-ion electrospray mass spectrometry of neutral underivatized oligosaccharides. Anal Chem 73:651-657.

Cheetham NWH, Fiala-Beer E, Walker GJ. 1990. Dextran structural details from high-field proton NMR spectroscopy. Carbohydr Polym 14:149-158.

Chen A, Wu D, Johnson CS. 1995. Determination of molecular weight distributions for polymers by Diffusion-Ordered NMR. J Am Chem Soc 117:7965-7970.

Chung CH, Day DF. 2002. Glucooligosaccharides from *Leuconostoc mesenteroides* B-742 (ATCC 13146): A potential prebiotic. J Ind Microbiol Biotechnol 29:196.

Ciucanu I, Kerek F. 1984. A simple and rapid method for the permethylation of carbohydrates. Carbohydr Res 131:209-217.

Claudio P. 2006. The universe of food quality. Food Qual Prefer 17:3-8.

Čmelík R, Chmelík J. 2010. Structural analysis and differentiation of reducing and non-reducing neutral model starch oligosaccharides by negative-ion electrospray ionization ion-trap mass spectrometry. Int J Mass Spectrom 291:33-40.

Côt GL. 2002 Alternan. In: Vandamme EJ, De Baets S, Steinbuchel A. Eds. Biopolymers. Polysaccharides I: polysaccharides from prokaryotes. Wiley-VCH, Weinheim, Germany, pp. 232− 350.

Côte GL, Ahlgren JA. 2000. Microbial Polysaccharides. Kirk-Othmer Encyclopedia of Chemical Technology. John Wiley & Sons, Inc.,

Côté GL, Robyt JF. 1982. Isolation and partial characterization of an extracellular glucansucrase from *Leuconostoc mesenteroides* NRRL B-1355 that synthesizes an alternating (1→6), (1→3)-α-d-glucan. Carbohydr Res 101:57-74.

De Belder AN. 1993. Dextran. In: Whistler RL, BeMiller JN. Eds. Industrial Gums: Polysaccharides and their derivatives. Academic Press, San Diego, pp. 399-425.

De Vuyst L, Degeest B. 1999. Heteropolysaccharides from lactic acid bacteria. FEMS Microbiol Rev 23:153-177.

De Vuyst L, Neysens P. 2005. The sourdough microflora: biodiversity and metabolic interactions. Trends Food Sci Technol 16:43-56.

Decock P, Cappelle S. 2005. Bread technology and sourdough technology. Trends Food Sci Technol 16:113-120.

Delsuc MA, Malliavin TE. 1998. Maximum Entropy Processing of DOSY NMR Spectra. Anal Chem 70:2146-2148.

Di Cagno R, De Angelis M, Limitone A, Minervini F, Carnevali P, Corsetti A, Gaenzle M, Ciati R, Gobbetti M. 2006. Glucan and Fructan Production by Sourdough *Weissella cibaria* and *Lactobacillus plantarum*. J Agric Food Chem 54:9873-9881.

Dols M, Simeon MR, Willemot RM, Vignon MR, Monsan PF. 1997. Structural characterization of the maltose acceptor-products synthesized by *Leuconostoc mesenteroides* NRRL B-1299 dextransucrase. Carbohydr Res 305:549-559.

Domon B, Costello CE. 1988. A systematic nomenclature for carbohydrate fragmentations in FAB-MS/MS spectra of glycoconjugates. Glycoconj J 5:397-409.

Duenas-Chasco MT, Rodriguez-Carvajal MA, Tejero-Mateo P, Espartero JL, Irastorza-Iribas A, Gil-Serrano AM. 1998. Structural analysis of the exopolysaccharides produced by *Lactobacillus* spp. G-77. Carbohydr Res 307:125-133.

Dueñas-Chasco MT, Rodríguez-Carvajal MA, Mateo PT, Franco-Rodríguez G, Espartero J, Irastorza-Iribas A, Gil-Serrano AM. 1997. Structural analysis of the exopolysaccharide produced by *Pediococcus damnosus* 2.6. Carbohydr Res 303:453-458.

Duus JO, Gotfredsen CH, Bock K. 2000. Carbohydrate Structural Determination by NMR Spectroscopy: Modern Methods and Limitations. Chem Rev 100:4589-4614.

Fabre E, Bozonnet S, Arcache A, Willemot R, Vignon M, Monsan P, Remaud-Simeon M. 2005. Role of the two catalytic domains of DSR-E dextransucrase and their involvement in the formation of highly α-(1→2) branched dextran. J Bacteriol 187:296-303.

Gaborieau M, Castignolles P. 2011. Size-exclusion chromatography (SEC) of branched polymers and polysaccharides. Anal Bioanal Chem 399:1413-1423.

Galle S, Schwab C, Arendt E, Gänzle M. 2010. Exopolysaccharide-forming *Weissella* strains as starter cultures for sorghum and wheat sourdoughs. J Agric Food Chem 58:5834-5841.

Gänzle M, Schwab C. 2009. Ecology of exopolysaccharide formation by lactic acid bacteria: sucrose utilisation, stress tolerance, and biofilm formation. In: Ullrich M, Ed. Bacterial polysaccharides: current innovations and future trends. Caister Academic Press, Norfolk, UK, pp.263-278.

Garozzo D, Giuffrida M, Impallomeni G, Ballistreri A, Mon taudo G. 1990. Determination of linkage position and identification of the reducing end in linear oligosaccharides by negative ion fast atom bombardment mass spectrometry. Anal Chem 62:279-286.

Gelinas P, McKinnon C, 2000. Fermentation and microbiological process in cereal foods. In: Kulp C, ve Ponte JG, Handbook of Cereal Science and Technology. Second edition. New York, Marcel Dekker, pp. 741-754.

Geyer H, Geyer R. 2006. Strategies for analysis of glycoprotein glycosylation. Biochim Biophys Acta-Proteins & Proteomics 1764:1853-1869.

Gidley MJ, Hanashiro I, Hani NM, Hill SE, Huber A, Jane J, Liu Q, Morris GA, Rolland-Sabate A, Striegel AM, Gilbert RG. 2010. Reliable measurements of the size distributions of starch molecules in solution: Current dilemmas and recommendations. Carbohydr Polym 79:255-261.

Gruter M, Leeflang BR, Kuiper J, Kamerling JP, Vliegenthart JFG. 1992. Structure of the exopolysaccharide produced by *Lactococcus lactis* subspecies *cremoris* H414 grown in a defined medium or skimmed milk. Carbohydr Res 231:273-291.

Hammes WP, Gänzle MG. 1998. Sourdough bread and related products. In: Wood BJB, Ed. Microbiology of fermented food. Blackie academic & professional, Thomson science, London, UK, pp. 199-215

Hakomori S. 1964. A Rapid Permethylation of Glycolipid, and Polysaccharide Catalyzed by Methylsulfinyl Carbanion in Dimethyl Sulfoxide. J Biochem 55:205-208.

Heinze T, Liebert T, Heublein B, Hornig S. 2006. Functional Polymers Based on Dextran. In: Klemm D, Ed. Polysaccharides II. Springer Berlin, Heidelberg, pp. 199-291.

Hofmeister GE, Zhou Z, Leary JA. 1991. Linkage position determination in lithium-cationized disaccharides: Tandem mass spectrometry and semiempirical calculations. J Am Chem Soc 113:5964-5970.

Ioan CE, Aberle T, Burchard W. 2001 Structure properties of dextran. 3. Shrinking factors of individual clusters. Macromolecules 34:3765-3771

Ioan CE, Aberle T, Burchard W. 2000. Structure properties of dextran. 2. Dilute solution. Macromolecules 33:5730-5739.

Irague R, Rolland-Sabaté A, Tarquis L, Doublier JL, Moulis C, Monsan P, Remaud-Siméon M, Potocki-Vr onèse G, Bul o n A. 2012. Structure and property engineering of α-d-glucans synthesized by dextransucrase mutants. Biomacromolecules 13:187-195.

Jeanes A, Haynes WC, Wilham CA, Rankin JC, Melvin EH, Austin M, Cluskey JE, Fisher BE, Tsuchiya HM, Rist CE. 1954. Characterization and Classification of Dextrans from Ninety-six Strains of Bacteria 1b. J Am Chem Soc 76:5041-5052.

Jerschow A, Müller N. 1997. Suppression of convection artifacts in stimulated-echo diffusion experiments. double-stimulated-echo experiments. J Magn Reson 125:372-375.

Jiang Y, Cole RB. 2005. Oligosaccharide analysis using anion attachment in negative mode electrospray mass spectrometry. J Am Soc Mass Spectrom 16:60-70.

JohnsonJr. CS. 1999. Diffusion ordered nuclear magnetic resonance spectroscopy: principles and applications. Prog Nucl Magn Reson Spectrosc 34:203-256.

Kaditzky S, Seitter M, Hertel C, Vogel RF. 2008. Performance of *Lactobacillus sanfranciscensis* TMW 1.392 and its levansucrase deletion mutant in wheat dough and comparison of their impact on bread quality. Eur Food Res Technol 227:433-442.

Kaditzky S, Vogel RF. 2008. Optimization of exopolysaccharide yields in sourdoughs fermented by lactobacilli. Eur Food Res Technol 228:291-299.

Katina K. 2005. Sourdough : a tool for the improved flavour, texture and shelf-life of wheat bread, PhD Thesis, University of Helsinki.

Khalikova E, Susi P, Korpela T. 2005. Microbial dextran-hydrolyzing enzymes: fundamentals and applications. Microbiol Mol Biol Rev 69:306-325.

Kim D, Robyt JF, Lee SY, Lee JH, Kim YM. 2003. Dextran molecular size and degree of branching as a function of sucrose concentration, pH, and temperature of reaction of *Leuconostoc mesenteroides* B-512FMCM dextransucrase. Carbohydr Res 338:1183-1189.

König S, Leary JA. 1998. Evidence for linkage position determination in cobalt coordinated pentasaccharides using ion trap mass spectrometry. J Am Soc Mass Spectrom 9:1125-1134.

Korakli M, Rossmann A, Ganzle MG, Vogel RF. 2001. Sucrose metabolism and exopolysaccharide production in wheat and rye sourdoughs by *Lactobacillus sanfranciscensis*. J Agric Food Chem 49:5194-5200.

Kralj S, van Geel-Schutten GH, Dondorff MM, Kirsanovs S, van der Maarel MJ, Dijkhuizen L. 2004. Glucan synthesis in the genus *Lactobacillus*: isolation and characterization of glucansucrase genes, enzymes and glucan products from six different strains. Microbiology 150:3681-3690.

Kralj S, Stripling E, Sanders P, van Geel-Schutten GH, Dijkhuizen L. 2005. Highly hydrolytic reuteransucrase from probiotic *Lactobacillus reuteri* strain ATCC 55730. Appl Environ Microbiol 71:3942-3950.

Kulp K. 2003. Baker's yeast and sourdough technologies in the production of U.S. bread products. In: Kulp K, Lorenz K. Eds. Handbook of dough fermentations. Marcel Dekker, New York, USA, pp.101-148.

Kuramitsu HK, Wondrack L. 1983. Insoluble glucan synthesis by *Streptococcus mutans* serotype c strains. Infect Immun 42:763-770.

Lacaze G, Wick M, Cappelle S. 2007. Emerging fermentation technologies: Development of novel sourdoughs. Food Microbiol 24:155-160.

Larm O, Lindberg B, Svensson S. 1971. Studies on the length of the side chains of the dextran elaborated by *Leuconostoc mesenteroides* NRRL B-512. Carbohydr Res 20:39-48.

Laws AP, Marshall VM. 2001. The relevance of exopolysaccharides to the rheological properties in milk fermented with ropy strains of lactic acid bacteria. Int Dairy J 11:709-721.

Leathers TD. 2002. Dextran. In: Vandamme EJ, De Baets S, Steinbuchel A. Eds. Biopolymers. Polysaccharides I: polysaccharides from prokaryotes. Wiley-VCH, Weinheim, Germany, pp. 299-321.

Leon AE, Duran E, Benedito De Barber C. 2002. Utilization of enzyme mixtures to retard bread crumb firming. J Agric Food Chem 50:1416-1419.

Mitsuishi Y, Kobayashi M, Matsuda K. 1984. Structures of three α-(1→2)-branched oligosaccharides isolated from *Leuconostoc mesenteroides* NRRL B-1299 dextran. Carbohydr Res 127:331-337.

Monchois V, Willemot R, Monsan P. 1999. Glucansucrases: mechanism of action and structure–function relationships. FEMS Microbiol Rev 23:131-151.

Mondal A, Datta AK. 2008. Bread baking – A review. J Food Eng 86:465-474.

Monsan P, Bozonnet S, Albenne C, Joucla G, Willemot R, Remaud-Siméon M. 2001. Homopolysaccharides from lactic acid bacteria. Int Dairy J 11:675-685.

Moulis C, Joucla G, Harrison D, Fabre E, Potocki-Veronese G, Monsan P, Remaud-Simeon M. 2006. Understanding the polymerization mechanism of glycoside-hydrolase family 70 glucansucrases. J Biol Chem 281:31254-31267.

Mourey T. 2004. SEC molecular-weight-sensitive detection. Int.J.Polym.Anal.Charact.; Int J Polym Anal Charact 9:97-135.

Mulloy B, Hart GW, Stanely P. 2008. Structural analysis of glycans. In: Varki A, Cummings RD, Esko JD, Freeze HH, Stanley P, Bertozzi CR, Hart GW, and Etzler ME Eds. Essentials of glycobiology. Second edition. Cold Spring Habour Laboratory Press, New York, USA, pp. 661-678.

Mulroney B, Traeger JC, Stone BA. 1995. Determination of both linkage position and anomeric configuration in underivatized glucopyranosyl disaccharides by electrospray mass spectrometry. J Mass Spectrom 30:1277-1283.

Naessens M, Cerdobbel A, Soetaert W, Vandamme EJ. 2005. *Leuconostoc* dextransucrase and dextran: production, properties and applications. J Chem Technol Biotechnol 80:845-860.

Nilsson M. 2009. The DOSY Toolbox: A new tool for processing PFG NMR diffusion data. J Magn Reson 200:296-302.

Nordmeier E. 1993. Static and dynamic light-scattering solution behavior of pullulan and dextran in comparison. J Phys Chem 97:5770-5785.

Nyberg NT, Duus JO, Sorensen OW. 2005. Heteronuclear Two-Bond Correlation: Suppressing Heteronuclear Three-Bond or Higher NMR Correlations while Enhancing Two-Bond Correlations Even for Vanishing 2JCH. J Am Chem Soc. 127:6154-6155.

Padmanabhan PA, Kim D, Pak D, Sim SJ. 2003. Rheology and gelation of water-insoluble dextran from *Leuconostoc mesenteroides* NRRL B-523. Carbohydr Polym 53:459-468.

Pasanen S, Jänis J, Vainiotalo P. 2007. Cello-, malto- and xylooligosaccharide fragmentation by collision-induced dissociation using QIT and FT-ICR mass spectrometry: A systematic study. Int J Mass Spectrom 263:22-29.

Patel S, Majumder A, Goyal A. 2012. Potentials of Exopolysaccharides from Lactic Acid Bacteria, Indian J Microbiol 52:3-12.

Politi M, Groves P, Chávez MI, Cañada FJ, Jiménez-Barbero J. 2006. Useful applications of DOSY experiments for the study of mushroom polysaccharides. Carbohydr Res 341:84-89.

Rantanen H, Virkki L, Tuomainen P, Kabel M, Schols H, Tenkanen M. 2007. Preparation of arabinoxylobiose from rye xylan using family 10 *Aspergillus aculeatus* endo-1,4-β-D-xylanase. Carbohydr Polym 68:350-359.

Rehm BH. 2010. Bacterial polymers: biosynthesis, modifications and applications. Nat Rev Microbiol 8:578-592.

Reis A, Domingues MRM, Domingues P, Ferrer-Correia AJ, Coimbra MA. 2003. Positive and negative electrospray ionisation tandem mass spectrometry as a tool for structural characterisation of acid released oligosaccharides from olive pulp glucuronoxylans. Carbohydr Res 338:1497-1505.

Remaud-Simeon M, Willemot R, Sarçabal P, Potocki de Montalk G, Monsan P. 2000. Glucansucrases: molecular engineering and oligosaccharide synthesis. J Mol Catal B: Enzym 10:117-128.

Robyt JF. 1986. Dextran. In: Kroschwitz JI, Eds. Encyclopedia of Polymer Science and Engineering. Wiley-VCH, New York, pp. 752-767.

Robyt JF, Yoon SH, Mukerjea R. 2008. Dextransucrase and the mechanism for dextran biosynthesis. Carbohydr Res 343:3039-3048.

Robyt JF, Kimble BK, Walseth TF. 1974. The mechanism of dextransucrase action , : Direction of dextran biosynthesis. Arch Biochem Biophys 165:634-640.

Robyt JF, Taniguchi H. 1976. The mechanism of dextransucrase action: Biosynthesis of branch linkages by acceptor reactions with dextran. Arch Biochem Biophys 174:129-135.

Roslund MU, Tähtinen P, Niemitz M, Sjöholm R. 2008. Complete assignments of the 1H and 13C chemical shifts and JH,H coupling constants in NMR spectra of d-glucopyranose and all d-glucopyranosyl-d-glucopyranosides. Carbohydr Res 343:101-112.

Ruas-Madiedo P, Salazar N, De los Reyes-Gavilan CG. 2009. Biosynthesis and chemical composition of exopolysaccharides produced by lactic acid bacteria. In: Ullrich M, Ed. Bacterial Polysaccharides: Current Innovations and Future Trends. Caister Academic Press, Norfolk, UK, pp.279-312.

Ruas-Madiedo P, De los Reyes-Gavilan CG. 2005. Invited Review: Methods for the screening, isolation, and characterization of exopolysaccharides produced by lactic acid bacteria. J Dairy Sci 88:843-856.

Ruas-Madiedo P, Hugenholtz J, Zoon P. 2002. An overview of the functionality of exopolysaccharides produced by lactic acid bacteria. Int Dairy J 12:163-171.

Russell RRB, Gilpin ML, Mukasa H, Dougan G. 1987. Characterization of glucosyltransferase expressed from a *Streptococcus sobrinus* gene cloned in *Escherichia coli*. J Gen Microbiol 133:935-944.

Sabatié J, Choplin L, Doublier JL, Arul J, Paul F, Monsan P. 1988. Rheology of native dextrans in relation to their primary structure. Carbohydr Polym 9:287-299.

Sawen E, Huttunen E, Zhang X, Yang Z, Widmalm G. 2010. Structural analysis of the exopolysaccharide produced by *Streptococcus thermophilus* ST1 solely by NMR spectroscopy. J Biomol NMR 47:125-134.

Schmitz S, Dona AC, Castignolles P, Gilbert RG, Gaborieau M. 2009. Assessment of the Extent of Starch Dissolution in Dimethyl Sulfoxide by 1H NMR Spectroscopy. Macromol Biosci 9:506-514.

Schwab C, Mastrangelo M, Corsetti A, Gänzle M. 2008. Formation of Oligosaccharides and Polysaccharides by *Lactobacillus reuteri* LTH5448 and *Weissella cibaria* 10M in Sorghum Sourdoughs. Cereal Chem 85:679-684.

Senti FR, Hellman NN, Ludwig NH, Babcock GE, Tobin R, Glass CA, Lamberts BL. 1955. Viscosity, sedimentation, and light-scattering properties of fraction of an acid-hydrolyzed dextran. J Polym Sci A Polym Chem 17:527-546.

Setford SJ. 1999. Measurement of native dextran synthesis and sedimentation properties by analytical ultracentrifugation. J Chem Technol Biotechnol 74:17-24.

Seymour FR, Slodki ME, Plattner RD, Jeanes A. 1977. Six unusual dextrans: methylation structural analysis by combined g.l.c.—m.s. of per-O-acetyl-aldononitriles. Carbohydr Res 53:153-166.

Seymour FR, Knapp RD, Chen ECM, Jeanes A, Bishop SH. 1979c. Structural analysis of dextrans containing 2-O-α--glucosylated α--glucopyranosyl residues at the branch points, by use of 13C-nuclear magnetic resonance spectroscopy and gas-liquid chromatography-mass spectrometry. Carbohydr Res 71:231-250.

Seymour FR, Knapp RD. 1980. Structural analysis of dextrans, from strains of *leuconostoc* and related genera, that contain 3-*O*-α-glucosylated α-glucopyranosyl residues at the branch points, or in consecutive, linear positions. Carbohydr Res 81:105-129.

Seymour FR, Knapp RD, Bishop SH. 1976. Determination of the structure of dextran by 13C-nuclear magnetic resonance spectroscopy. Carbohydr Res 51:179-194.

Seymour FR, Chen ECM, Bishop SH. 1979a. Methylation structural analysis of unusual dextrans by combined gas-liquid chromatography-mass spectrometry. Carbohydr Res 68:113-121.

Seymour FR, Knapp RD, Bishop SH. 1979b. Correlation of the structure of dextrans to their 1H-n.m.r. Spectra. Carbohydr Res 74:77-92.

Sidebotham RL. 1974. Dextrans. Adv Carbohydr Chem Biochem; 30:371-444.

Simoes J, Domingues P, Reis A, Nunes FM, Coimbra MA, Domingues MR. 2007. Identification of anomeric configuration of underivatized reducing glucopyranosyl-glucose disaccharides by tandem mass spectrometry and multivariate analysis. Anal Chem 79:5896-5905.

Slodki ME, England RE, Plattner RD, Dick WE. 1986. Methylation analyses of NRRL dextrans by capillary gas-liquid chromatography. Carbohydr Res 156:199-206.

Smitinont T, Tansakul C, Tanasupawat S, Keeratipibul S, Navarini L, Bosco M, Cescutti P. 1999. Exopolysaccharide-producing lactic acid bacteria strains from traditional Thai fermented foods: isolation, identification and exopolysaccharide characterization. Int J Food Microbiol 51:105-111.

Spengler B, Dolce JW, Cotter RJ. 1990. Infrared laser desorption mass spectrometry of oligosaccharides: Fragmentation mechanisms and isomer analysis. Anal Chem 62:1731-1737.

Stampfli L, Nersten B. 1995. Emulsifiers in bread making. Food Chem 52:353-360.

Striegel AM, Isenberg SL, Cote GL. 2009. An SEC/MALS study of alternan degradation during size-exclusion chromatographic analysis. Anal Bioanal Chem 394:1887-1893.

Suarez ER, Syvitski R, Kralovec JA, Noseda MD, Barrow CJ, Ewart HS, Lumsden MD, Grindley TB. 2006. Immunostimulatory polysaccharides from *Chlorella pyrenoidosa*. A new galactofuranan. measurement of molecular weight and molecular weight dispersion by DOSY NMR. Biomacromolecules 7:2368-2376.

Sundberg A, Sundberg K, Lillandt C, Holmbom B. 1996. Determination of hemicelluloses and pectins in wood and pulp fibers by acid methanolysis and gas chromatography. Nord Pulp Pap Res J 11:216-219, 226.

Sutherland IW. 1990. Biotechnology of microbial exopolysaccharides. Cambridge University Press, Cambridge, pp. viii, 163s.

Taylor C, Cheetham NWH, Walker GJ. 1985. Application of high-performance liquid chromatography to a study of branching in dextrans. Carbohydr Res 137:1-12.

Tieking M, Korakli M, Ehrmann MA, Gänzle MG, Vogel RF. 2003. In situ production of exopolysaccharides during sourdough fermentation by cereal and intestinal isolates of lactic acid bacteria. Appl Environ Microbiol 69:945-952.

Tieking M, Ganzle MG. 2005. Exopolysaccharides from cereal-associated lactobacilli. Trends Food Sci Technol 16:79-84.

Tirtaatmadja V, Dunstan DE, Boger DV. 2001. Rheology of dextran solutions. J Nonnewton Fluid Mech 97:295-301.

Tramesel D, Catherinot V, Delsuc M-. 2007. Modeling of NMR processing, toward efficient unattended processing of NMR experiments. J Magn Reson 188:56-67.

Usui T, Ogata M, Murata T, Ichikawa K, Sakano Y, Nakamura Y. 2009. Sequential analysis of α-glucooligosaccharides with α-(1→4) and α-(1→6) linkages by negative Ion Q-TOF MS/MS spectrometry. J Carbohydr Chem 28:421-430.

Vandamme EJ, Renard CEFG, Arnaut FRJ, Vekemans NMF, Tossut PPA, 1997 Process for obtaining improved structure build-up of baked products. European Patent, EP 0 790 003A1.

van Leeuwen SS, Kralj S, van Geel-Schutten IH, Gerwig GJ, Dijkhuizen L, Kamerling JP. 2008a. Structural analysis of the α-d-glucan (EPS180) produced by the *Lactobacillus reuteri* strain 180 glucansucrase GTF180 enzyme. Carbohydr Res 343:1237-1250.

van Leeuwen SS, Kralj S, van Geel-Schutten IH, Gerwig GJ, Dijkhuizen L, Kamerling JP. 2008b. Structural analysis of the α-d-glucan (EPS35-5) produced by the *Lactobacillus reuteri* strain 35-5 glucansucrase GTFA enzyme. Carbohydr Res 343:1251-1265.

van Leeuwen SS, Leeflang BR, Gerwig GJ, Kamerling JP. 2008c. Development of a 1H NMR structural-reporter-group concept for the primary structural characterisation of α-d-glucans. Carbohydr Res 343:1114-1119.

van Leeuwen SS, Kralj S, Gerwig GJ, Dijkhuizen L, Kamerling JP. 2008d. Structural analysis of bioengineered α-D-glucan produced by a triple mutant of the glucansucrase GTF180 enzyme from *Lactobacillus reuteri* strain 180: Generation of (α-(1→4) linkages in a native (1→3)(1→6)-α-D-glucan. Biomacromolecules 9:2251-2258.

Viel S, Capitani D, Mannina L, Segre A. 2003. Diffusion-ordered NMR spectroscopy: a versatile tool for the molecular weight determination of uncharged polysaccharides. Biomacromolecules 4:1843-1847.

Vilaplana F, Gilbert RG. 2010. Characterization of branched polysaccharides using multiple-detection size separation techniques. J Sep Sci 33:3537-3554.

Vink H, Dahlstrom G. 1967. Refractive index increments for polymers in solutions in multicomponent solvents. Makromol Chem 109:249-252.

Vujičić-Žagar A, Pijning T, Kralj S, López CA, Eeuwema W, Dijkhuizen L, Dijkstra BW. 2010. Crystal structure of a 117 kDa glucansucrase fragment provides insight into evolution and product specificity of GH70 enzymes. Proceedings of the National Academy of Sciences 107:21406-21411.

Watanabe T, Chiba M, Matsuda Y, Sakurai F, Kobayashi M, Matsuda K. 1980. Acetolysis of *Leuconostoc mesenteroides* NRRL B-1299 dextran. Isolation and characterization of oligosaccharides containing secondary linkages from the borate-soluble fraction. Carbohydr Res 83:119-127.

Waldherr F, Vogel RF. 2009. Commercial exploitation of homo-exopolysaccharides in non-dairy food systems. In: Ullrich M Ed. Bacterial polysaccharides: current innovations and future trends. Caister Academic Press, Norfolk, UK, pp.313-330.

Welman A. 2009. Exploitation of Exopolysaccharides from Lactic Acid Bacteria: Nutritional and Functional Benefits. In: Ullrich M. Ed. Bacterial polysaccharides: current innovations and future trends. Caister Academic Press, Norfolk, UK, pp.331-344.

Welman A, Maddox I. 2003. Exopolysaccharides from lactic acid bacteria: perspectives and challenges. Trends Biotechnol 21:269-274.

Wirtz R. 2003. Grain, Baking, and Sourdough Bread. In: Kulp K, Lorenz K. Eds. Handbook of dough fermentations. Marcel Dekker, New York, USA, pp.1-24.

Wittgren B, Wahlund K. 1997. Fast molecular mass and size characterization of polysaccharides using asymmetrical flow field-flow fractionation-multiangle light scattering. J Chromatogr, A 760:205-218.

Wu C. 1993. Laser light-scattering characterization of the molecular weight distribution of dextran. Macromolecules 26:3821-3825.

Wuhrer M, de Boer AR, Deelder AM. 2009. Structural glycomics using hydrophilic interaction chromatography (HILIC) with mass spectrometry. Mass Spectrom Rev 28:192-206.

Xu X, Li H, Zhang Z, Qi X. 2009. Hydrodynamic properties of aqueous dextran solutions. J Appl Polym Sci 111:1523-1529.

Yamagaki T, Sato A. 2009. Isomeric oligosaccharides analyses using negative-ion electrospray ionization ion mobility spectrometry combined with collision-induced dissociation MS/MS. Anal Sci 25:985-988.

Zaia J. 2004. Mass spectrometry of oligosaccharides. Mass Spectrom Rev 23:161-227.

Zhang H, Brokman SM, Fang N, Pohl NL, Yeung ES. 2008. Linkage position and residue identification of disaccharides by tandem mass spectrometry and linear discriminant analysis. Rapid Commun Mass Spectrom 22:1579-1586.

Zurbriggen BZ, Bailey MJ, Penttilä ME, Poutanen K, Linko M. 1990. Pilot scale production of a heterologous Trichoderma reesei cellulase in *Saccharomyces cerevisiae*, J Biotechnol 13:267-278.